

For Reference

NOT TO BE TAKEN FROM THIS ROOM

For Reference

NOT TO BE TAKEN FROM THIS ROOM

Ex LIBRIS
UNIVERSITATIS
ALBERTAENSIS



Thesis
1966
#4D

THE UNIVERSITY OF ALBERTA

THE EFFECT OF VALENCY ON DIFFUSION
IN A MAGNETIC FIELD

A Thesis

Submitted to the Faculty of Graduate Studies
In Partial Fulfilment of the Requirements
for the Degree of Doctor of Philosophy

DEPARTMENT OF MINING AND METALLURGY

by

JOHN RAYMOND CAHOON

EDMONTON, ALBERTA

January, 1966

UNIVERSITY OF ALBERTA
FACULTY OF GRADUATE STUDIES

The undersigned certify that they have read and
recommend to the Faculty of Graduate Studies for acceptance,
a thesis titled

THE EFFECT OF VALENCY ON DIFFUSION
IN A MAGNETIC FIELD

submitted by JOHN RAYMOND CAHOON

in partial fulfilment of the requirements for the degree of
Doctor of Philosophy.

ABSTRACT

The effect of a magnetic field on diffusion in the heterovalent Cu-Zn (γ -brass) system and in the homovalent Ag(rich)-Cu system is investigated with the general aim of elucidating the electronic nature of the diffusion process. Standard sandwich diffusion couples were annealed both with and without a magnetic field of 30,000 oersteds applied perpendicular to the diffusion direction. The diffusion constants for γ -brass were obtained via an analysis of the motion of a phase boundary; for the Ag-Cu system, concentration-penetration curves were obtained by electron probe microanalysis and diffusion constants determined by the familiar Boltzmann - Matano treatment. No statistically significant field effect was found in either system. For γ -brass, (58-61 at.% Zn) the diffusion coefficient is given as $7.1 \pm 0.6 \times 10^{-9} \text{ cm}^2/\text{sec.}$ at 509°C ; for the Ag-Cu system the frequency factor and activation energy calculated from the diffusion data are $0.03^{+.03}_{-.016} \text{ cm}^2/\text{sec.}$ and $37.8 \pm 1.5 \text{ kcal/g-atom}$ respectively. The absence of a diffusion inhibition effect by the field in heterovalent γ -brass, which was present in the heterovalent Al(rich)-Cu system, is associated with the low electrical conductivity of γ -brass. The absence of a field effect in the Ag-Cu system, which has a relatively high electrical conductivity, is associated with the absence of effective electron density (per atom) gradients for the

corresponding concentration and density gradients. The influence of the electronic structure on the plasma-magnetohydrodynamic properties of the alloy is considered in the light of the field diffusion results obtained for the γ -brass, Ag(rich)-Cu, and Al(rich)-Cu alloy systems; specifically, such factors as conductivity, effective mass of the electron, electron density gradients, and electron ground state energies are discussed in relation to the diffusion process.

ACKNOWLEDGEMENTS

I am glad to have this opportunity to thank Dr. W.V. Youdelis for his supervision during the course of this project. His guidance and friendship over the past five years are greatly appreciated.

I would like to thank other members (present and former) of the Department, particularly Dr. D.R. Colton, Dr. M.J. Bibby, and Mr. R.M. Scott for their helpful discussions and assistance. I am also very grateful to my wife for her patience and perserverance in typing this thesis.

The financial assistance of the National Research Council of Canada who provided a scholarship and an equipment grant (NRC-A-836) is gratefully acknowledged.

TABLE OF CONTENTS

	PAGE
INTRODUCTION	1
HISTORICAL REVIEW	6
A. DIFFUSION IN γ -BRASS	7
B. DIFFUSION IN SILVER(RICH)-COPPER ALLOYS	8
C. ELECTRONIC THEORIES OF DIFFUSION	13
D. DIFFUSION IN A MAGNETIC FIELD	18
1. Thermodynamic Considerations	19
2. Magnetohydrodynamics	19
3. Plasma Dynamics	22
4. Plasma Oscillation and Charge Screening	30
E. THE MAGNETIC DIFFUSION EFFECT IN FERROMAGNETIC METALS AND ALLOYS	35
EXPERIMENTAL METHODS	47
A. PREPARATION OF ALLOYS	47
1. γ and $\gamma + \beta$ Brass	47
2. Silver-Copper Alloys	48
3. Preparation of Silver	50
B. PREPARATION OF DIFFUSION COUPLES	52
1. γ -Brass Diffusion Couples	52
2. Silver-Silver Copper Sandwich Diffusion Couples	54
C. THE DIFFUSION ANNEALS	56
D. THE MAGNET	61
E. MEASUREMENTS	62
1. Direct Measurement of the Kirkendall Shift	62

	PAGE
2. Measurement of the Boundary Motion in the γ -Brass Diffusion Couples	63
3. Electron Probe Analysis of the Silver-Copper Diffusion Couples	65
F. TREATMENT OF DATA FROM PROBE ANALYSIS	67
RESULTS	70
A. DIFFUSION IN γ -BRASS	70
B. DIFFUSION OF COPPER IN SILVER	73
1. Direct Measurement of Kirkendall Shift	73
2. Diffusion Results for the Diffusion of Copper in Silver	74
DISCUSSION	83
A. DIFFUSION IN γ -BRASS	83
B. DIFFUSION OF COPPER IN SILVER	88
C. DISCUSSION OF ERRORS	95
1. Measurement of Temperature	96
2. Analysis	97
3. Inhomogeneity of Base Alloys	98
4. Welding	98
5. Computational Errors	98
D. DIFFUSION IN THE MAGNETIC FIELD	99
1. Electron Density Difference	100
2. Electron Ground State Energy	105
3. Screening	112
SUMMARY AND CONCLUSIONS	114
BIBLIOGRAPHY	116

APPENDICES

I. ANALYSIS OF MATERIALS	120
II. DETERMINATION OF THE DIFFUSIVITY BY THE BOUNDARY SHIFT BETWEEN A SINGLE PHASE AND A TWO PHASE REGION	122
III. CONCENTRATION PROFILES FOR THE Ag-Cu DIFFUSION COUPLES	125
IV. DETERMINATION OF THE AVERAGE DISTANCE TRAVERSED BY AN ION DURING DIFFUSION	134

LIST OF FIGURES

FIGURE	PAGE
1. Diffusion coefficients in δ -brass.	9
2. Previous results for the diffusion of copper in silver.	12
3. Variation of the field and no-field interdiffusion coefficients with temperature in the Al(rich)-Cu system.	29
4. The magnetic diffusion effect in alpha-iron.	36
5. Precipitation of a silver-copper-oxygen compound in the diffusion zone.	51
6. Welding assembly for δ -brass diffusion couples.	53
7. Welding assembly for silver-copper diffusion couples.	55
8. Furnace used for the diffusion anneals.	58
9. Phase boundary motion in δ -brass for diffusion couple Br-F-1.	64
10. Electron probe concentration profile for couple Ag-F-6.	66
11. Electron probe concentration profile for couple Ag-F-7.	66
12. Calculation of diffusion coefficient for couple Ag-F-6 annealed at 754°C for 45 hrs.	69
13. Boundary shift for $\delta/\delta + \beta$ brass diffusion couples.	72

FIGURE	PAGE
14. Probability plots for couples Ag-F-3 and Ag-NF-3 annealed at 630°C for 48 hrs.	75
15. Probability plots for couples Ag-F-5 and Ag-NF-5 annealed at 699°C for 96 hrs.	76
16. Probability plots for couples Ag-F-6 and Ag-NF-6 annealed at 755°C for 45 hrs.	77
17. Probability plots for couples Ag-F-7 and Ag-NF-7 annealed at 803°C for 25 hrs.	78
18. Variation of D with concentration in couple Ag-NF-7.	81
19. Variation of the diffusivity with temperature in the Ag(rich)-Cu system.	82
20. Comparison of the grain sizes in couples annealed at 630°C and 756°C.	91
21. Comparison of previous data with present results.	92
22. Different grain sizes in couple Ag-NF-7 annealed at 803°C for 24 hrs.	94
23. Two-band representation for N(E) vs. E in the Al-Cu and Ag-Cu alloy systems.	108
24a. Phase diagram showing limiting concentrations for diffusion from a two phase into a single phase region.	123

FIGURE	PAGE
24b. Concentration profile after diffusion at temperature 'T' for time 't'.	123
25. Penetration curve for couple Ag-F-3 annealed at 629°C for 48 hrs.	126
26. Penetration curve for couple Ag-NF-3 annealed at 630°C for 48 hrs.	127
27. Penetration curve for couple Ag-F-5 annealed at 699°C for 96 hrs.	128
28. Penetration curve for couple Ag-NF-5 annealed at 698°C for 96 hrs.	129
29. Penetration curve for couple Ag-F-6 annealed at 754°C for 45 hrs.	130
30. Penetration curve for couple Ag-NF-6 annealed at 756°C for 45 hrs.	131
31. Penetration curve for couple Ag-F-7 annealed at 802°C for 25 hrs.	132
32. Penetration curve for couple Ag-NF-7 annealed at 803°C for 25 hrs.	133

LIST OF TABLES

TABLE	PAGE
I. RESULTS OF SEITH AND PERETTI	10
II. DIFFUSIVITY FOR DIFFUSION IN γ -BRASS	71
III. KIRKENDALL SHIFT AND DIMENSIONAL CHANGES FOR DIFFUSION OF COPPER IN SILVER	73
IV. SUMMARY OF DIFFUSION RESULTS IN THE SILVER - COPPER SYSTEM	79

INTRODUCTION

Work in the past on the theory of diffusion in solids has been based chiefly on a thermodynamic approach. The frequency factor, D_0 , and activation energy, Q , of the diffusion constant are expressed in thermodynamic quantities, and diffusion experiments are then designed and carried out for a semi-empirical determination of these parameters. The atomistics of the diffusion process is minimally involved, and then only in a statistical way in the calculation of correlation factors for the atom jump process, which determines the magnitude of the frequency factor. The emphasis on the thermodynamic approach by the theorist resulted more from necessity than chance, for an atomistic approach in the broad sense of the term requires the description of the diffusion process on a quantum mechanical (electronic) level. For this, a knowledge of the perturbation potential surrounding an impurity atom in a metal lattice and its interaction with defects (vacancies) is required. It is only relatively recently that more satisfactory theories on fields around impurity atoms in metals have been developed, and only now are they being applied to an analytical study of the atomistics of diffusion, and to an interpretation of the activation energy on the basis of electronic models.

The first serious attempt to relate the activation energy of the diffusion process to the electronic configuration of the activated solute-vacancy system was that of Lazarus¹,

who calculated the effect of screening on the diffusion of the solute Sb in Ag. The diffusion of Sb in Ag for very dilute concentrations is considerably faster than the self diffusion of Ag, and it was shown that this was due to the attraction of the negatively charged vacancies for the screened and positively charged Sb ions. The theory of the screened potential of the impurity atom and its interaction with a vacancy was developed more extensively in a series of papers by Alfred and March^{2,3,4}, in which the usual Thomas - Fermi approximation for electron density is used, but where the first order or linearization approximation of the Poisson equation used by Lazarus and others is avoided. The result is that the perturbation potentials are more effectively shielded for impurity atoms of valency $Z+1$ dissolved in a monovalent metal. Le Claire⁵, in a very extensive paper, applied the results of Alfred and March to develop a more comprehensive theory for the diffusion of heterovalent solutes in monovalent metals. The differences in the activation energies between solute and self diffusion, calculated using Le Claire's theory, showed remarkably good agreement with experimental results for impurity elements immediately following the noble metal solvent in the periodic table. The agreement however was poor for those solutes with negative values for Z (transition metals), and this was attributed to the gross uncertainty in the value of Z to be taken and the actual form of the screening constant.

The recent investigations of Youdelis, Colton, and

Cahoon^{6,7} on the effect of a magnetic field on diffusion and solidification in alloys was a further significant step in the direction of describing the diffusion process on the basis of electronic models. It was shown that diffusion of Cu in Al in a transverse magnetic field of 30,000 oersteds was inhibited at least 25%, with no field effect observed when diffusion was parallel to the field direction. A theory based on the plasma-magnetohydrodynamic properties of the alloy was developed to account for the results. According to the theory, the magnetic field decreases the diffusivity by the factor $1/(1+\omega_{ce}^2/\nu_e^2)$, where ω_{ce} and ν_e are the cyclotron and collision frequencies respectively of the diffusion transported electrons. For diffusion inhibition to occur, it was shown that there must be a finite (even though small) electron density gradient associated with the solute concentration gradient, and that Hall diffusion currents must close to prevent the build-up of (electrostatic) Hall fields which would cancel the Lorentz force on the electrons. The plasma oscillation screening factor (Thomas - Fermi form) was discussed, and it was shown (by a theoretical argument) that it is not affected by the field, and as a consequence it was proposed that the decrease in the diffusivity was effected through a decrease in the frequency factor D_0 , and not through an increase in the activation energy for diffusion. The results of the solidification experiments in a magnetic field, both for chill-cast ingots⁷ and directionally (slow) solidified ingots⁸, supported the field diffusion-inhibition

hypothesis. It was found that the segregation in the field-solidified ingots differed from that obtained for the no-field ingots, and a theory consistent with the diffusion-inhibition effect of the magnetic field was presented to explain the segregation differences. By applying irreversible thermodynamic principles, it was shown that the segregation changes in the field-solidified ingots are a manifestation of the decreased entropy production of the diffusion, convective mixing, and viscous processes of solidification in a magnetic field. For the Al-Cu ingots there is order-of-magnitude agreement between the observed segregation change and the decreased diffusion rate in the magnetic field.

The theory of diffusion in a magnetic field, as developed by Youdelis, Colton, and Cahoon, is in need of further elaboration, for the equations developed for diffusion in a magnetic field are applicable only to the extent that a particular alloy exhibits plasma-like properties. In diffusion the roles exercised by the various electronic factors, such as for example: the magnitude of the electron density gradient, electron ground state energies, effective mass of the electron, conductivity, screening, etc., should be examined more closely, particularly their effect on the plasma nature of the metal. It was decided, therefore, that as a complement to the heterovalent diffusion investigation of Cu in Al, a study of homovalent diffusion ($Z=0$) in a magnetic field would be useful in clarifying some of the points raised above.

Also, it was decided to study diffusion in the hetero-valent γ -brass in a magnetic field because the effective mass of the electron in this system is supposedly very low⁴⁵. The low effective mass should cause a high cyclotron frequency and thus diffusion in a magnetic field should be severely inhibited.

In this present investigation the Ag(rich)-Cu system was chosen for the study of homovalent diffusion (Cu in Ag) in a magnetic field, and for the following reasons: (1) The almost complete lack of reliable diffusion data on this (commercially) important alloy system. Only two diffusion investigations have been published and there is little agreement of results between the authors. It was felt, therefore, that accurate diffusion data on this system would itself be a valuable contribution to the literature. (2) Ag(rich)-Cu alloys have the lowest resistivity compared to other possible homovalent systems. The importance of this quantity in determining the magnitude of the field effect is evident in considering the factor by which the diffusivity is reduced in the field, viz., $1/(1+\omega_{ce}^2/\nu_e^2)$. The collision frequency (resistivity) dependency of the field effect is developed in more detail in the text of this thesis. (3) The ground state energies of the electrons of Cu and Ag differ sufficiently to permit a limited analysis of this effect.

HISTORICAL REVIEW

Except for the recent work on diffusion and solidification in magnetic fields undertaken by Youdelis and his collaborators (including the author) there have been no previous direct investigations on the effect of a magnetic field on processes involving mass transport in alloy systems. Therefore, the review of the subject must necessarily include those topics which are indirectly related to the present work. Previous work on diffusion in the Ag(rich)-Cu system and the δ -brass system will be considered first, followed by a brief review of the theories of Lazarus and Le Claire on the electronic nature of the diffusion process. The "magnetic diffusion effect" as observed in ferromagnetic alloys is also considered as it bears some relationship indirectly to the present investigation. An extensive and detailed account is given of the theory on diffusion in a magnetic field, for although now in print, it was largely developed during the initial stages of this work and so forms part of this thesis. Its inclusion in the historical review section is partly for reasons of convenience in thesis format.

A. DIFFUSION IN δ -BRASS

The δ phase in the alloy system Cu-Zn is an exceedingly brittle intermetallic compound, and as such is a difficult system in which to study diffusion by conventional means; i.e. using solid-solid diffusion couples and a sectioning technique for analysis. This is probably why there has been only one reported investigation concerning diffusion in δ -brass, that of Mehl and Lutz¹⁰ in 1961. Mehl and Lutz used a vapor-solid diffusion system for alloy preparation and an electron probe for analysis. The experimental technique consisted of making an alloy of $\delta + \epsilon$ brass, powdering and placing a quantity of it at either end of a β -brass cylindrical rod located in a pyrex or vycor glass cylinder. The glass cylinder was then evacuated to 10^{-5} mm. of Hg, sealed, and heated to the appropriate diffusion annealing temperature ranging from 375°C to 650°C for periods of four to thirty hours. The δ phase from the two phase ($\delta + \epsilon$) alloy evaporated and plated onto the surface of the brass cylinder to form a "dynamic" diffusion couple; i.e. a diffusion couple having non-stationary boundaries. It was necessary to use the two phase alloy ($\delta + \epsilon$) so that the concentration at the surface of the diffusion couple remained constant with time as a consequence of chemical equilibrium. On evaporation, the surface concentration remained constant at the composition of the $\delta / \delta + \epsilon$ boundary (or $\delta / \delta + \delta$ boundary at higher temperatures), whereas if

the powdered δ -phase was used alone, the surface concentration was found to vary with time.

Following the diffusion anneal, the sample was quenched in water, measured and weighed, then electroplated with copper to prevent fracture of the brittle δ phase during sectioning and polishing. Concentration-distance curves were obtained using an electron probe, and diffusion coefficients were determined by means of the Boltzmann - Matano method, shown by Jost¹¹ to be valid for diffusion systems exhibiting concentration discontinuities at phase boundaries as well as for ordinary single phase diffusion systems. A plot of the diffusion coefficients for δ -brass for various zinc concentrations versus $1/T$ is given in Figure 1.

B. DIFFUSION IN SILVER(RICH)-COPPER ALLOYS

With the abundant data published concerning diffusion in silver-rich alloys it is surprising that there have been only two reported investigations concerning the diffusion of copper in silver. The first was conducted by Seith and Peretti¹² in 1936. They used a technique somewhat similar to that used in the present investigation. A 2 at.% alloy cylinder, 6.5 mm. in diameter and 3 mm. long, was vacuum welded to a pure silver cylinder of similar dimensions. A welding temperature of 750°C and a pressure of 20 p.s.i. were maintained for a period of one-half to one hour. Diffusion anneals were then conducted at 895°C for 16 days,

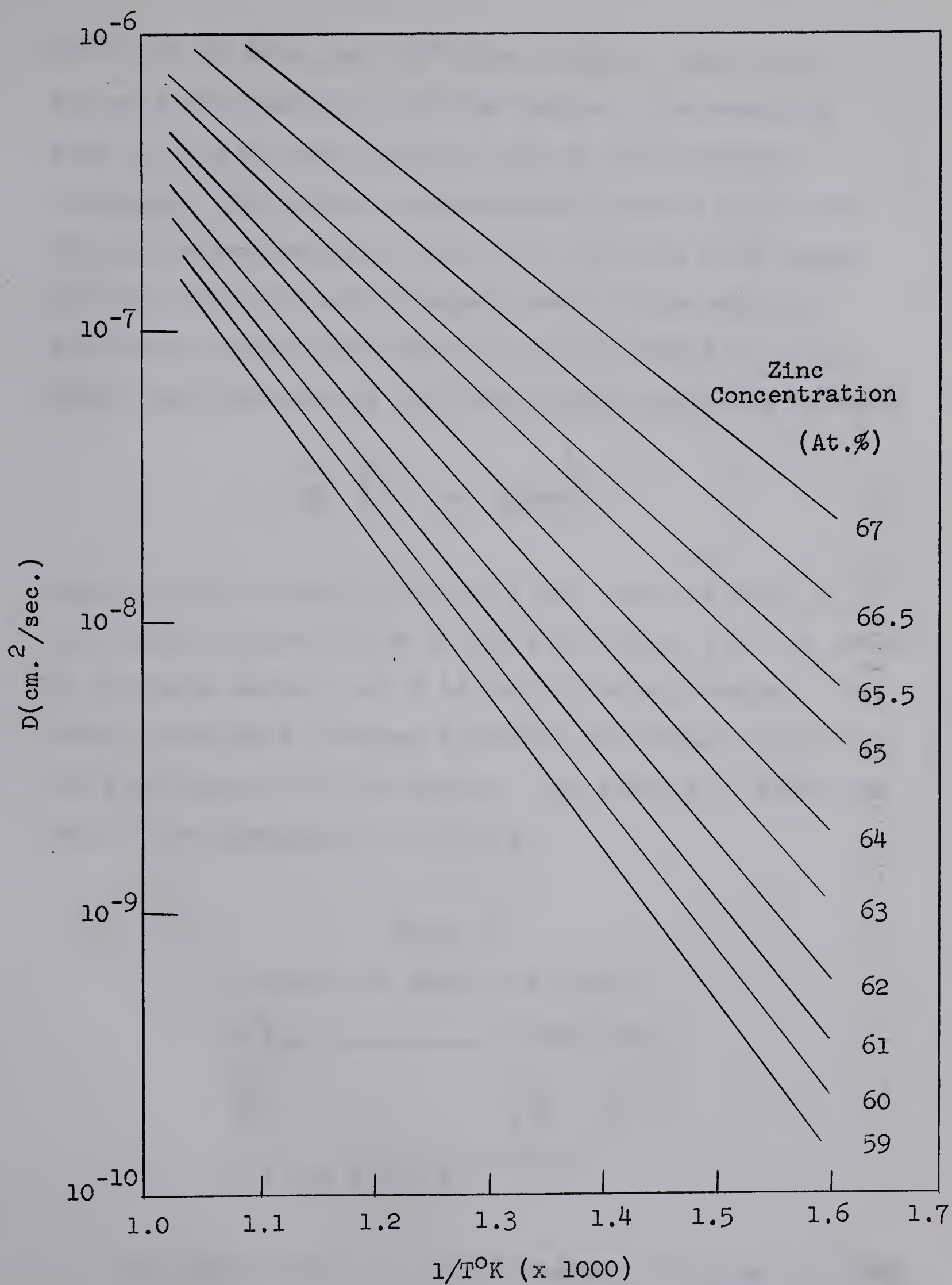


Figure 1. Diffusion coefficients in γ -brass (After Mehl and Lutz¹¹).

800°C for 29 days, and 760°C for 12 days. Samples for analysis were machined from the sample at intervals of 0.05 to 0.10 mm. and analyzed using a spectrographic technique. Only three concentration-distance points were obtained corresponding to 0.3, 0.1, and 0.03 at.% copper as these were the only standards used in the analysis. From these points three diffusion coefficients for each sample were obtained by the Grube method using the equation

$$C = \frac{C_0}{2} \left(1 - \operatorname{erf} \frac{x}{2\sqrt{Dt}} \right), \quad (1)$$

where C is the concentration at x cm. from the weld, C_0 is the initial concentration of the bulk alloy, t is the length of diffusion anneal, and D is the diffusion constant. The three values were averaged to obtain an average value for the particular diffusion anneal. The results of Seith and Peretti are summarized in Table I.

Table I

Results of Seith and Peretti

$T^{\circ}\text{C}$	$D \text{ cm.}^2/\text{sec.}$
895	9.4×10^{-10}
800	5.9×10^{-10}
760	3.6×10^{-10}

$$D = 5.9 \times 10^{-5} e^{-24,800/RT}$$

The second investigation of copper diffusion in silver was that of Sawatzky¹³ in 1957. He used a tracer technique

to establish the self diffusion coefficient of copper in single crystals of silver. The tracer technique employed by Sawatzky consisted of plating a small quantity of radioactive tracer (initial activity 100,000 counts per minute) onto the surface of a pure silver cylinder, 1/2 cm. long and 1.6 cm. in diameter. The specimen was then diffusion annealed at temperatures ranging from 700°C to 950°C for periods of five to forty five hours depending upon the temperature. Following the diffusion anneal, the specimens were sectioned for analysis by machining off about twenty 0.001 cm. layers on a jeweller's lathe. These layers were then analyzed by measuring the activity with a gieger counter. The diffusivity, D , was determined using the equation

$$C(x,t) = \frac{A}{Dt} e^{-x^2/4Dt}, \quad (2)$$

where A is the total amount of tracer material plated onto the silver, and $C(x,t)$ is the concentration at distance x from the plated surface after a diffusion anneal of time t . The concentration of copper was assumed directly proportional to the number of counts per minute and the diffusivity was determined from a plot of log activity versus x^2 , which according to equation (2) yields a straight line of slope $-1/4Dt$. The log D versus $1/T$ plot obtained by Sawatzky along with that of Seith and Peretti is given in Figure 2, from which it is evident there is little agreement between the two investigations.

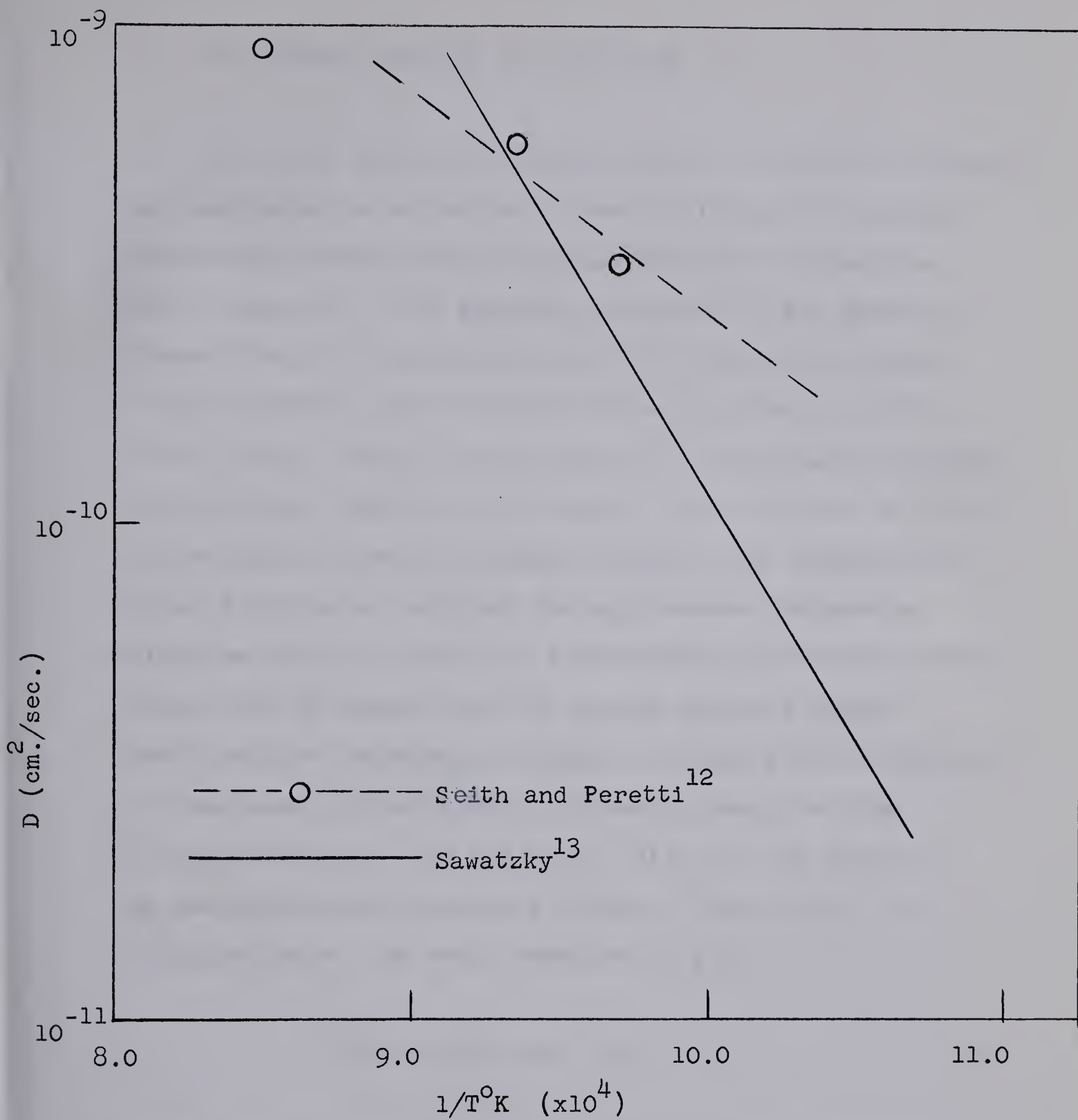


Figure 2. Previous results for the diffusion of copper in silver.

C. ELECTRONIC THEORIES OF DIFFUSION

The first work on diffusion theory in which the process was considered to be basically one involving electrostatic interaction between the diffusing atom and a vacancy was that of Lazarus¹. For impurity diffusion it was generally assumed that at low concentrations the diffusivity should be approximately equal to that for self diffusion of the solvent metal, since vacancy motion is predominantly through (or involving) solvent metal atoms. In an attempt to account for the high diffusion constant for Sb in Ag, compared to the self diffusion constant for Ag, Lazarus proposed a diffusion model in which the electrostatic attraction energy between the Sb atoms (ions) of excess positive charge ($Z=+4$) and the negatively charged vacancies ($Z=-1$) contribute to a decrease in the overall activation energy of the diffusion process. The potential, $V(r)$, of the impurity ion was calculated assuming a Thomas - Fermi model and linearization of the basic equation to give

$$V(r) = \frac{Ze}{r} \exp(-qr) \quad , \quad (3)$$

where Z is the excess charge units, and q the screening constant defined as

$$q = \left[4 \pi e^2 N(E_F) \right]^{1/2} . \quad (4)$$

$N(E_F)$ is the energy level density near the Fermi surface. In a monovalent metal a vacancy is assumed to be equivalent to an effective charge $(-e)$ at the vacant site, corresponding to the removal of an ion of charge $(+e)$. Then if a is the nearest-neighbor distance, the excess energy ΔE required to form a vacancy at a site next to an impurity atom is given by $-eV(a)$, thus

$$\Delta E = \frac{-Z e^2}{a} \exp(-qa) , \quad (5)$$

which for the case of Sb in Ag is negative since Z is positive. In the vacancy mechanism of diffusion the vacancy formation energy constitutes a part of the overall activation energy for the diffusion process, and any change in it would result in an equivalent change in the diffusion activation energy. Lazarus shows that the activation energy for diffusion of Sb in Ag is less than that for Ag self diffusion by approximately the amount calculated for ΔE .

Le Claire⁵ extended the ideas of Lazarus to include a consideration of the electrostatic interaction of the impurity ion and vacancy during their reciprocal motion as well as in vacancy formation. He proposed that the difference in diffusion coefficients between impurity diffusion (D_2) and self diffusion (D_0) arises principally from the corresponding difference ΔQ in activation energies Q_2 and Q_0 , which he gives as

$$\Delta Q = \Delta H_2 + \Delta E - R \partial \ln f_2 / \partial (1/T) . \quad (6)$$

ΔH_2 is the difference between the activation energy for a jump of an impurity atom into a neighboring vacant site and the activation energy for the jump, in pure solvent, of a solvent atom into a vacant site. The last term in the equation allows for the temperature dependence of the correlation factor f_2 for impurity diffusion, and is a complicated quantity involving, in addition to ΔH_2 , the activation energies for solvent atom jumps near the impurity. ΔE has the same significance as in the theory of Lazarus, except that $V(r)$ is now calculated without the linearization approximation of the Thomas - Fermi equation and is given by

$$V(r) = \frac{\alpha Ze}{r} \exp(-qr) , \quad (7)$$

where α is a constant depending only on Z .

When an atom is at the saddle point of its jump from one site to the next, there is in effect a half-vacancy on each side of the migrating atom. If the effective charge of $-1/2e$ is assigned to each of the half-vacancies, then

$$\Delta H_2 = 2 \left(-e/2 \right) V(x) + eV(a) , \quad (8)$$

so that

$$\Delta H_2 + \Delta E = -eV(x) . \quad (9)$$

x is the distance of the effective centers of the half-vacancies from the migrating atom at the saddle point, which Le Claire assumes is approximately $11a/16$, corresponding to the position of the centroids of the hemispheres constituting the major parts of the half-vacancies. Using the above expressions for ΔE and ΔH_2 , Le Claire calculated ΔQ for a large number of heterovalent impurities in noble metals. Good agreement with experimental values of ΔQ was obtained for impurity elements immediately following in the periodic table the noble metal solvent, but the agreement was poor for the so-called "negative Z" impurities (transition elements in noble metal solvents). This was attributed to uncertainty in what value to assign to Z and the correct form of the screening constant q . For negative Z values it is noted that in the Thomas - Fermi method, electrons are not allowed in regions of negative kinetic energy, and hence requires that there be a sphere of radius r_e around the negative point charge in which there are no electrons. For this reason exact solutions for $V(r)$ are not possible. Alfred and March³ have obtained approximate solutions for this case (monovalent solvent) by matching solutions at $r = r_e$ to obtain α , where $V(r) = E_F$ at $r = r_e$ and also the potential and its first derivative are continuous.

Le Claire⁹ has applied his general theory developed for heterovalent impurity diffusion in monovalent solvent metals to the problem of homovalent impurity diffusion.

He shows that for a homovalent alloy the wave equation for an electron is equivalent (to a good approximation) to the wave equation for a free electron scattered by a potential $U = E_A^0 - E_B^0$ below the constant zero potential of the solvent lattice outside the Wigner - Seitz sphere of radius R , where E_A^0 and E_B^0 are the ground state energies of the solvent and solute electrons respectively in their respective pure metals. If U is positive there is a potential well at the impurity atom site and electrons are attracted into its cell, giving it a net negative charge. Vacancies with their effective negative charge are repelled from such an impurity and as a consequence the activation energy for diffusion should increase, i.e. ΔQ is positive for comparison with self diffusion. When U is negative a potential hump exists at the impurity site and ΔQ is correspondingly negative. The effect of the potential well is to polarize the conduction electrons in the immediate vicinity of the impurity atom, and this redistribution of charge adds another term, $v_e(r)$, to the potential, so that the total self-consistent potential with respect to the pure solvent as zero becomes

$$\left. \begin{aligned} V(r) &= U/e + v_e(r) \quad , \quad r < R \\ V(r) &= v_e(r) \quad , \quad r > R \end{aligned} \right\} \quad (10)$$

In the linearized approximation of the Thomas - Fermi equation the potential $V(r)$, subject to the boundary conditions in (10), becomes for $r > R$

$$V(r) = \frac{-U}{2er} \frac{(qR-1)}{q} \exp (q (R-r)) . \quad (11)$$

Since (7) and (11) are of the same form in their dependence on r , a homovalent solute atom has the same potential as a heterovalent solute atom of excess charge Z given by $(ZQ)_{\text{eff.}} = - (U/2qe^2) (qR - 1)\exp qR$. Using equation (11) for $V(r)$, Le Claire has calculated ΔQ for impurity diffusion of the noble metals in one another. The calculated and observed values for ΔQ agreed remarkably well. In particular, the experimental result that ΔQ is largest for Au in Ag and least for Au in Cu is reproduced theoretically, both with respect to sign and magnitude of ΔQ . Although the theory gives results which agree very well with experiment for the monovalent metals, Le Claire cautions the use of equation (11) for systems having higher electron densities, in particular where the solvent is trivalent. This is due to the oscillatory nature of $V(r)$, with the oscillations occurring at shorter distances as the electron density increases.

D. DIFFUSION IN A MAGNETIC FIELD

In dealing with the theory of the effect of a magnetic field on diffusion, it is necessary to explore in some detail all possibilities wherein some effect may be expected. Therefore, the effect of a magnetic field on the thermodynamics of the (diffusion) system, the magnetohydrodynamic

and plasma nature of the alloy, and the effect of a magnetic field on charge screening is considered in the following.

1. Thermodynamic Considerations

Generally, the effect of a magnetic field on the thermodynamic functions of a system will be in the order of the ratio of the induced magnetic energy to the total energy of the system (specifically, the enthalpy at 0°K). The induced magnetic energy in a system is given by $\frac{1}{2} \chi H^2$, where χ and H are the magnetic susceptibility and field strength respectively.* For silver ($\chi = 0.2 \times 10^{-6}$ c.g.s./gm.) this induced energy is 2×10^{-4} cal./mole, as compared to 5.7 cal./mole for the specific heat and over 20,000 cal./mole for the activation energy for diffusion. The induced magnetic energy is therefore negligible, and any effect of the magnetic field on the thermodynamic functions of the diffusion system can be ignored¹⁴.

2. Magnetohydrodynamics

The magnetohydrodynamic equation of macroscopic fluid motion is the ordinary hydrodynamic equation modified to

- - - - -

* Electromagnetic and c.g.s. units are used throughout unless otherwise specified.

take account of the interaction between fluid motion and the electric and magnetic fields. The equation as derived from the Boltzmann transport equation is given by¹⁵

$$\rho \frac{d\vec{v}}{dt} + \rho(\vec{v} \cdot \nabla)\vec{v} = -\nabla p + \rho \vec{g} - \nu \rho \nabla^2 \vec{v} + \mu \vec{j} \times \vec{H} \quad , \quad (12)$$

where \vec{v} is the macroscopic velocity of a fluid having density ρ , magnetic permeability μ , and kinematic viscosity ν . In equation (12), p is the pressure, \vec{g} the gravitational acceleration, \vec{H} the magnetic field strength, and \vec{j} is defined by Ohm's law (assuming the existence of the continuum property) thus:

$$\vec{j} = \sigma (\vec{E} + \mu \vec{v} \times \vec{H}) \quad , \quad (13)$$

where σ is the conductivity of the fluid and \vec{E} is the applied electric field. The effect of the magnetic field on the motion of the fluid is found in the $\mu \vec{j} \times \vec{H}$ term (eqn. 12) known as the pondermotive force. From equation (13),

$$\mu \vec{j} \times \vec{H} = \mu \sigma (\vec{E}_\perp \times \vec{H}) - \mu^2 \sigma H^2 \vec{v}_\perp \quad , \quad (14)$$

where \vec{E}_\perp and \vec{v}_\perp are components transverse to the magnetic field. The quantity $\mu^2 \sigma H^2 \vec{v}_\perp$ is the induction drag which opposes motion across the lines of force, and may be regarded as a magnetic viscous force analogous to the ordinary viscous force ($\nu \rho \nabla^2 \vec{v}$). The non-linear term $\rho(\vec{v} \cdot \nabla)\vec{v}$ in equation (12)

is the inertia (convective) component of the force. The magnitudes of the latter two forces are comparable with $\nu \rho v l^{-2}$ and $\rho v^2 l^{-1}$ respectively, where l is a characteristic length of the system. Therefore, the magnetic viscous force in the fluid will dominate over the ordinary viscous and convective forces if the respective parameters $\mu^2 H^2 l^2 \sigma (\rho \nu)^{-1}$ and $\mu^2 H^2 l^2 \sigma (\rho v)^{-1}$ are large compared with unity, which is the case for systems having large dimensions and/or strong magnetic fields.

During the process of diffusion, the magnetic field will inhibit diffusion perpendicular to the field in that there is a density change associated with the concentration change and hence a small macroscopic motion of the center of mass of fluid (or solid). However, for solid or liquid diffusion, the velocity of this motion is relatively slow or negligible because density changes are very small so that the magnetic viscous force can generally be neglected. For example, for diffusion in mercury where $\rho \nu \sim 10^{-1}$, $\sigma \sim 10^{-5}$ e.m.u., and for $H = 30,000$ oersteds, $\mu^2 H^2 l^2 \sigma (\rho \nu)^{-1} \sim 10^{-1}$ for a gradient length of 10^{-3} cm. Thus, the magnetic viscous force is less than the ordinary viscous force which is itself negligible for diffusion processes. Therefore, the magnetic viscosity will play a negligible role in diffusion in solid or liquid systems.

3. Plasma Dynamics

It was shown previously that the effect of a magnetic field on macroscopic motion was negligible. However, the macroscopic magnetohydrodynamic viscous force represents the sum total of the magnetic forces acting on the individual particles, i.e. the electrons and ion cores of the solid or liquid. These forces will influence the relative motion or diffusion of the individual particles, in that the Lorentz force will cause them to gyrate around the magnetic lines of force with frequency $\omega_c = eH/m^*$, where m^* is the effective mass of the particle. (We have assumed particles of single charge.) Equations (12) and (13) are valid only when the collision frequency of the electrons, ν_e , greatly exceeds the gyration frequency, ω_{ce} ; i.e. $\omega_{ce}/\nu_e \ll 1$. If the gyration radius is in the order of the mean free path or smaller, the classical description of the transport properties breaks down and recourse to the fundamental Boltzmann equation is necessary to describe the two-fluid plasma system in which Ohm's law is no longer valid.

Two basic plasma dynamic equations (Spitzer¹⁶) are the linearized equation of motion in the steady state and the reduced force equation:

$$\vec{\nabla} p = \mu \vec{j} \times \vec{H} , \quad (15)$$

and

$$\vec{E} + \mu \vec{v} \times \vec{H} = \vec{j}/\sigma + \frac{1}{en_e} (\vec{\nabla} p_i) , \quad (16)$$

where n_e is the volume density of electrons, σ the electrical conductivity of the plasma, and the subscript "i" refers to the ions. (The force of gravity which Spitzer included has been neglected.) Solving for \vec{v} in equation (16) and substituting for \vec{j} (equation 15) the transverse velocity of the fluid in a magnetic field is

$$\vec{v}_\perp = \frac{\vec{H}}{\mu H^2} \times \left(-\vec{E} + \frac{\vec{\nabla} p_i}{en_e} \right) - \left(\frac{1}{\sigma \mu^2 H^2} \right) \vec{\nabla} p . \quad (17)$$

A concentration gradient in an alloy will give rise to a corresponding free electron gradient¹⁷, which is analogous to a density or pressure gradient in an electron plasma ($\vec{\nabla} p$ in eqn. 17). The interaction of the magnetic field with the gradient results in a drift of the plasma transverse to the direction of the field. In the absence of electron-ion collisions, the motion of the plasma is perpendicular to both the magnetic field and the pressure gradient $\vec{\nabla} p$, while electron-ion collisions result in a "diffusion" flow component parallel to $\vec{\nabla} p$, the magnitude of which is given by the second term in equation (17).

It is not possible to compare the component of plasma flow velocity along the pressure gradient to normal diffusion velocities because of their essentially different natures. The pressure gradient in (17) is a result of the magnetic field itself ($\vec{\nabla} p$ vanishes as H vanishes), and the "diffusion"

is the flow of electrons and ions together (ambipolar diffusion), not motion of one species relative to another. This equation does, however, show the nature of the magnetic diffusion inhibition in the direction of the pressure or density gradient. Diffusion along the gradient is inversely proportional to both σ and H^2 , and becomes increasingly smaller as either H or σ is increased.

It is possible to obtain more quantitative equations relating to the currents and hence mass transfer, by considering the effect of the magnetic field on the diffusing electrons alone. In the non-steady state the effect of the field on the electrons compared to that on the ions will be in the order of the inverse ratio of their masses, approximately 10^5 . Therefore, the forces on the ions will be essentially electrical in nature, associated with the deviation from electrical neutrality as the ions tend to drift away from the electrons which are retarded by the Lorentz force in tending to make them gyrate about the lines of force. The Debye shielding distance, defined by (e in e.s.u.)

$$h_D = \left(\frac{kT}{4\pi n_e e^2} \right)^{1/2}, \quad (18)$$

is a measure of the extent to which the charge distribution (ref. 16, page 22) can deviate from the equilibrium distribution. For example, over a region ten times the thickness of the Debye shielding distance, the electron

density must be within one percent of the equilibrium value. If, for metals, it is assumed that the thermal energy of the electrons can be replaced by the Fermi energy, E_F , then the extent to which appreciable charge separation can occur is in the order of an angstrom unit or less than a lattice spacing. Since appreciable charge separation cannot normally occur, it is reasonable to assume that ion motion is controlled by electron motion and any effect of the magnetic field on the motion of the electrons will be transferred to the motion of the ions. Equations are therefore derived for the electron diffusion flux of the alloy in a magnetic field and it is assumed that the ion flux (chemical diffusion) will be affected similarly.

In the derivation of the electron flux equation it is assumed that the free electrons of the metal constitute a gas moving with velocity \vec{V} relative to an ionic gas velocity \vec{v} in a stationary magnetic field, \vec{H} . If the electrons lose an amount of momentum equivalent to $m_e^* \vec{V}$, during each electron-ion collision of frequency ν_e , then the drag force due to collisions is $-n_e m_e^* \vec{V} \nu_e$, where n_e is the electron density. The other operative forces are the electric field force, $n_e e (\vec{E}' + \mu \vec{V} \times \vec{H})$, where $\vec{E}' = (\vec{E} + \mu \vec{V} \times \vec{H})$, \vec{E} being an applied field, and the force due to the electron pressure gradient, $-\vec{\nabla} p_e$. Since the electron has negligible mass to accelerate, these forces are assumed in equilibrium; therefore (ref. 15, page 101),

$$\vec{\nabla} p_e + n_e e (\vec{E}' + \mu \vec{V} \times \vec{H}) + n_e m_e^* \vec{V} \nu_e = 0. \quad (19)$$

If the electron flux is given by $\vec{j}_e = -n_e e \vec{V}$, then by substituting $-\vec{j}_e/n_e e$ for \vec{V} and using the equation relations $\sigma = n_e e^2/m_e^* \nu_e$, and $\omega_{ce} = \mu e H/m_e^*$, equation (19) becomes

$$\sigma (\vec{E}' + \frac{1}{n_e e} \vec{\nabla} p_e) = \vec{j}_e + \frac{\omega_{ce}}{H \nu_e} \vec{j}_e \times \vec{H}. \quad (20)$$

For normal diffusion processes, the ionic velocity, \vec{V} , is extremely small and also no external field is applied; therefore $\vec{E}' \sim 0$. Solving equation (20) for \vec{j}_e by taking the cross product with \vec{H} , and setting $\vec{\nabla} p_e$ perpendicular to \vec{H} , i.e. $\vec{\nabla} p_e = \hat{i} \partial p_e / \partial x$,

$$\vec{j}_e = \frac{\sigma}{(1 + \omega_{ce}^2 / \nu_e^2)} \cdot \left[\frac{1}{n_e e} \hat{i} \frac{\partial p_e}{\partial x} - \frac{\omega_{ce}}{H n_e e \nu_e} \frac{\partial p_e}{\partial x} \times \vec{H} \right]. \quad (21)$$

The pressure gradient, $\partial p_e / \partial x$, is related to the chemical potential, which, for free electrons in metals, is equivalent to the Fermi energy, E_F . Therefore, $\partial p_e / \partial x$ in equation (21) can be replaced by $\partial E_F / \partial n_e \cdot \partial n_e / \partial x$ (for $\vec{\nabla} T = 0$). The electron flux parallel to the electron density gradient becomes

$$\vec{j}_{e_x} = \frac{\sigma}{(1 + \omega_{ce}^2 / \nu_e^2)} \cdot \left[\frac{1}{n_e e} \cdot \frac{\partial E_F}{\partial n_e} \cdot \frac{\partial n_e}{\partial x} \right], \quad (22)$$

and the flux perpendicular to the gradient becomes

$$\vec{j}_{ey} = \frac{\sigma}{(1 + \omega_{ce}^2 / \nu_e^2)} \cdot \frac{\omega_{ce}}{\nu_e} \cdot \left(\frac{1}{n_e} \cdot \frac{\partial E_F}{\partial n_e} \cdot \frac{\partial n_e}{\partial x} \right), \quad (23)$$

where the magnetic field is considered to be in the Z direction.

Equation (22) shows that the electron flux along the concentration gradient is reduced by the factor

$1 / (1 + \omega_{ce}^2 / \nu_e^2)$ due to the magnetic field, and since

the Debye distance is small (10^{-8} cm.) the ion current and

thus the chemical diffusion along the concentration gradient

is similarly reduced. Therefore, Fick's first law for

diffusion transverse to a magnetic field becomes

$$J_{\perp} = D_{\perp} \left(-\frac{\partial C}{\partial x} \right), \quad (24)$$

where the transverse diffusivity D_{\perp} is related to the normal diffusivity D by

$$D_{\perp} = \frac{D}{(1 + \omega_{ce}^2 / \nu_e^2)}. \quad (25)$$

Equation (25) shows that diffusion is inhibited by the factor $1 / (1 + \omega_{ce}^2 / \nu_e^2)$, and is independent of both diffusion velocity and electron gradient as long as a small but finite gradient does exist (again a consequence of the very short Debye shielding distance).

Equation (23) gives the magnitude of the electron

flux (Hall flux) transverse to the concentration gradient. There is, however, no corresponding ion current in the Hall direction since the electron density distribution is not altered by the Hall flux. The medium here is assumed infinite so charge accumulation (Hall field) against surfaces cannot occur. In finite samples, where bounding surfaces are present, the Hall currents must close to prevent charge accumulation and the resultant Hall potential, as the Hall field will cancel (to the first order) the Lorentz force on the electron. However, even for the latter case an effect of the magnetic field remains, due to the component of transverse magnetoresistance arising from the non-spherical symmetry of the Fermi surface¹⁸. For most metals this effect is small even at extremely low temperatures and becomes vanishingly small as room temperature is approached¹⁹.

Youdelis et al⁶ have shown that a magnetic field of 30,000 oersteds decreases the diffusivity of copper in dilute aluminum-copper alloys by about 25% (see Fig. 3). This is in good agreement with the theoretical result obtained from equation (25) providing $\nu_e = 10^{12}$ and $m_e^* = m_e$. From conductivity data, assuming a semi-classical model for electron transport, the collision frequency for the electron is calculated to be in the range $10^{12} - 10^{14}$ per second²⁰. The collision frequency is in fact, a function of the wave vector \vec{k} , and it is assumed that a collision frequency spectrum exists for the electrons in a metal. Therefore, it is a reasonable assumption that at least

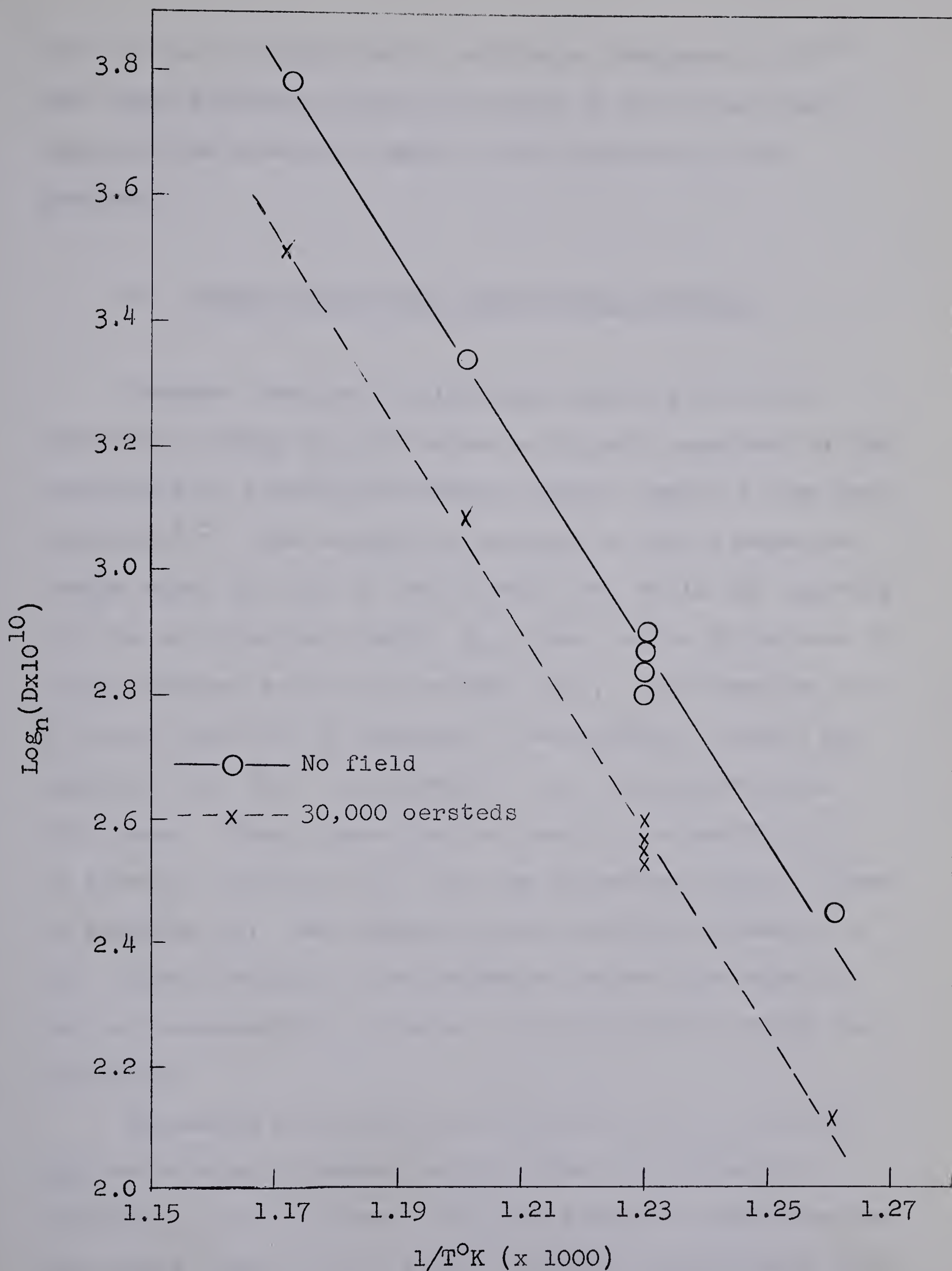


Figure 3. Variation of field and no-field interdiffusion coefficients with temperature in the Al(rich)-Cu system. (After Youdelis et al⁶)

some of the electrons have a collision frequency of 10^{12} and these electrons control the rate of diffusion since they are the slowest to move in the direction of the gradient.

4. Plasma Oscillation and Charge Screening

Current theories of diffusion indicate that the activation energy for diffusion is largely comprised of the electrostatic interaction energy between impurity ions and vacancies^{1,5}. The vacancy is assumed to have a negative charge equal to that of the solvent ion, while the impurity ion has an effective charge, Z_e , equal to the difference in charge between solute and solvent ions, and therefore can be either positive or negative. The potential around the impurity ion, $V(r)$, at distance r , as calculated using the Thomas - Fermi approximation (see Alfred and March³) is given by equation (7); with the screening constant given by equation (4). Any change in the screening parameter q will cause a change in the potential around the impurity ion and consequently a change in the activation energy for diffusion.

Screening and organized oscillations of an electron gas are related phenomena arising from the collective behavior of the electrons. The oscillation of the electron gas arises from the long range Coulombic force between the electrons. If for some reason a non-equilibrium charge

distribution (defect) appears in the electron gas, the whole gas contracts or expands collectively in an attempt to smooth out the charge distribution. In doing so it will over-correct causing an opposite polarization and a regular oscillation of the gas will set in. Ziman (ref. 18, page 161) has shown that the electron gas (plasma) oscillation frequency is given by (e in e.s.u.)

$$\omega_p = \left(\frac{4\pi n_e e^2}{m_e^*} \right)^{1/2}, \quad (26)$$

which is $\sim 10^{16}$ /second for the ordinary electron densities in metals. Actually, the plasma frequency is a function of the wave number k , the two being related through the plasma dispersion relation. Bohm and Pines²¹ have shown that there is a maximum wave number for a collective mode (corresponding to a minimum wave length) beyond which collective interaction ceases. The critical wave number, k_c , is shown to be of the same order of magnitude as the screening parameter q in equation (4). Thus, screening is a collective electron interaction phenomenon and the screening parameter relates to the minimum wavelength possible for this collective interaction. For a classical (non-degenerate) plasma, the critical wave number is the reciprocal of the Debye distance²¹.

Comparing equations (4) and (26), the screening parameter and the plasma frequency are related thus:

$$q = \omega \left(\frac{m_e^*}{n_e} N(E_F) \right)^{1/2}. \quad (27)$$

Therefore, any change in the plasma frequency due to a magnetic field will result in a corresponding change in q , which in turn will be reflected in the activation energy for diffusion. The effect of a magnetic field on the plasma oscillation frequency and screening has been studied for the case of a non-degenerate electron gas, as approximated by the charge carriers in semi-conductors. Bonch - Bruevich and Mironov²² have shown that the screening parameter is increased by a magnetic field for distances $\gg h_D$, while for distances $\ll h_D$ the parameter is increased. Using the equations developed by Bonch - Bruevich and Mironov, it can be shown that a magnetic field of strength 10^5 oersteds changes the screening factor (e.g. for germanium) by less than 1% for distances $1A^0$ (interatomic distance). This change will have negligible effect on the potential, $V(r)$, surrounding an impurity ion, and therefore will have an equally negligible effect on the activation energy for diffusion.

The arguments presented above show that a magnetic field of moderate strength has negligible effect upon screening in a non-degenerate plasma (e.g. semi-conductors), but a fully degenerate plasma more closely approximates the electrons in a metal. Therefore, these arguments have been extended by Youdelis et al⁶ to show that a magnetic

field of moderate strength has negligible effect on screening in a fully degenerate plasma and thus has negligible effect on screening in metals.

The screening parameter is related to the plasma frequency, ω , and the density of energy levels, $N(E_F)$, by equation (27). A magnetic field does not alter the average density of energy levels though it does alter their detailed distribution. Any change in the detailed distribution will however, affect the plasma frequency and therefore must be taken into account when studying the effect of a magnetic field on ω .

Stephen²³ has shown that the plasma frequency parallel to the magnetic field in a degenerate electron gas is given by

$$\omega_{\parallel}^2 = \omega_p^2 + \frac{6k^2 E_F}{5 m_e^*} \left\{ 1 + \frac{5}{16} \left[\left(\frac{h\omega_{ce}}{2\pi E_F} \right)^2 - \frac{1}{3} \left(\frac{h\omega_{ce}}{2\pi E_F} \right)^2 \right] \right\}, \quad (28)$$

where ω_p is defined by equation (26), and h is Planck's constant. The effect of the magnetic field is located in the terms in the square brackets, the first being due to electron spin and the second to orbital motion. Using the Fermi energy for silver and an effective mass of the electron equivalent to the ordinary mass, the term $(h\omega_{ce}/2\pi E_F)^2$ becomes significant only at fields of $10^7 - 10^8$ oersteds. It is therefore concluded that a magnetic field of ordinary strengths has no effect on parallel oscillations.

The case of oscillation perpendicular to the magnetic field is complicated by the occurrence of gaps in the frequency spectrum²⁴ which occur at multiples of the cyclotron frequency and are comparable to the forbidden energy bands for electrons in a solid. Wave propagation in a plasma perpendicular to a magnetic field is thus, in some aspects similar to the propagation of an electron wave on a solid, in that there exist gaps at selective frequency (energy) intervals for which no wave propagation is possible. For the electron densities in metals, the frequency gaps are small and have negligible effect on the average frequency distribution spectrum. Stephen gives for the oscillation frequency perpendicular to the field,

$$\omega_{\perp}^2 = \omega_p^2 + \omega_{ce}^2 + \left\{ \frac{6k^2 E_F}{5 m_e^*} \cdot \frac{\omega_p^2}{\omega_p^2 - 3\omega_{ce}^2} \right\} \quad (29)$$

$$\times \left\{ 1 + \frac{5}{16} \left[\left(\frac{h\omega_{ce}}{2\pi E_F} \right)^2 + \frac{2}{3} \left(\frac{h\omega_{ce}}{2\pi E_F} \right)^2 \right] \right\},$$

The important factor in equation (29) is the cyclotron frequency, ω_{ce} , as we have previously shown that $(h\omega_{ce}/2\pi E_F)^2 \ll 1$ for field strengths of 10^7 or less, and therefore the term in the square brackets can be neglected. An approximate calculation shows that for a field strength of 30,000 oersteds, $\omega_{ce} \sim 10^{12}$, which is also negligible compared to the basic plasma frequency, $\omega_p = 10^{16}$, (c.f. eqn. 26).

In the preceding discussion it was shown that a magnetic field of moderate strength does not appreciably change the thermodynamics or the charge screening of a solid metal diffusion system. The above considerations require that the effect of the magnetic field is via the plasma-magnetohydrodynamic forces as expressed through the change in chemical diffusivity in equation (25), and is a change manifested through the frequency factor, D_0 , not the activation energy, Q , in the Arrhenius equation $D = D_0 e^{-Q/RT}$.

E. THE MAGNETIC DIFFUSION EFFECT IN FERROMAGNETIC METALS AND ALLOYS

The magnetic diffusion effect observed in ferromagnetic materials relates to the discontinuity in the $\log D$ versus $1/T$ plots in the vicinity of the Curie temperature. A number of investigations on iron and cobalt and their alloys show that the diffusivity below the Curie temperature is lower than that expected from an extrapolation of diffusivities obtained at temperatures above the Curie temperature (see Fig. 4).

The "abnormal" decrease in diffusivity is associated with the onset of ferromagnetism on crossing the Curie temperature and was first noticed by Birchenall²⁵ in 1958, but the accuracy of the diffusion measurements did not permit a conclusive determination of the effect. Later, Borg and Birchenall²⁶ determined accurately the self diffusion

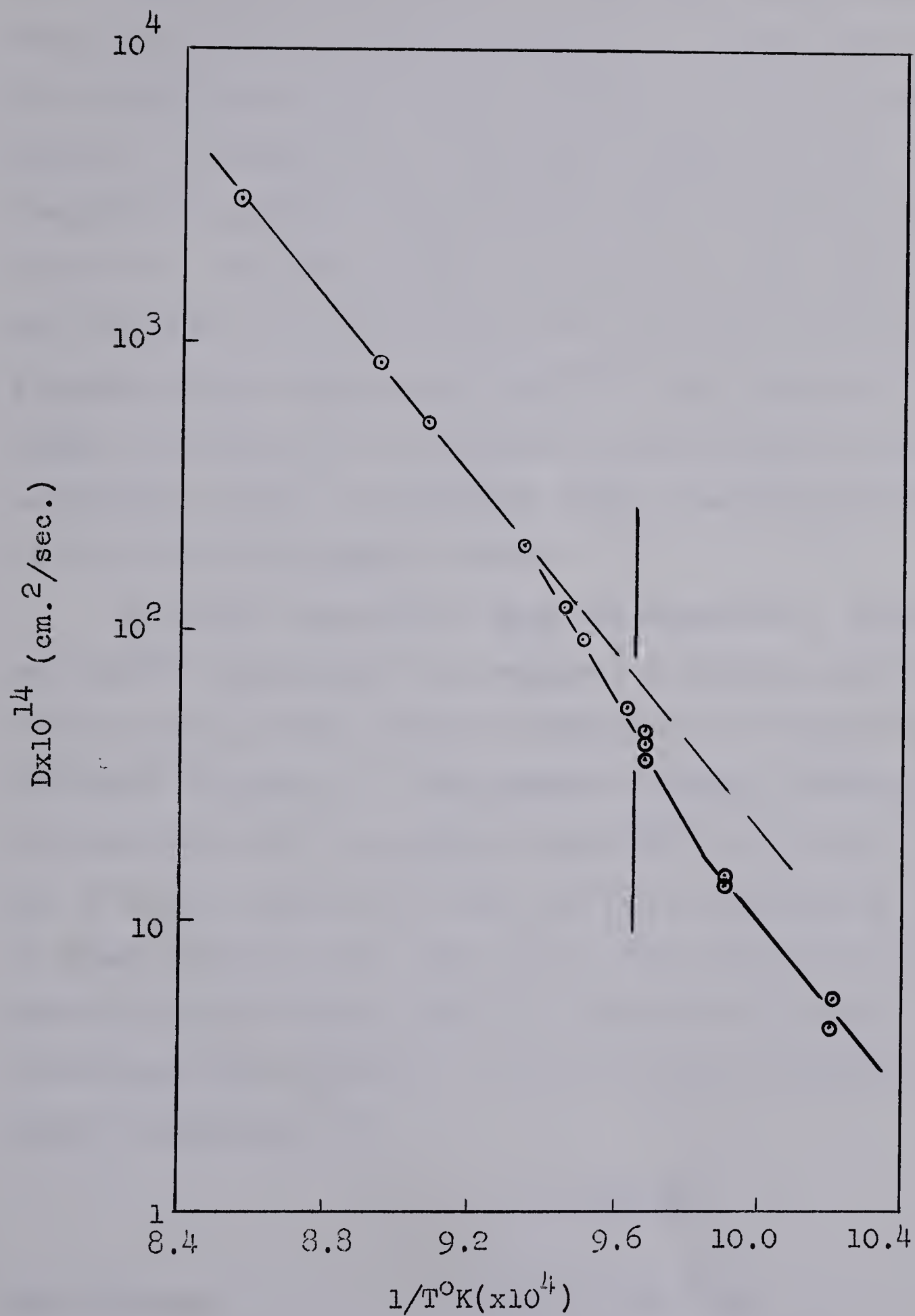


Figure 4. The magnetic diffusion effect in alpha-iron.
(After Borg and Birchenall²⁶)

coefficients for Fe in alpha iron both above and below the Curie temperature (c.f. Fig. 4), but these results were still not accurate enough to determine whether the decrease in diffusivity was due to an increase in the activation energy, a decrease in the frequency factor, or both. A theoretical argument indicated that the decreased diffusivity is due to a decreased number of vacancies which results from the increase in binding energy with the onset of 3d spin alignment (about 2000 cal./mole)²⁶. This decrease in the number of vacancies is reflected by an increase in the activation energy for diffusion with a resulting decrease in D in the ferromagnetic state.

Following the work by Borg and Birchenall, Stanley and Wert²⁷ investigated the magnetic diffusion effect in iron-vanadium alloys using a combination of tracer and anelastic techniques. The purpose of adding vanadium was to raise the Curie temperature some 60°C in an effort to get a larger temperature range below the Curie point in which to study diffusion and thus obtain more accurate results. Stanley and Wert established that for an iron alloy containing 18% vanadium, diffusion in the paramagnetic state is described by

$$D = 3.9 \cdot e^{-58,500/RT} ,$$

and diffusion in the ferromagnetic state by

$$D = 0.25 \cdot e^{-61,900/RT} .$$

The decrease in D_0 by a factor of over 10, and the increase in Q (3,400 calories) result in a diffusivity in the ferromagnetic state just below the transition temperature of 1/100 of that expected from an extrapolation from values in the paramagnetic state. Stanley and Wert do not state whether the increase in activation energy is due to an increase in the formation energy for vacancies, an increase in motional energy, or both. The decrease in the frequency factor, D_0 , is attributed to a decrease in the entropy of motion of the vacancies. If the increase in the free energy of a lattice due to the strain of a diffusing atom is given by

$$\Delta F = 1/2 \mu \epsilon^2$$

where μ is the shear modulus and ϵ the total strain, then the free energy change is a linear function of μ . Therefore, the entropy change and thus the frequency factor is a function of the temperature derivative of the shear modulus. There is some evidence that $d\mu/dT$ does increase as the temperature decreases below the Curie temperature, but Stanley and Wert admit that the increase in $d\mu/dT$ is not sufficient to cause a ten-fold decrease in the frequency factor, D_0 , even though the sign of the change is correct.

A few comments on the work of Stanley and Wert are in order. First, the diffusion coefficients in the paramagnetic state were determined by tracer methods and those in the ferromagnetic region were obtained by anelastic methods. It is generally accepted that diffusion results

obtained by the same methods are comparable, but diffusion results obtained by independent methods may differ appreciably either because of inherent experimental technique errors or conceptual difficulties in relating diffusion data to theory. Stanley and Wert's comparison of activation energies for the two states may be quite valid; however, the accuracy of $\pm 30\%$ claimed for the frequency factors and the 1000% decrease in D_0 is somewhat suspect. Also, in the anelastic technique a 100 oersted magnetic field was used to suppress enormous magneto-elastic damping of the Zener relaxation peaks. This applied field was sufficient to saturate the alloy giving a magnetic induction in the alloy of over 20,000 gauss. Therefore, some of the decrease in D_0 may have been a result of the magnetic diffusion inhibition effect found by Youdelis et al⁶.

At about the same time that the work of Stanley and Wert appeared, Buffington et al²⁸ published their results on the investigation of self diffusion in iron, and Hirano et al²⁹ on the diffusion of nickel in iron. Buffington et al used radioactive tracer techniques to determine the self diffusion coefficients of iron at temperatures for 700°C to 905°C and confirmed the earlier work of Borg and Birchenall²⁶, that the diffusivity in the ferromagnetic state is about three times lower than that expected from an extrapolation of the values in the paramagnetic state. They found that for the paramagnetic state

$$D = 1.9 e^{-57,200/RT} ,$$

and for the ferromagnetic state,

$$D = 2.0 e^{-60,000/RT} ,$$

where the values in the transition region between 750°C and 790°C have been excluded. As is the case in the previous investigations, the errors of $\pm 2\%$ in the activation energies and $\pm 25\%$ in the frequency factors are too large to establish (with any confidence) whether the effect is through an increase in activation energy or a decrease in frequency factor so a plausible theoretic case was presented in which the decrease in diffusivity is ascribed to an increase in the energy required to form a vacancy in the ferromagnetic state. It was pointed out by Hume - Rothery³⁰ that the results of Buffington et al appear to be in error in that the plot of $\log D$ versus $1/T$ (Fig. 2, ref. 28) ignored one particular point in the ferromagnetic region. As only four results were obtained for this region, Hume - Rothery contends that had this particular result been included, the activation energy for the ferromagnetic state would be identical with that for the paramagnetic state, and that the decrease in diffusivity is due to a decrease in frequency factor rather than an increase in activation energy. However, if one analyzes the data of Buffington et al (Table 2, ref. 28) using linear regression theory, one finds that the frequency factor and activation energy they report is computationally correct. Therefore, there is some support for the theory contending that an increase in activation energy is

responsible for the decreased diffusivity in ferromagnetic iron even though the difference in activation energies between the para and ferromagnetic regions is not statistically significant.

In support of the activation energy increase theory, Buffington et al²⁸ state that if the decrease in diffusivity were attributed solely to a decrease in frequency factor, then the latter would have to be lowered by three or four orders of magnitude and the corresponding changes that would occur in vibrational frequency, lattice spacing, and activation entropy are highly unlikely. However, a simple calculation shows that, assuming no change in activation energy between the two states, the diffusivity in the ferromagnetic state can be represented by

$$D = 0.42 e^{-57,200/RT}$$

compared to

$$D = 1.9 e^{-57,200/RT}$$

for the paramagnetic state. The frequency factor is therefore decreased only by a factor of 5, and a decrease in D_0 cannot be entirely ruled out.

In 1961, Hirano et al²⁹ reported that the diffusion coefficient of nickel in the ferromagnetic state is less than that expected from an extrapolation of values obtained for the paramagnetic state. They determined that for the paramagnetic state

$$D = 1.3 e^{-56,000/RT} ,$$

and for the ferromagnetic state,

$$D = 1.4 e^{-58,700/RT} .$$

The decreased diffusivity was again attributed to an increase in the energy of formation of vacancies in the ferromagnetic state. In 1962 Hirano et al³¹ reported their results on the diffusion of Co and Ni in Co and Co-Ni alloys. They reported a magnetic diffusion effect similar in magnitude to that reported for Fe and Fe alloys. Using a conventional radioactive tracer technique they determined the self diffusivity of Co in the paramagnetic state to be

$$D = 0.17 e^{-62,200/RT} ,$$

and for the ferromagnetic state,

$$D = 0.50 e^{-65,400/RT} .$$

Their results for the diffusivities of Co and Ni in Co alloys up to 51% Ni are similar, showing an increase in frequency factor of 50-100% and an increase in activation energy of 1000-3000 calories upon entering the ferromagnetic state. (The increase in activation energy is sufficient to offset the increase in frequency factor.) The increase in D_0 combined with the increase in activation energy makes it rather difficult to ascertain the magnetic diffusion effect in the low-nickel alloys, although the effect is obvious in the higher nickel alloys (30% and 51% Ni). Borg³² has

re-analyzed the data of Hirano et al³¹ and has stated that "the complete absence of the magnetic effect is obvious" in the alloys up to 20% Ni. A careful plot of the data shows that Borg's criticism is justified for the results in pure cobalt, but appears somewhat doubtful for the alloys containing 10% and 20% Ni.

Hirano et al attribute the magnetic diffusion effect to the additional energy required to form a vacancy in the ferromagnetic state. This additional energy arises from the interaction of electron spin with the Weiss field and is in the order of the thermal energy of an electron at the Curie temperature, i.e. kT_c . It is obvious that this value is about 2000 cal./mole and agrees with the diffusion results, both in magnitude and direction. Borg, however, criticizes this theory, maintaining that the increase in vacancy formation energy is not sufficient to account for the decrease in diffusivity. He proposes an alternate theory based on the influence of ferromagnetism on the elastic constants, but this theory has not appeared in print to date.

In regard to the magnetic diffusion effect in cobalt, a very important factor seems to have been overlooked. Colton³³ has pointed out that there is considerable evidence indicating a phase transformation (f.c.c. to h.c.p.) at or near the Curie temperature in cobalt^{34,35}. This transformation could mask the magnetic diffusion effect and could possibly account for the anomalously high frequency factors reported for the ferromagnetic state.

Borg and Lai³⁶, in an effort to shed more light on the problem of the magnetic effect, studied the self diffusion of Au, Co, and Ni in paramagnetic and ferromagnetic α -iron. These elements were chosen for their different magnetic moments, which should have some influence on the free energy of motion of the vacancies. The magnetic effect was again obvious for the diffusion of these three elements, but the magnetic moment had no effect, as the magnitude of the magnetic diffusion effect was similar for all three. Due to the limited number of observations, Borg and Lai do not calculate frequency factors or activation energies for the ferromagnetic state for comparison with values obtained in the paramagnetic state. They do, however, state that the effect is too large to be accounted for by the decreased vacancy hypothesis and suggest that a change in vacancy mobility is responsible, the theory of which was to be discussed in a forthcoming publication. (This publication has not yet appeared in print.)

To increase the temperature range for studying diffusion in paramagnetic iron, Borg et al³⁷ studied the self diffusion of Fe and Co in delta iron (δ -Fe is b.c.c. and its properties are assumed to extrapolate from the α phase). They report that the diffusivity of Fe in δ -Fe is given by

$$D = 1.9 e^{-57,000/RT} .$$

They compare this to the equation determined by Borg and Birchenall²⁶ for diffusion of Fe in α Fe, namely

$$D = 118 e^{-67,200/RT} .$$

Borg et al state that the remarkable differences in D_0 and Q between the two phases, (α and δ iron) are the most important consequence of the investigation. They seem to have ignored the work of Buffington et al²⁸ who obtained for self diffusion of Fe in paramagnetic α iron,

$$D = 1.9 e^{-57,200/RT} ,$$

which may be considered identical to the result for δ iron considering the accuracy of diffusion work. Also, Buffington et al report one value for diffusion in δ iron which agrees well with values obtained by Borg et al. In view of this it seems possible that the "remarkable differences" of D_0 and Q between α and δ iron as reported by Borg et al are a consequence of insufficient accuracy of results.

In conclusion, there is no doubt concerning the existence of the magnetic diffusion effect in ferromagnetic systems. The diffusivities of Fe, Au, Co, and Ni in Fe in the ferromagnetic state are less by a factor of at least three than that expected from extrapolations of values obtained in the paramagnetic state. While the decrease itself is statistically significant, the results are not sufficiently accurate to determine experimentally whether the decrease in diffusivity is due to an increase in activation energy or a decrease in the frequency factor, though most investigators tend to support the activation

energy increase theory. While it is true that each individual experiment is not accurate enough to attribute the magnetic effect to either the activation energy or the frequency factor, almost all the investigations show an increase in activation energy for the ferromagnetic state. This fact tends to lend some weight to the activation energy increase theory, and therefore, at least part of the magnetic effect is likely due to the resultant decrease in the number of vacancies. Hume - Rothery³⁰ and Borg³² tend to support a theory proposing a decrease in the frequency factor, but to attribute the entire magnetic diffusion effect to this decrease appears somewhat presumptuous in view of the evidence to the contrary.

EXPERIMENTAL METHODS

A. PREPARATION OF ALLOYS

1. δ and $\delta + \theta$ Brass

These alloys were prepared from high purity zinc (99.999%) obtained from the Consolidated Mining and Smelting Co. of Canada, Ltd., and high purity copper (99.999%) obtained from Johnson, Matthey and Co., Ltd., (A detailed analysis of these materials is given in Appendix I). The zinc was supplied in 1" square bars 8" long which were cut to facilitate handling, washed thoroughly with soap and water and then cleaned in concentrated H Cl. The copper was supplied in 0.25" diameter bars 5" long, from which smaller pieces were cut with a hacksaw and cleaned in H NO₃. The alloys were prepared in 350 gram lots by first melting the freshly cleaned zinc and then adding the proper amount of copper. High purity graphite molds were used to contain the alloy which was melted in an open electric muffle furnace. It was necessary to add the copper in small amounts starting at a melt temperature of 500°C and increasing the temperature about 50°-100°C after each addition. Using this procedure, the temperature of the melt was never more than 50°-100°C above the liquidus temperature of the alloy, this precaution being necessary to prevent vaporization and oxidation of the highly volatile zinc in the alloy. After the copper

had been dissolved the alloy was stirred vigorously with a graphite rod three times, the alloy being re-heated after each stirring to prevent solidification. Ingots 0.8" in diameter and 5" long were cast from a bottom pour mold into a pre-heated graphite mold mounted on a steel baseplate. By impinging water onto the baseplate, the ingots were solidified unidirectionally to obtain a predictable solute distribution³⁸. After solidification, 1" was cropped from each end of the ingot, thus removing the most severely segregated regions; the remainder was annealed at a temperature of 500°C (650°C for the two phase $\gamma + \beta$ alloy) for seven days to eliminate interdendritic micro-segregation. Sections from the ingots were removed, examined metallographically and analyzed chemically to insure that the alloy was of the proper composition and homogeneity.

Considerable caution was required in handling and cutting the γ -brass ingots because of their extreme brittleness. This was done using a Servomet sparkcutter, supplied by Metals Research Ltd., Cambridge, England, as it was impossible to machine or cut the ingots by conventional means.

2. Silver-Copper Alloys

These alloys were prepared from high purity silver (99.999%) obtained from the Consolidated Mining and Smelting Co. of Canada, Ltd., and high purity copper (99.999%)

obtained from J. Light and Co, Colnbrook, England. (A detailed analysis of these materials is given in Appendix I.) The silver was supplied in the form of clean shot which was ready for melting. The copper was supplied in rod form, 0.20" in diameter and 5" long, from which pieces of appropriate weight were cut and then cleaned in an aqueous solution of HNO_3 . The alloys were prepared in 450 gram lots by first melting the silver then adding the copper in the form of freshly cleaned pellets. High purity graphite crucibles were used to contain the melts in an open electric muffle furnace. When the copper was completely dissolved, the alloy was thoroughly mixed by pouring back and forth between crucibles a total of nine times. (The alloy was poured back and forth three times on each of three occasions, being reheated between mixings to prevent solidification and the accompanying segregation.) An alloy ingot 0.8" in diameter and 5" long was cast and solidified in the same manner as the brass ingots. One inch was cropped from each end of the alloy ingot where segregation was greatest, and the remainder was hot worked to remove any porosity due to gas evolution during solidification. After hot working, the ingot was machined to remove surface contamination and then given a homogenization anneal at 800°C for seven days to eliminate interdendritic segregation. Before making disks for diffusion couples the surface was again machined to remove any contamination picked up during the homogenization anneal.

3. Preparation of Silver

The silver was supplied in shot form and it was therefore necessary to melt and cast ingots from which disks for diffusion couples could be machined. Initially, diffusion couples were made using silver disks machined from ingots which had been melted and cast in air. However, during the diffusion anneal, oxygen dissolved in the silver diffused into the silver-copper alloy forming a Ag-Cu-O compound, which precipitated throughout the diffusion zone making it impossible to establish accurate concentration-penetration curves (see Fig. 5*). Therefore, to prevent oxygen absorption by the silver during preparation of the ingots it was necessary to melt the silver shot and solidify the ingot in a vacuum. The silver shot was contained in a graphite crucible, 0.8" in diameter and 6" long and was melted in a dynamic vacuum of 10^{-3} mm. of mercury. The molten silver was held in the vacuum at a temperature of 1050°C for one hour and then was solidified unidirectionally by removing the crucible from the furnace at a rate of 10" per hour. When the silver was prepared in the above manner, no problems with oxide precipitation were encountered.

- - - - -

* Figure 5 is actually an extreme case of precipitation as the alloy shown contains 6% copper compared to 1% used in most of the experiments.

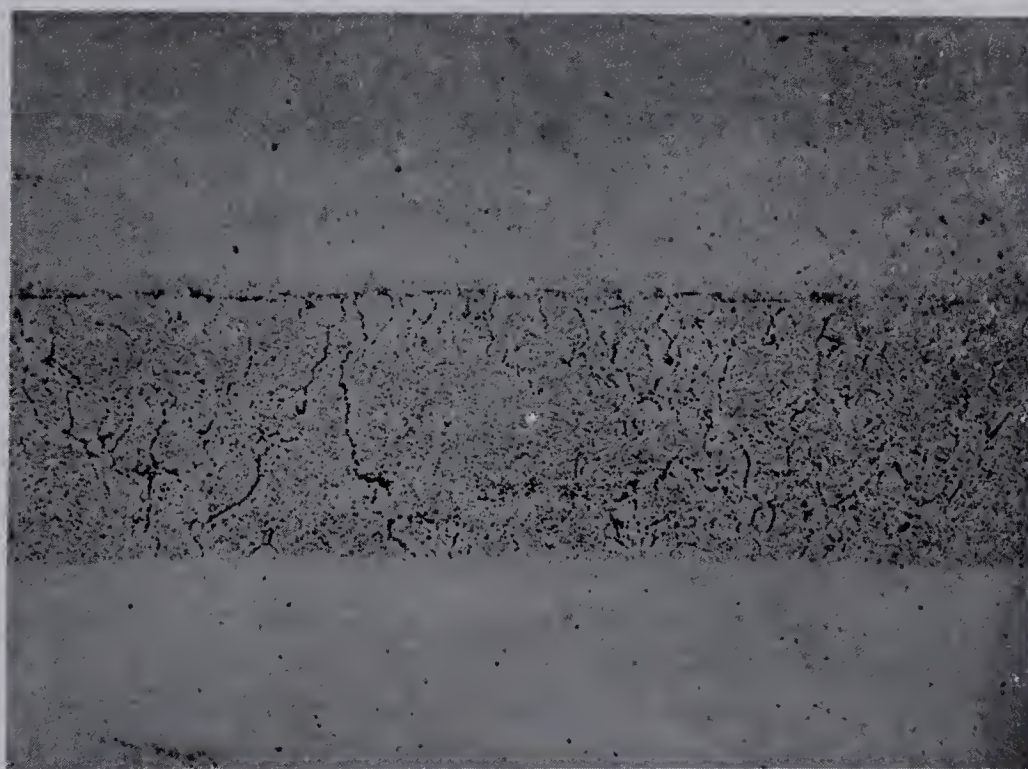


Figure 5. Precipitation of a silver-copper-oxygen compound in the diffusion zone. X70.

The copper alloy showed no evidence of the Ag-Cu-O precipitate even though it was prepared in air. The precipitate formed during melting but remained on the surface of the melt as slag.

B. PREPARATION OF DIFFUSION COUPLES

1. δ -Brass Diffusion Couples

A circular disk 0.75" in diameter and 0.25" long was cut from each of the homogenized δ and $\delta + \beta$ brass ingots using the Servomet sparkcutter. The faces of the disk were planed parallel and as smooth as possible with the planing attachment for the sparkcutter. One face of each disk was then polished, starting with 600 grit paper and finishing with "Linde B", .05 micron abrasive. After polishing, the disks were thoroughly cleaned with soap and water, dried with acetone, then immediately placed in the steel mold shown in Figure 6. (After cleaning and drying, the disks were handled only with tongs or rubber gloves to prevent contamination of the surface.) The mold was flushed with argon before the top end piece was inserted. When the mold was assembled it was placed in an induction heating coil and clamped with just sufficient pressure to hold the assembly together. Power was supplied to the induction unit at a rate sufficient to reach the welding temperature in five minutes. The welding temperature of 500°C was maintained

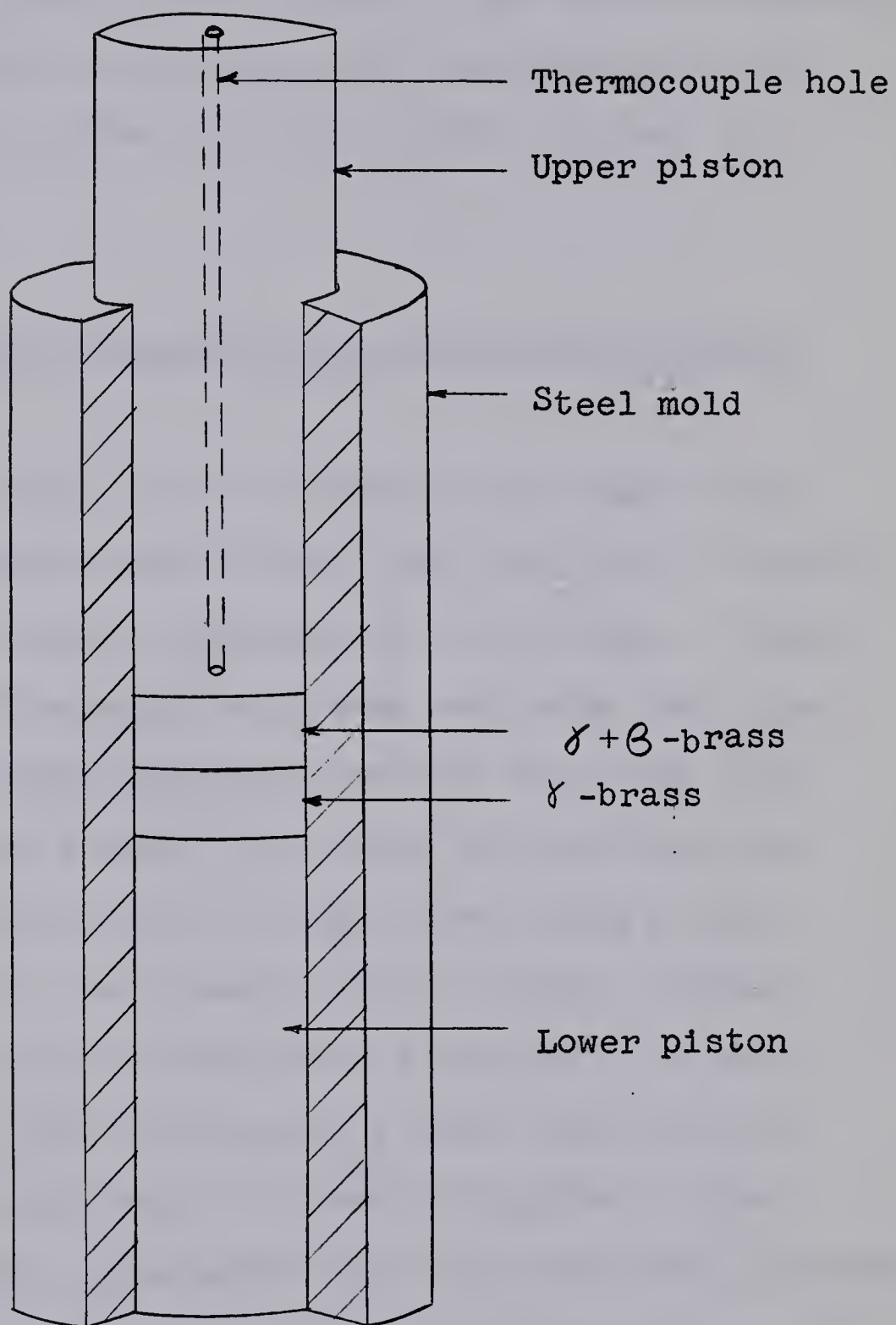


Figure 6. Welding mold for γ -brass diffusion couples.

for fifteen minutes after which the induction unit was shut off and the mold allowed to cool slowly. The welded composite was then removed from the mold and cut longitudinally for two diffusion couple halves, one for a field run and one for a no-field run.

2. Silver-Silver Copper Sandwich Diffusion Couples

Two circular disks 0.75" in diameter and 0.25" long were cut from the vacuum-cast silver ingot and one of similar dimensions was cut from the homogenized alloy ingot. These disks were cleaned thoroughly with soap and water and dried with acetone after which they were handled only with clean metal tongs or rubber gloves. The faces of the disks were machined on a precision lathe at high speed using a very sharp tool to obtain a very smooth, shiny finish. After machining, the disks were immediately assembled in a small steel capsule with tight fitting end pieces, which was in turn placed in the steel mold as shown in Figure 7. The mold was flushed with argon before the end pieces were inserted. It was then placed in an induction coil and clamped securely with a heavy steel clamp. The assembly was heated to the welding temperature of 720°C which was maintained for fifteen minutes. The pressure reached during welding due to the expansion of the diffusion couple against the steel restraining clamp was sufficient to extrude the silver. After welding, the mold was removed from the induction unit

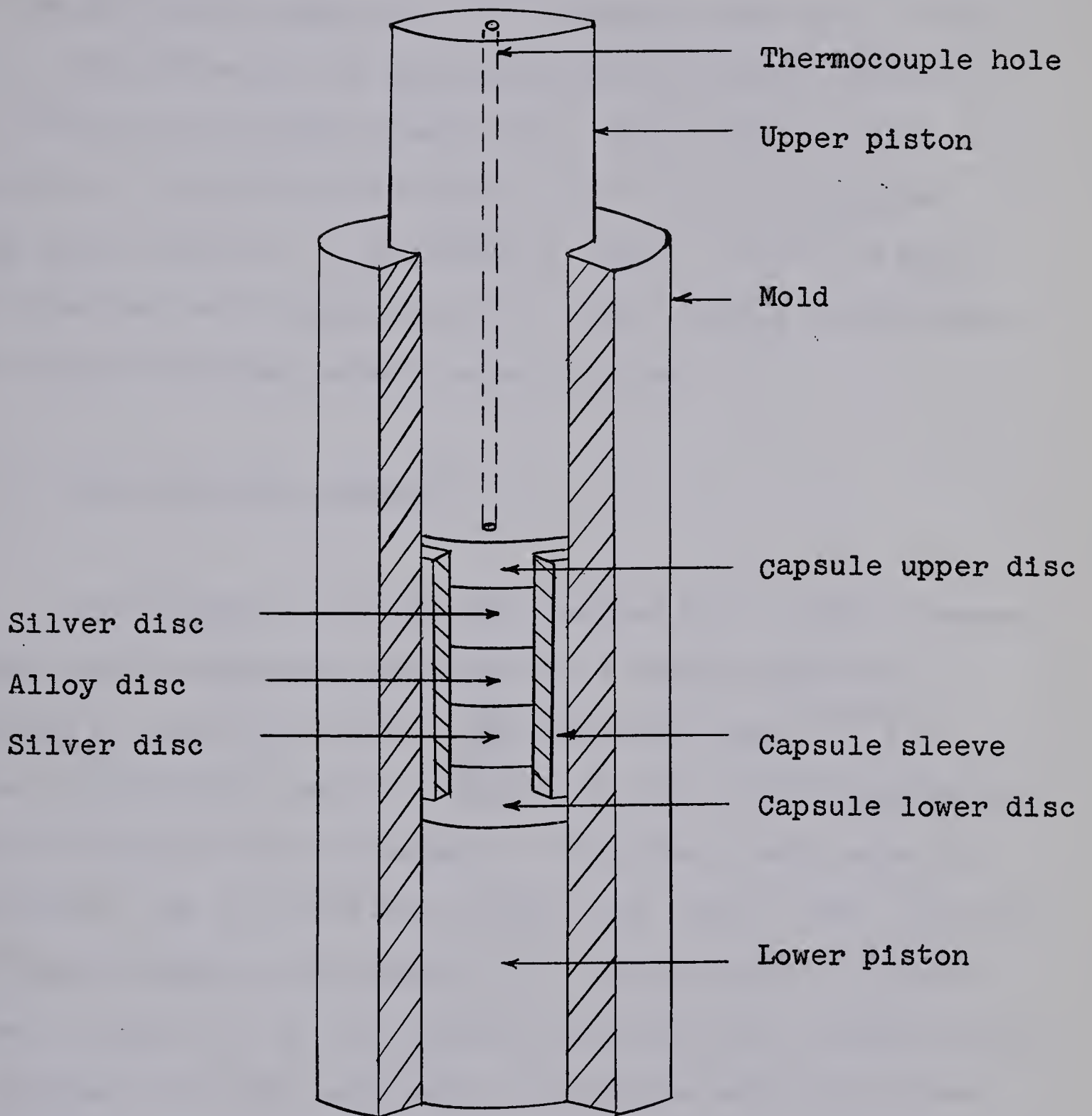


Figure 7. Welding assembly for silver-copper diffusion couples.

and quenched in water. The capsule was forced from the mold, and the steel casing of the capsule was machined free of the diffusion composite. The composite was then cut in two, longitudinally, to make duplicate diffusion couples for field and no-field experiments. Each couple, after mechanical polishing and etching with a freshly prepared $\text{NaCN-H}_2\text{O}_2$ solution, (3 gm. NaCN in 100 ml. 30 vol. % H_2O_2) was examined metallographically for any defects in the weld. Any couples showing defects were rejected.

C. THE DIFFUSION ANNEALS

The diffusion anneals were carried out in tube furnaces under argon atmosphere and controlled temperatures for periods of time (calculated from published data^{10,12}) to give a reasonable length of diffusion zone without requiring unduly long runs on the magnet. All anneals were made in duplicate, one with and one without the field. The δ -brass diffusion couples were wrapped in aluminum foil to prevent direct contact of the diffusion couple with the furnace walls. No suitable foil was available in which to wrap the silver-copper diffusion couples so they were wired to two thermocouple insulators to prevent direct contact of the couple with the furnace tube. Before starting a run the furnace was flushed with argon at a rapid rate for ten minutes and continued at a reduced rate during the heating up period. During the annealing the argon pressure in the furnace was

maintained at a few inches of mercury. For runs lasting longer than twenty-four hours, the furnace was flushed with argon for a few minutes every day.

The small amount of space between the pole pieces of the magnet (1.5") necessitated the construction of tube furnaces which would reach 800°C with very little insulation. The tube furnace shown in Figure 8 consisted of mullite tubing, 1.25" I.D. and 18" long, with a Kanthal A heating element ribbon wound uniformly around the central nine inches. The ribbon was wound directly on the mullite tube and the furnace was then insulated by wrapping with asbestos tape and coating with asbestos furnace cement. The two furnaces constructed in this manner were used without failure for more than eight hundred hours at temperatures ranging from 500°C - 800°C. Firebrick plugs placed at each end of the hot-zone in the furnace served to reduce the temperature gradients along the length of the furnace. The temperature distribution, obtained by advancing a thermocouple embedded in a block of silver along the length of furnace, showed that the central two inches of the furnace in which the diffusion couples were located was uniform to $\pm 2^{\circ}\text{C}$.

The furnace temperature was controlled by a Thermo Electronic Model 80025, on-off controller, which controlled the "high-low" power supply to the furnace. The controller is a potentiometric type instrument which uses a chromel-alumel thermocouple as a sensing element, and is sensitive

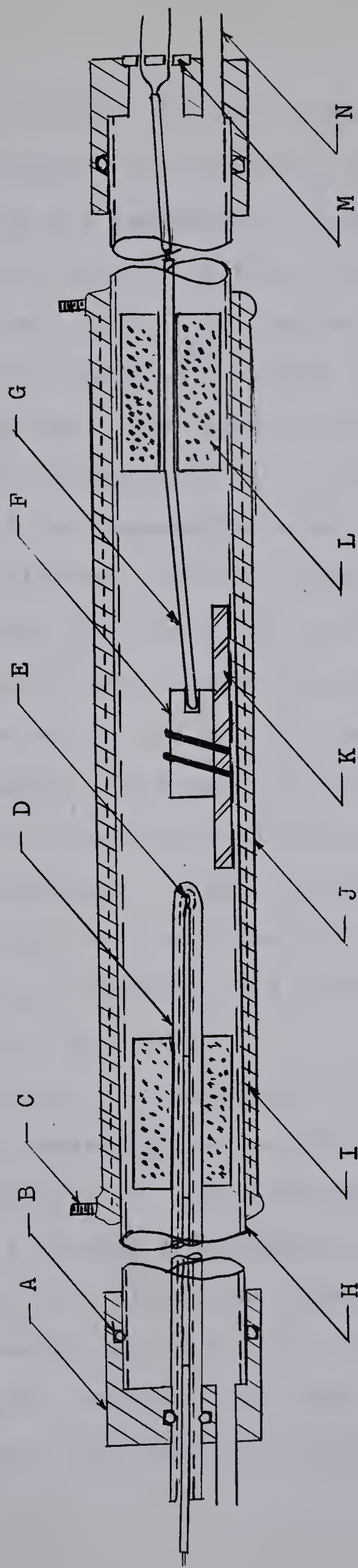


Figure 8. Furnace used for the diffusion anneals. A, brass end piece; B, 'o'-ring seal; C, terminal; D, control thermocouple shield (alumina tube); E, control thermocouple; F, sample wired to insulators; G, measuring thermocouple; H, mullite tube; I, Kanthal A winding; J, insulation; K, thermocouple insulators; L, porous plug; M, Stupakoff insulator; N, gas inlet.

to a change of 0.03°C . During a diffusion experiment the sensing thermocouple was enclosed in a heavy alumina tube (c.f. Fig. 8) so the temperature of the sensing thermocouple did not change as rapidly as that of the diffusion couple. This resulted in a cyclic fluctuation of the temperature of the diffusion couple in the order of 0.5°C .

The "high-low" power supply consisted essentially of two variable transformers and a relay. One transformer was set to hold the temperature about 15°C above the set temperature, while the other was adjusted to maintain the temperature about 15°C below the set point. The controller switched back and forth between the transformers maintaining the temperature within $\pm 1^{\circ}\text{C}$ of the set point. It was necessary to supply the furnace with direct current as the magnetic field acting on alternating current quickly disrupted the windings. Direct current was obtained by passing the output of the "high-low" power supply through a full-wave bridge rectifier and a simple filter comprising a choke and four capacitors.

Chromel-alumel thermocouples (28 guage) were used throughout the investigation for both the control and measuring thermocouples. The instrument used for measuring temperatures, a Tinsley Potentiometer type 3184D, could be read accurately to $\pm 20 \mu$ volts which corresponds to a temperature sensitivity of $\pm 0.5^{\circ}\text{C}$. The potentiometer was used only for accurate spot checks of the temperature, a constant check being made by recording the temperature

on a Westronics M11B/U/DV2H multipoint recorder on which a change of $\pm 1^{\circ}\text{C}$ was easily discernible.

The measuring thermocouple was insulated along its length inside the furnace by two-hole alumina insulators and was inserted into the end of the diffusion couple to a depth of 0.20" so that the actual temperature of the specimen and not that of the ambient atmosphere was measured. The thermocouple wires passed out of the furnace via a Stupakoff insulator which was soldered into the brass end piece, and were insulated outside the furnace with plastic spaghetti tubing. The thermocouple leads were joined to copper potentiometer leads immersed in an ice bath to give a 0°C reference temperature. The measuring couples were initially calibrated against the melting point of pure aluminum (99.999%) and were periodically checked during the course of the experiments by comparison with a standard platinum-platinum-10% rhodium thermocouple calibrated to $\pm 1^{\circ}\text{C}$ by the National Research Council of Canada. The thermocouple checks were carried out in the diffusion furnaces by embedding the thermocouples in a block of silver and comparing them at three or four temperatures within the experimental range. During a diffusion anneal the furnace temperature was checked with the potentiometer several times daily and a continuous record between spot checks was kept using the strip-chart recorder. After completion of each diffusion anneal the temperature record was carefully examined for any deviations away from the set point. If the temperatures deviated from

the set values for an appreciable period of time, the equivalent time at the required temperature was calculated using published diffusion data and this correction was applied to the total time for the diffusion anneal.

The multipoint recorder was also used to maintain a continuous record of the current supplied to the magnet. This signal was supplied by the voltage drop across a 1200 amp, 50 millivolt shunt built into the generator power supply of the magnet. This precaution was necessary in case of power failure so that the exact time of shutdown would be known. A simple safety device consisting of a relay powered by the voltage drop across the magnet was installed so that the magnet diffusion furnace would shut off in the event of magnet failure.

D. THE MAGNET

The magnetic field for the experiments was obtained by a water cooled, iron-clad electromagnet which was constructed from a design based on that of Bitter³⁹. It is equipped with soft iron pole pieces which have a face diameter of 4" and a gap of 1.5". Power was supplied by a 36 kilowatt D.C. generator which has a voltage ripple of less than 5% at 40 volts. The magnet is capable of operating continuously at fields in excess of 30,000 gauss.

E. MEASUREMENTS

1. Direct Measurement of the Kirkendall Shift

These measurements were performed only on the silver-copper diffusion couples as these were sandwich-type whereas the δ -brass couples were not. Measurements of the shift were made on a Tukon Hardness Tester manufactured by Wilson Mechanical Instrument Co., New York. The instrument is equipped with a displaceable stage which could be moved in two directions by means of micrometer screws. The scales on the micrometers are marked in 0.01 mm. divisions and by interpolation it is possible to reproduce measurements to a precision of ± 0.002 mm. The measurements were performed by carefully positioning the diffusion couple such that the welds were parallel to one direction of travel and then measuring the distance between the welds before and after diffusion. (It has been shown that inclusions in the weld serve the same purpose as inert markers^{33,40}.) Thirteen measurements were taken at 0.5 mm. intervals across the central 6 mm. of the couple, with the same area being measured before and after the diffusion anneal. The welds were revealed by first mechanically polishing then etching the couples with a freshly prepared NaCN-H₂O₂ solution.

The length and width of the diffusion couples were also measured with a micrometer before and after diffusion to detect any change in overall dimensions during the diffusion anneals.

2. Measurement of the Boundary Motion in the γ -Brass Diffusion Couples.

After an appropriate length of diffusion anneal, the foil-wrapped couple was removed from the furnace and quenched in water. The surface was sanded down to 600 grit paper and was then chemically polished for three minutes with the following solution⁴¹:

66% acetic acid
17% orthophosphoric acid
17% nitric acid

(All percentages are in volume percent.) About five measurements of the boundary shift (Fig.9) were taken on the Tukon Hardness Tester utilizing the Filar Micrometer eyepiece in which one division is equivalent to approximately one micron using the 16 mm. objective. The specimen was again sanded and polished and the boundary position re-measured. This procedure was repeated until further sanding and polishing revealed no change in the boundary shift, thus insuring that all surface effects had been removed. Over twenty measurements of the boundary shift were taken at 0.5 mm. intervals on the central portion of the diffusion couple to insure sufficient accuracy of the diffusion coefficient to be calculated from the boundary shift data. The twenty measurements were then averaged to give the shift.

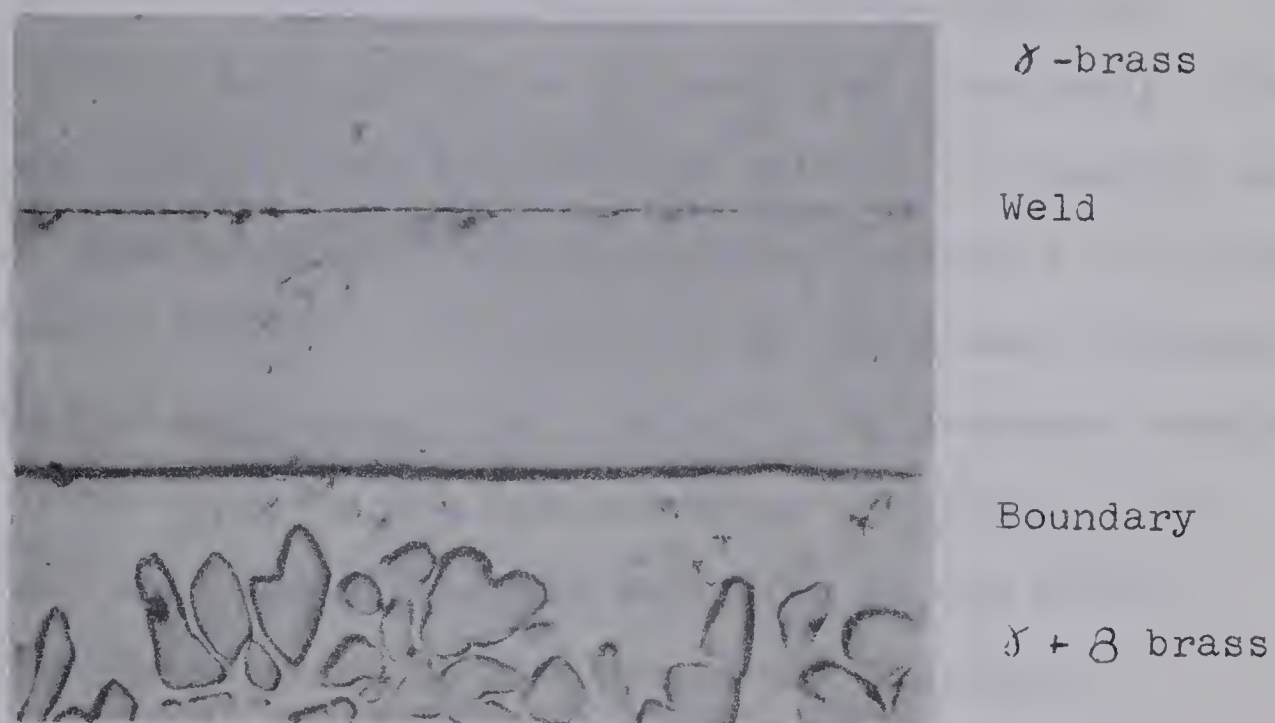


Figure 9. Phase boundary motion in γ -brass for diffusion couple Br-F-1. X 100.

3. Electron Probe Analysis of the Silver-Copper Diffusion Couples

Following a diffusion anneal, the diffusion couple was removed from the furnace and quenched rapidly in water. The couple was sanded, polished, and etched, and the Kirkendall shift was measured as described previously. The couple was then mounted in bakelite using a 1" diameter mount and 1/16" was machined from the surface to remove the effects of surface diffusion. The bakelite mounting was necessary to prevent distortion of the couple due to pressure exerted by the lathe chuck during the machining operation. The couple was then sanded and polished down to one micron diamond abrasive prior to electron probe analysis.

The probe analysis was performed commercially by Materials Testing Laboratories, Los Angeles, California. Four continuous profiles of copper concentration versus distance were obtained for each diffusion couple, two across each weld. A 0.49 wt. % copper standard supplied by the author was used to calibrate the analysis. The accuracy of the probe was estimated to be ± 0.01 wt. % copper. Typical concentration profiles for the 1 wt. % and 7 wt. % couples are shown in Figures 10 and 11 respectively.

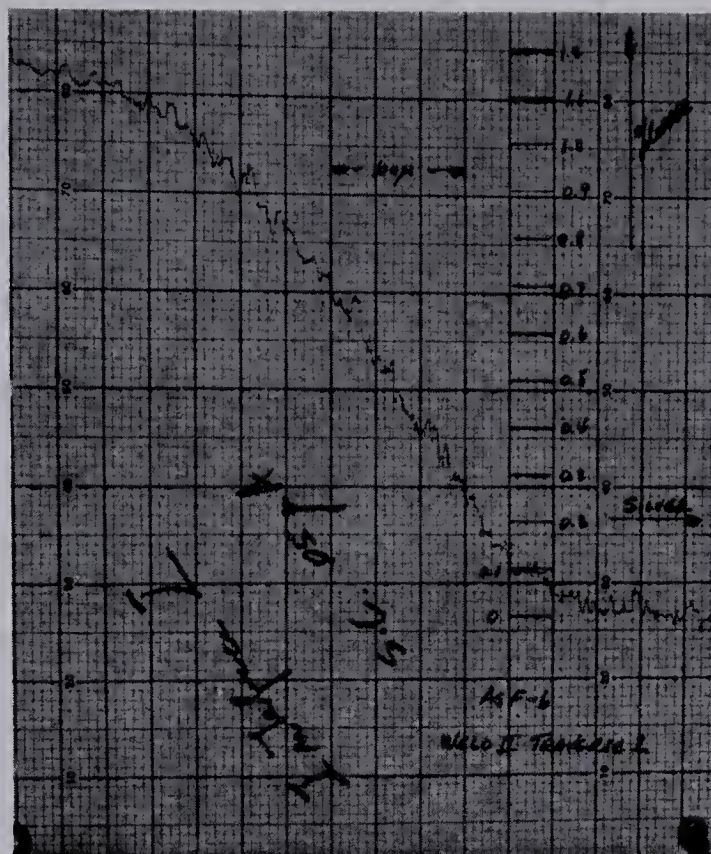


Figure 10. Electron probe concentration profile for couple Ag-F-6 (1 wt.% Cu). X 1/3.

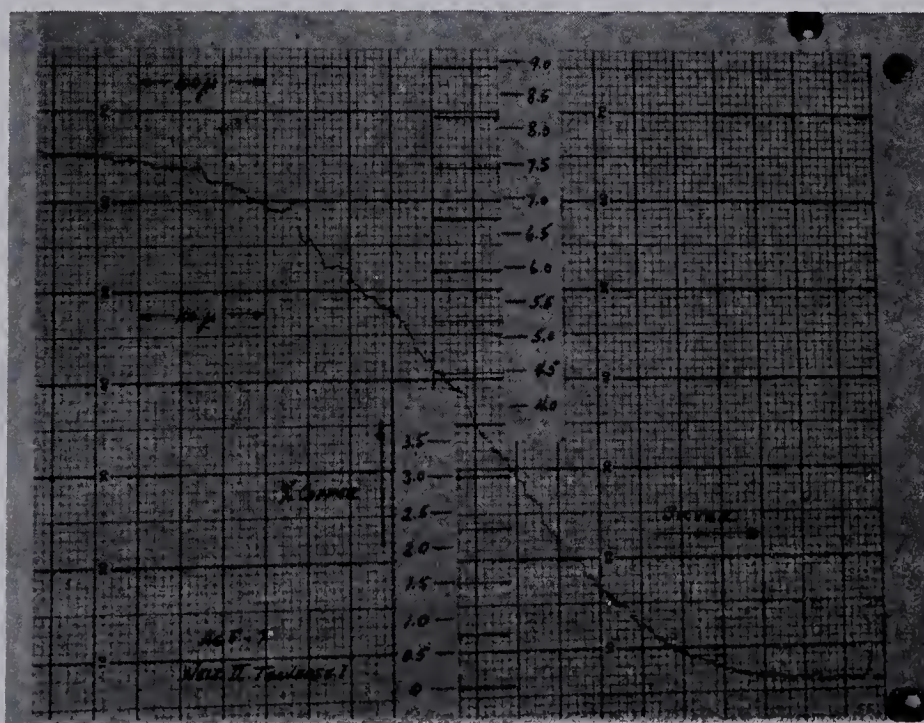


Figure 11. Electron probe concentration profile for couple Ag-F-7 (7 wt.% Cu). X 1/3.

F. TREATMENT OF DATA FROM PROBE ANALYSIS

Due to differences in the initial concentration (C_0) for each couple, and due to the failure of the analyst to locate the position of the weld, it was necessary to treat each profile independently. Each profile was re-plotted in atomic % and the Matano interface located by means of an area balance. The profile was then converted to a standard initial concentration which was the average of the eight initial concentrations for each of the four corresponding field and no-field profiles. The four standardized profiles were then averaged to obtain the final penetration curve. The diffusion coefficients were calculated from the final penetration curves using the Boltzmann - Matano method, in which no assumptions regarding a Kirkendall shift or concentration dependence of the diffusivity are required. Fick's second law of diffusion for the general case is given by⁴²

$$\frac{dc}{dt} = \frac{d}{dx} \left(D \frac{dc}{dx} \right). \quad (30)$$

Using the parameter $\eta = x/\sqrt{t}$, c becomes a function of η alone and equation (30) can be transformed into the ordinary homogeneous differential equation,

$$-\frac{\eta}{2} \frac{dc}{d\eta} = \frac{d}{d\eta} \left(D \frac{dc}{d\eta} \right). \quad (31)$$

The diffusivity is obtained by integration of equation (31) and is given by

$$D = \frac{1}{2t} \left(\frac{dx}{dc} \right)_{c=c_1} \int_0^{c_1} xdc \quad . \quad (32)$$

where the appropriate boundary conditions are

$$c = 0 \text{ for } x < 0 \text{ at } t = 0,$$

$$c = 0 \text{ for } x \rightarrow -\infty, \text{ all } t,$$

$$c = c_0 \text{ for } x > 0 \text{ at } t = 0,$$

$$c = c_0 \text{ for } x \rightarrow +\infty, \text{ all } t.$$

The quantities $\left(\frac{dx}{dc} \right)_{c=c_1}$ and $\int_0^{c_1} xdc$ in equation (32) are obtained graphically from the experimental concentration-distance curves. In this way the concentration dependence of the diffusivity can be determined. In the present investigation, the diffusivities were determined at the Matano interface as both the slope and the area can be determined with the greatest accuracy at this point. A sample penetration curve complete with the calculation of the diffusivity is given in Figure 12.

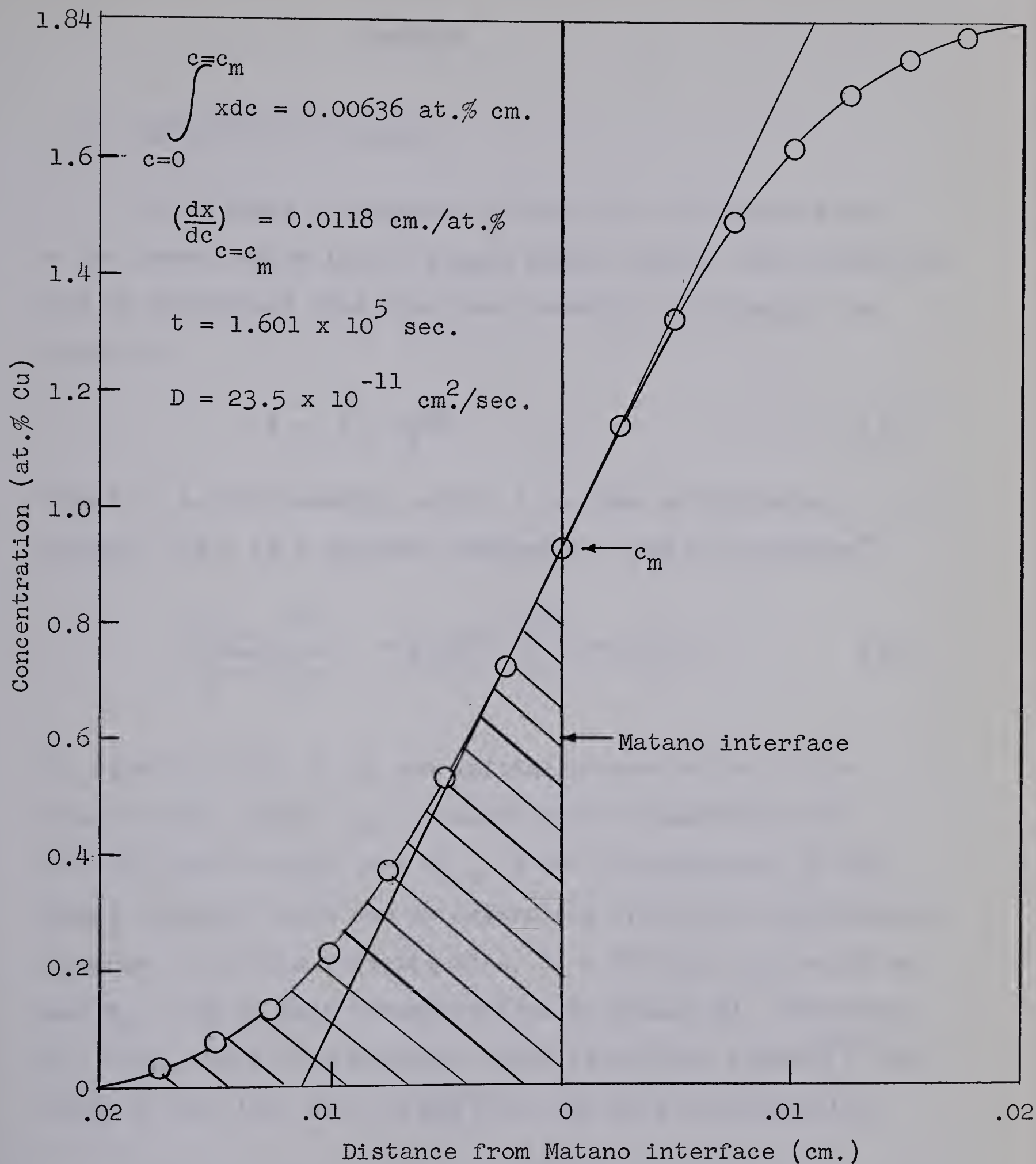


Figure 12. Calculation of diffusion coefficient for couple Ag-F-6 annealed at 754° C for 45 hrs.

RESULTS

A. DIFFUSION IN δ -BRASS

It is shown in Appendix II that, for diffusion from a two phase region into a single phase region, the diffusivity can be determined from the phase boundary shift using the equation

$$K = \epsilon / 2\sqrt{Dt} , \quad (33)$$

where ϵ is the boundary shift, t is time of diffusion anneal, and k is a constant determined from the equation*

$$\frac{C_{1,0} - C_1}{C_2 - C_{1,0}} = K \sqrt{\pi} e^{K^2} (\text{erf } K - 1) . \quad (34)$$

In equation (34), C_1 is the initial concentration of the single phase region, C_2 is the initial concentration of the two phase region, and $C_{1,0}$ is the concentration at the phase boundary which can be determined from the constitutional diagram. For this investigation, $C_1 = 61\%$ Zn, $C_{1,0} = 58\%$ Zn, and $C_2 = 55\%$ Zn (all concentrations in atomic %). Therefore $K = 0.35$, and if the boundary shift is plotted versus \sqrt{t} the slope of the line will be $2K\sqrt{D}$ or, for this investigation,

- - - - -

* Equation (34) holds only for the special case of diffusion from a two phase region into a single phase region.

$.70\sqrt{D}$. The \sqrt{t} plots for the γ -brass field and no-field couples are shown in Figure 13, and the corresponding diffusivities are given in Table II.

Table II

Diffusivity for Diffusion in γ -Brass

Couple	Temp ($^{\circ}\text{C}$)	Field (oersteds)	Diffusivity ($\times 10^9$ (cm. ² /sec))
B-NF-1	509 $^{\circ}\text{C}$	0	$6.8 \pm 0.6^*$
B-F-1	508 $^{\circ}\text{C}$	30,000	7.4 ± 0.6

* The error limits on D in Table II are calculated from the maximum and minimum slopes passing through the standard deviations of the boundary shift measurements (see Fig.13), and therefore give only the relative accuracy of the diffusivities. The calculated diffusivity is strongly dependent upon the values used for the initial concentrations and therefore the absolute error of the diffusivity may be somewhat larger.

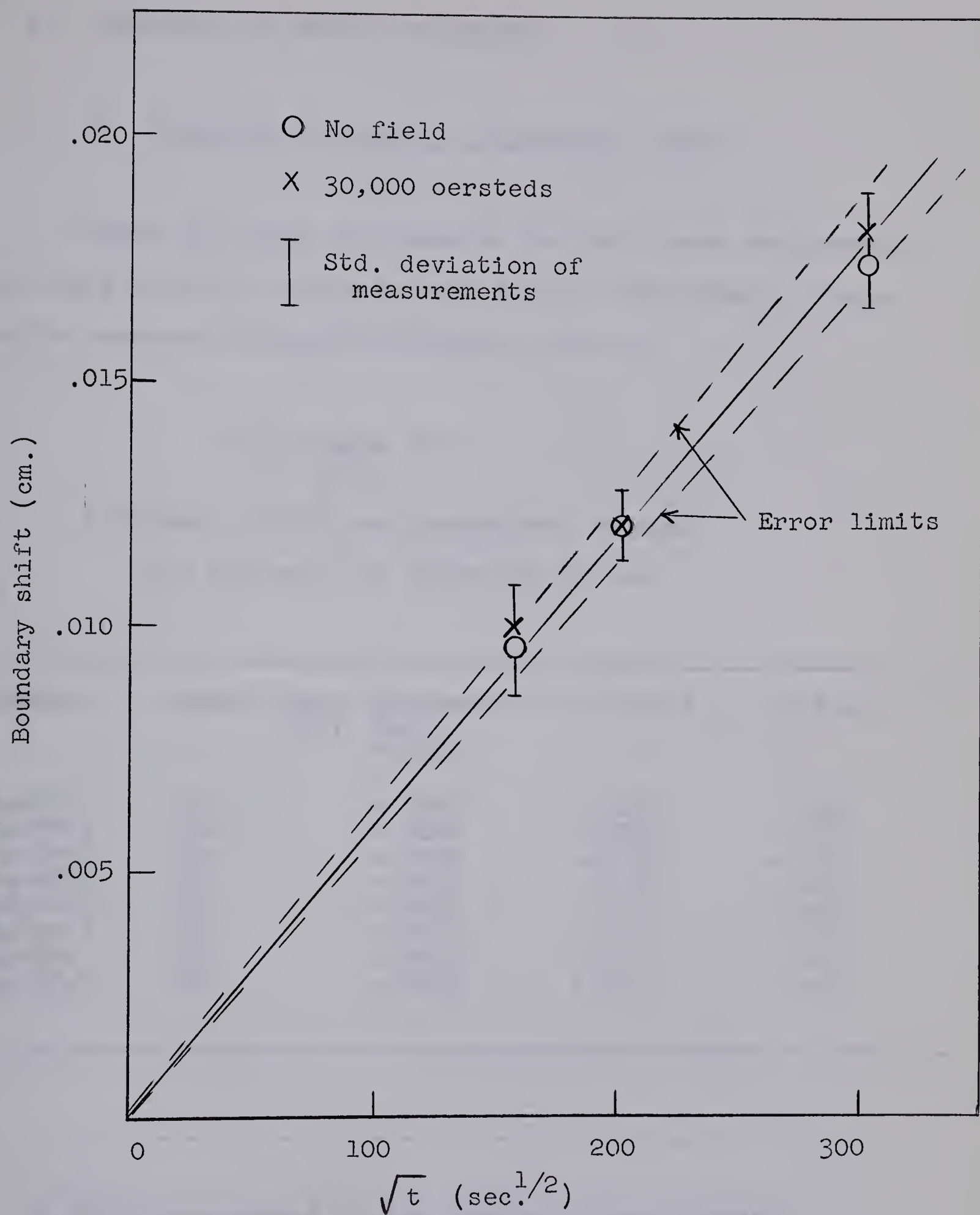


Figure 13. Boundary shift for $\delta/\delta+\beta$ brass diffusion couples.

B. DIFFUSION OF COPPER IN SILVER

1. Direct Measurement of Kirkendall Shift

Table III lists the results for the direct measurement of the Kirkendall shifts as well as the dimensional changes which occurred during the diffusion anneals.

Table III

Kirkendall Shift and Dimensional Changes
for Diffusion of Copper in Silver

Couple	Anneal Temp. (°C)	Kirkendall Shift *(cm.)	d1 (cm.)	dw (cm.)
Ag-F-3	629	+.0005	+.0025	+.002
Ag-NF-3	630	+.0004	+.0025	-.001
Ag-F-5	699	+.0012	+.0025	-.001
Ag-NF-5	698	+.0012	0.0	-.001
Ag-F-6	754	+.0011	0.0	-.002
Ag-NF-6	756	+.0024	+.001	+.002
Ag-F-7	802	+.0020	0.0	0.0
Ag-NF-7	803	+.0025	+.005	+.001

* This measurement is the change in the interweld distance, or twice the actual Kirkendall shift.

2. Diffusion Results for the Diffusion of Copper in Silver

If the diffusion coefficient is independent of concentration, a plot of the ratio $c(x)/c_0$ vs. x on probability paper will yield a straight line with the slope of the line proportional to the diffusivity. Therefore, for the detection of small relative changes in the diffusivity and also for indication of the concentration dependence of the diffusivity, a probability plot is convenient. The probability plots for the four sets of field and no-field diffusion couples are compared in Figures 14-17*. The diffusivities for the eight diffusion couples as calculated by the Boltzmann - Matano method at the Matano interface are presented in Table IV. Column 8 in Table IV gives the ratio of the squares of the Matano areas for each set of field and no-field couples. It can be shown for the case of no concentration dependence, that the square of the Matano area is proportional to the diffusivity. Therefore, because no slope measurement is required, the ratio of the Matano areas is the most accurate comparison of the

* The best fit lines for the probability plots for couples Ag-F-3, Ag-NF-3, Ag-F-6, and Ag-NF-6 were calculated using linear regression theory. The others were drawn by eye.

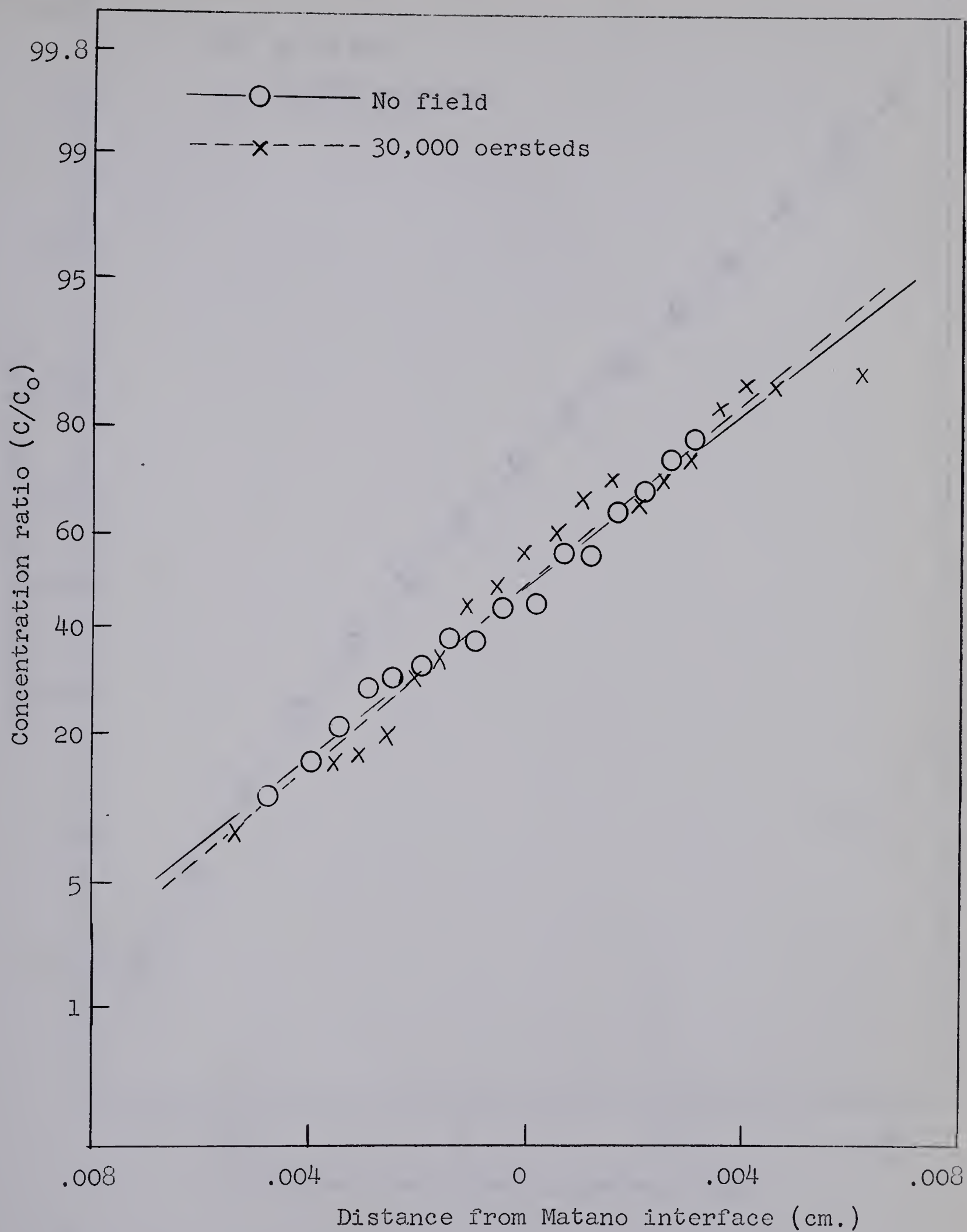


Figure 14. Probability plots for couples Ag-F-3 and Ag-NF-3 annealed at 630°C for 48 hrs.

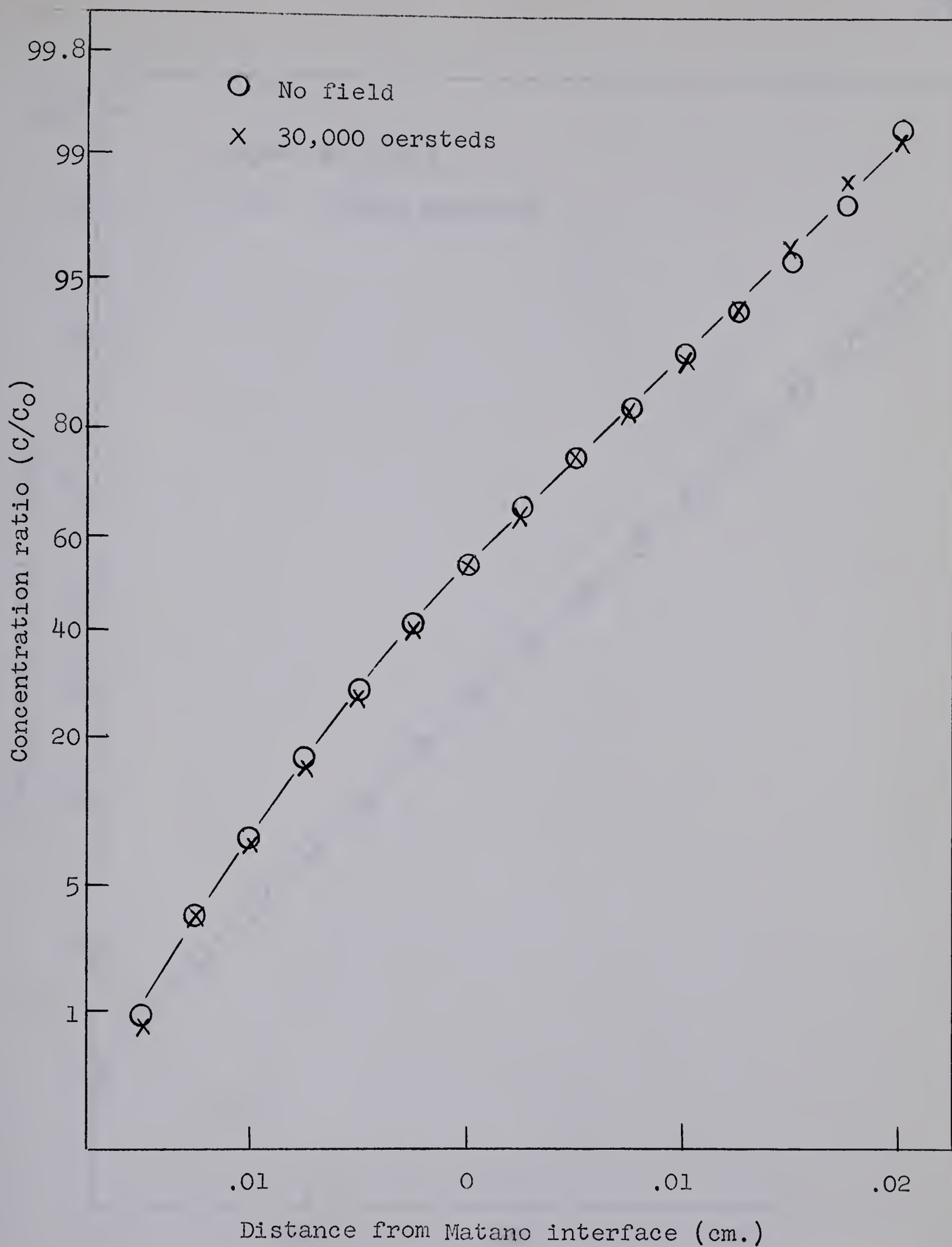


Figure 15. Probability plots for couples Ag-F-5 and Ag-NF-5 annealed at 699°C for 96 hrs.

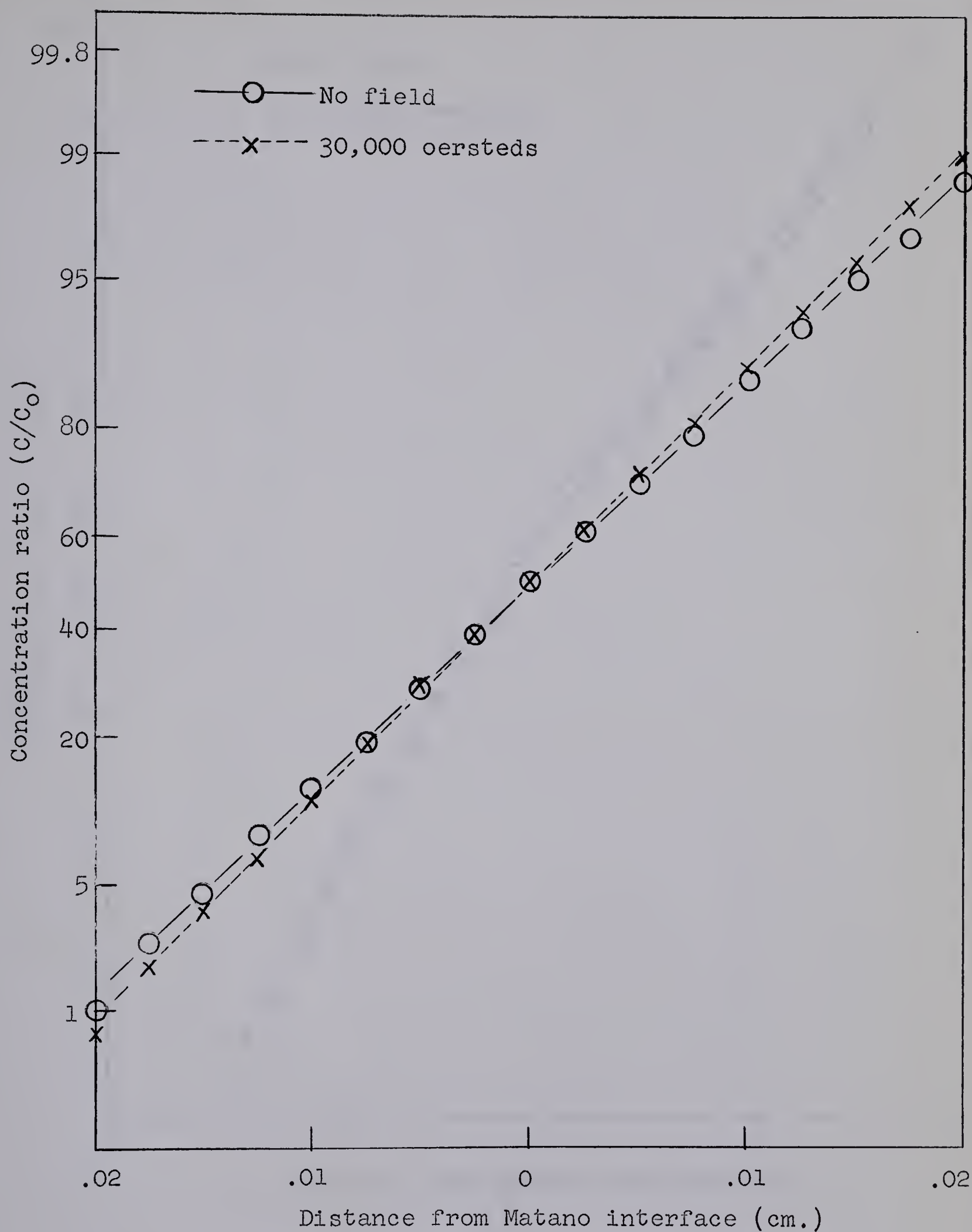


Figure 16. Probability plots for couples Ag-F-6 and Ag-NF-6 annealed at 755°C for 45 hrs.

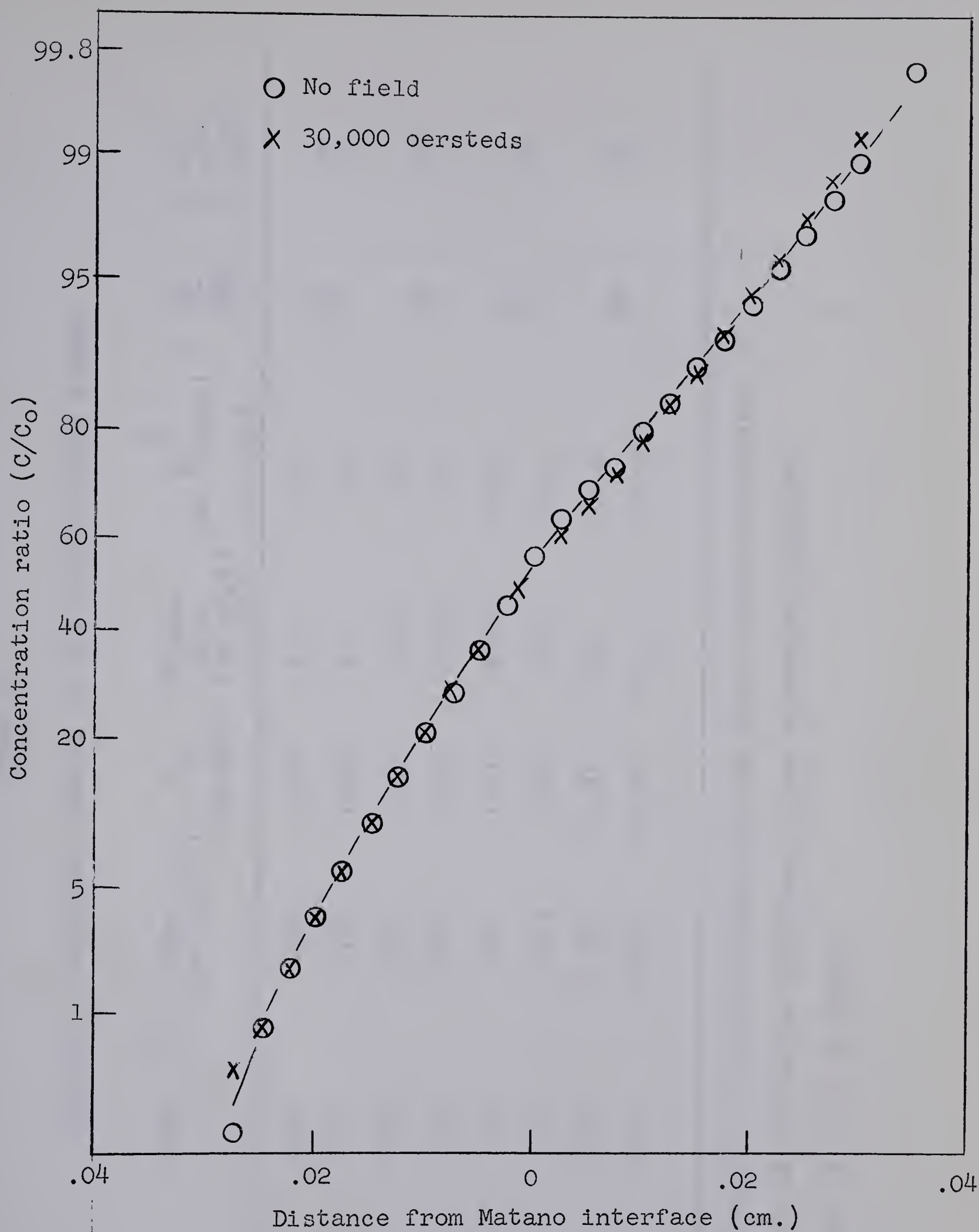


Figure 17. Probability plots for couples Ag-F-7 and Ag-NF-7 annealed at 803°C for 25 hrs.

TABLE IV

SUMMARY OF DIFFUSION RESULTS IN THE SILVER-COPPER SYSTEM

Couple	Temp, (°C)	Time (sec. x 10 ⁻⁵)	C ₀ (at. %Cu)	Matano Area (cm. at. %) x 10 ³	$\frac{D}{(\text{cm.}^2/\text{sec.})}$ x 10 ¹¹	$\frac{D_F}{D_{NF}}$	$\left(\frac{A_F}{A_{NF}}\right)^2$
Ag-F-3*	629	1.725	1.28	2.0	4.7	.94	.95
Ag-NF-3	630	1.725	1.28	2.1	5.0		
Ag-F-5	699	3.454	1.93	5.87	8.8		
Ag-NF-5	698	3.454	1.93	6.06	9.3	.95	.94
Ag-F-6	754	1.601	1.84	6.36	23.5		
Ag-NF-6	756	1.601	1.84	6.56	24.5	.96	.94
Ag-F-7	802	0.903	11.91	58.4	60.0 ⁺		
Ag-NF-7	803	0.903	11.91	59.3	64.0 ⁺	.94	.96

* Field strength is 30,000 oersteds for all field couples designated 'F'.

‡ Calculated at the Matano interface unless otherwise indicated.

+ Calculated at 1 at. % copper.

diffusivities. The concentration-distance curves for the 8 couples complete with the calculations for diffusivities are shown in Appendix III.

The concentration dependence of the diffusivity up to 11 at. % calculated for couple Ag-NF-7 is given in Figure 18. The temperature dependence of the diffusivities for the four sets of couples is shown in Figure 19.

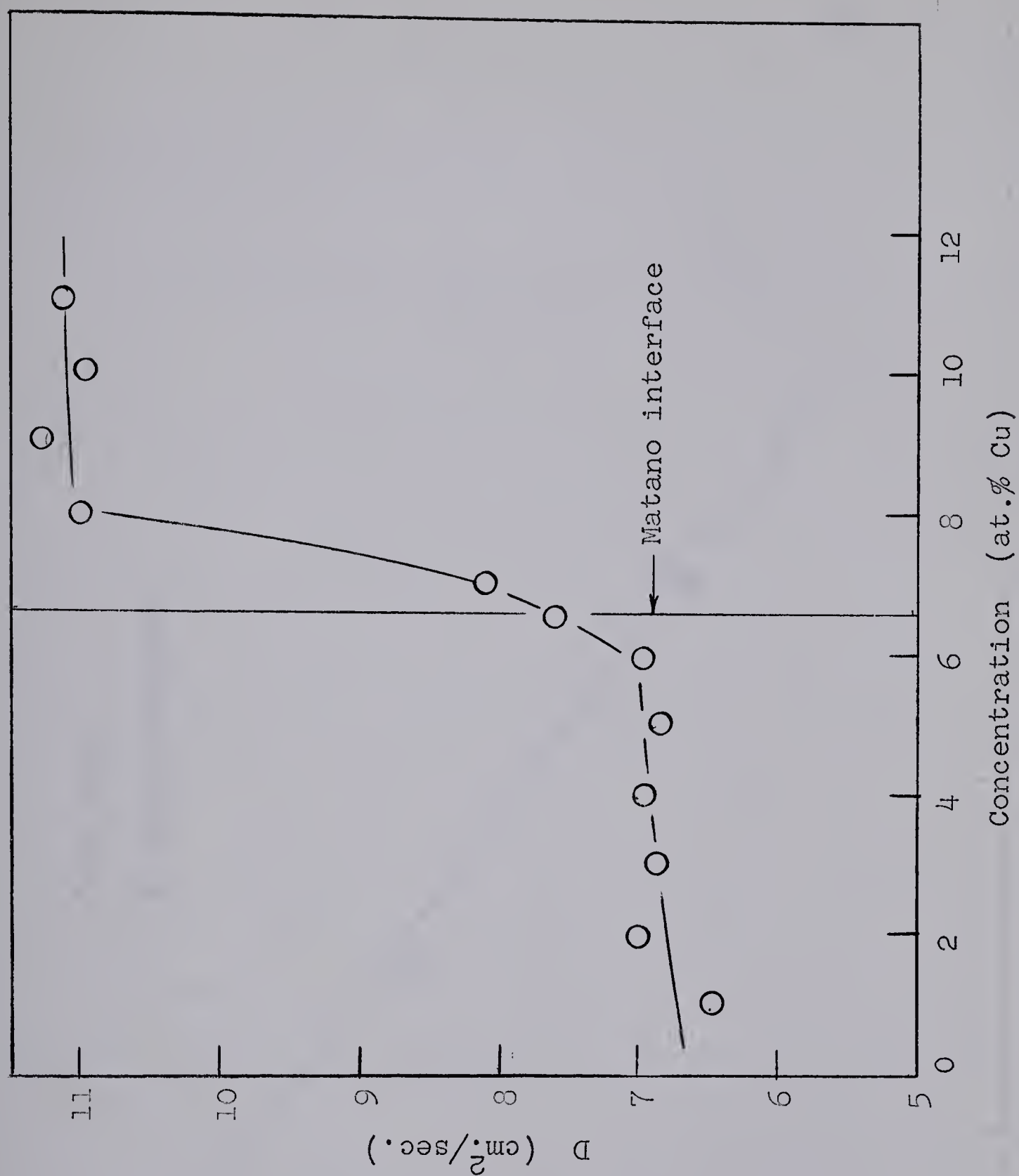


Figure 18. Variation of D with concentration in couple Ag-NF-7.

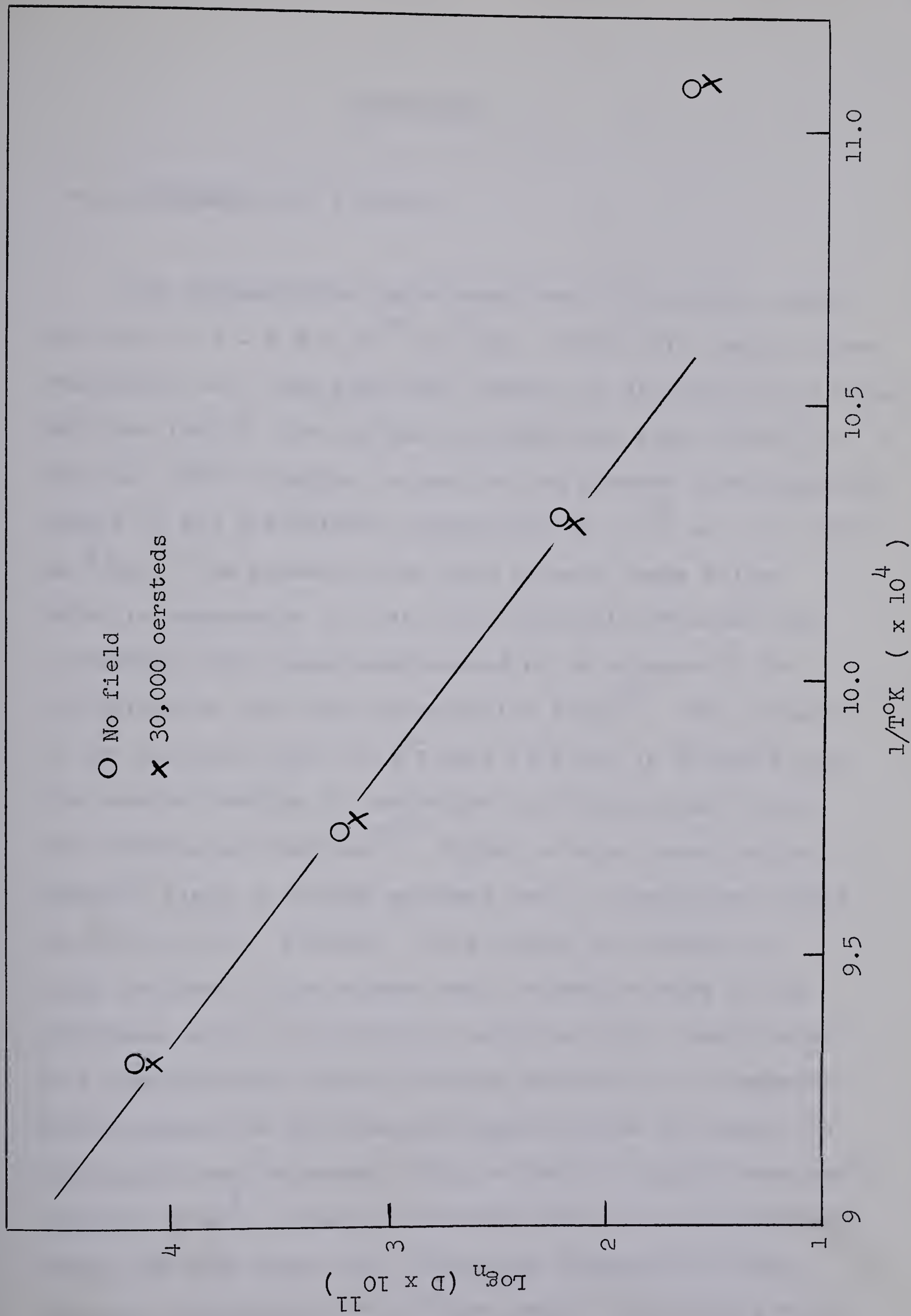


Figure 19. Variation of the diffusivity with temperature in the Ag(rich)-Cu system.

DISCUSSION

A. DIFFUSION IN γ -BRASS

The diffusivities calculated from the boundary shifts are about $7.1 \pm 0.6 \times 10^{-9}$ cm.²/sec. (Table II), which agrees reasonably well with published values for diffusion in γ -brass. Mehl and Lutz¹⁰ give for the concentration range (59-61) at. % zinc and 509°C (similar to that of the present investigation) values of the diffusivity ranging from 5×10^{-9} to 1.2×10^{-8} cm.²/sec. The present value lies between these values which is reasonable in that the diffusivity obtained from a boundary shift experiment should be an average of the diffusivities over the concentration range⁴³. The linearity of the boundary shift vs. \sqrt{t} plot (Fig.13) is evidence that the boundary motion is controlled by diffusion and not by the interfacial reaction⁴⁴. Figure 12 also shows that a magnetic field of 30,000 oersteds has no significant effect on diffusion in γ -brass. This system was chosen for study because of the assumed small effective mass of the electrons, which, according to equation (25), should result in a comparatively large diffusion inhibition in a magnetic field compared to the aluminum-copper system (in which the diffusivity was decreased 25% by a field of 30,000 oersteds⁶). Youdelis et al⁶, assuming the effective mass of the electron equals the rest mass, and a collision frequency for the effective electrons of $\sim 10^{12}$ per second, calculate a value

of 0.75 for the inhibition factor $1/(1 + \omega_{ce}^2/\nu_e^2)$ (eqn. 25), which agrees well with the experimental evidence.

From the equation⁴⁵

$$\chi = \frac{4\mu_o^2}{h^2} (3\pi^2 n_e)^{1/3} \cdot \left(m_e^* - \frac{m_o^2}{3m_e^*} \right), \quad (35)$$

where: χ is the volume magnetic susceptibility, μ_o is the Bohr Magneton, n_e is the number of electrons per unit volume, h is Planck's constant, and m_o is the rest mass of the electron, it is possible to calculate the effective mass of the electron, m_e^* . Using the values $\chi = -8.3 \times 10^{-6}$ (ref. 45, page 106) and $n = 1.66$ electrons per atom⁴⁶, the effective mass of the electrons in δ -brass is 0.4×10^{-28} gms. Using this value for the effective mass, the cyclotron frequency, ω_{ce} (eH/ m_e^*), becomes 12×10^{12} /sec., and, if it is assumed for the moment that the collision frequency of the electron in δ -brass is the same as in aluminum (10^{12} /sec.), then the diffusion inhibition factor $\frac{1}{1 + \omega_{ce}^2/\nu_e^2}$ becomes 1/145, which means diffusion in δ -brass should be severely reduced by a magnetic field. Since the magnetic field has no significant effect on diffusion in δ -brass it follows that the collision frequency must be much greater than 10^{12} per sec. However, values for the collision frequency are not readily available, and therefore it is convenient to relate the parameter ω_{ce}^2/ν_e^2 (eqn.25) to other physical parameters which are more easily obtained.

The collision frequency of the electrons, ν_e , is related to the bulk electrical conductivity in the solid, , by (ref. 20, page 295),

$$\nu_e = \frac{n_e e^2}{m_e^* \sigma} \quad , \quad (36)$$

where n_e is the number of free electrons per unit volume, e is the electronic charge, and m_e^* is the effective mass of an electron. Substituting equation (36) for ν_e and using $\omega_{ce} = eH/m_e^*$, the diffusion inhibition factor (eqn. 25) becomes

$$1 + \omega_{ce}^2 / \nu_e^2 = 1 + \left(\frac{\sigma H}{n_e e} \right)^2 \quad , \quad (37)$$

where H is the strength of magnetic field. Equation (37) is a useful means of evaluating the amount of diffusion inhibition in that it contains the phenomenological conduction coefficient, σ , which is easily measured, and the actual number of free electrons, n_e , which is generally considered to be equivalent to the valence of the solvent metal (per atom).

A different, but equivalent, relationship may be obtained if it is assumed that the mean free path of the electrons, Λ_e , is independent of energy⁴⁷. The collision frequency is then given by

$$\nu_e = v / \Lambda_e \quad , \quad (38)$$

where v is the velocity of the electrons. The velocity is related to the kinetic energy (here all the free electrons are considered) by

$$v = \left(\frac{2 \langle E \rangle}{m_e^*} \right)^{1/2}, \quad (39)$$

where $\langle E \rangle$ is the average kinetic energy of all the electrons. Using equations (38) and (39) the collision frequency is

$$\nu_e = \frac{1}{\Lambda_e} \left(\frac{2 \langle E \rangle}{m_e^*} \right)^{1/2}. \quad (40)$$

The average kinetic energy is three fifths of the Fermi energy and is given by^{*48}

$$\langle E \rangle = \frac{3}{10} \cdot \frac{h^2}{m_e^*} \cdot \left(\frac{3 n_e}{8 \pi} \right)^{2/3}, \quad (41)$$

Substituting equation (41) into (40) gives

$$\nu_e = \frac{1}{\Lambda_e} \left\{ \frac{3}{5} \cdot \frac{h^2}{m_e^{*2}} \cdot \left(\frac{3 n_e}{8 \pi} \right)^{2/3} \right\}^{1/2}. \quad (42)$$

Using equation (42) and the relation $\omega_{ce} = eH/m_e^*$, the

- - - - -

* For simplicity the Fermi energy at absolute zero is used. At a temperature of 800°C this assumption introduces an error in the energy of only about 5%.

diffusion inhibition factor becomes

$$1 + \omega_{ce}^2 / \nu_e^2 = 1 + \frac{5}{3} \cdot \frac{e^2 H^2 \Lambda_e^2}{h^2} \cdot \left(\frac{8\pi}{3 n_e} \right)^{2/3} . \quad (43)$$

The diffusion inhibition factor given by equation (43) is dependent only upon the mean free path of the electrons and their density. Note that the effective mass m_e^* does not appear. The mean free path is the more important variable, for diffusion inhibition goes as Λ_e^2 compared to $(1/n_e)^{2/3}$ for the electron density. If the mean free path is calculated from conductivity data, equations (37) and (43) are equivalent.

Youdelis et al⁶ propose that diffusion in a magnetic field is controlled by those electrons which have a collision frequency of $\sim 10^{12}$ per second, whereas conductivity measurements indicate that the average collision frequency is in the order of 10^{14} per second. Therefore equations (37) and (43) cannot be used for quantitative calculations for the inhibition factor if values for σ and Λ_e are obtained from conductivity measurements. However, equations (39) and (45) give the qualitative behavior of the factor, i.e. it is proportional to $(\sigma/n_e)^2$ (eqn. 37) or, $\Lambda_e^2/n_e^{2/3}$ (eqn. 43).

The values of σ and n_e for aluminum are 4×10^7 ohm⁻¹ cm.⁻¹ and 1.8×10^{23} electrons/cm.³ while the corresponding values for γ -brass are 0.7×10^7 ⁴⁹ and

1.0×10^{23} respectively. If $\omega_{ce}^2/\nu_e^2 = 0.3$ for aluminum, then for δ -brass, $\omega_{ce}^2/\nu_e^2 = 0.3 \times (.7/1.0)^2 \times (1.8/4)^2 = .03$. Assuming a straight proportionality relationship, diffusion inhibition in δ -brass would be only about 3% in a field of 30,000 oersteds which would be undetectable by the method used in this investigation.

The segregation change in Bi-Sb alloys upon solidification in a magnetic field was attributed to the small effective mass of the electron in that system, yet equation (43) shows that the effective mass cancels out in the diffusion inhibition term, $1/(1 + \omega_{ce}^2/\nu_e^2)$, when the collision frequency is defined in the classical phenomenological sense; i.e., $\nu_e = v/\lambda_e$. However, in bismuth the effective mass is highly anisotropic and the effect of the mass cannot be rigidly described by a classical treatment. Therefore, it is possible that the effective mass is important in determining the amount of diffusion inhibition by a magnetic field in some (anisotropic) systems.

B. DIFFUSION OF COPPER IN SILVER

An examination of the probability plots (see Figs. 14-17) and the diffusivities presented in Table IV, shows that a magnetic field of 30,000 oersteds has no appreciable effect on diffusion of copper in silver(rich) alloys. The probability plot for couple Ag-F-6 was analyzed using linear

regression theory* and the standard deviation of the slope (the slope is proportional to the diffusivity) was calculated to be $\pm 1.5\%$. It is reasonable to assume that this error is similar for all the couples.⁺ However, an error in the temperature of 1°C will change the diffusivity by 2.5% , and therefore it is impossible to claim better accuracy than $\pm 4\%$ for the diffusivities listed in Table IV. Even though the field diffusivities are consistently about 5% lower than the no-field diffusivities, this difference is not statistically significant, and in any case, a 5% decrease in the diffusivity is far less than the 25% decrease reported by Youdelis et al.⁶ for diffusion of copper in aluminum in a magnetic field of comparable strength. Therefore, for the purposes of this discussion it is assumed that a magnetic field has negligible effect on diffusion of copper in silver.

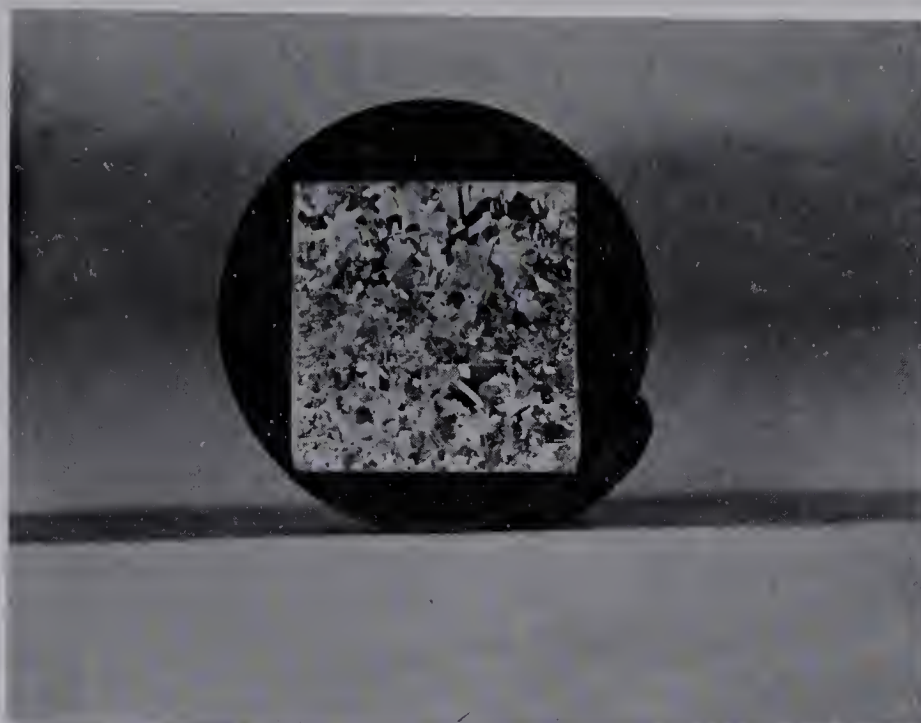
The Arrhenius plot ($\log D$ vs. $1/T$) for the eight diffusion couples is given in Figure 19, from which it is apparent that the diffusivities obtained at 630°C (lowest point) are anomalously high as they do not fit on the straight

- - - - -

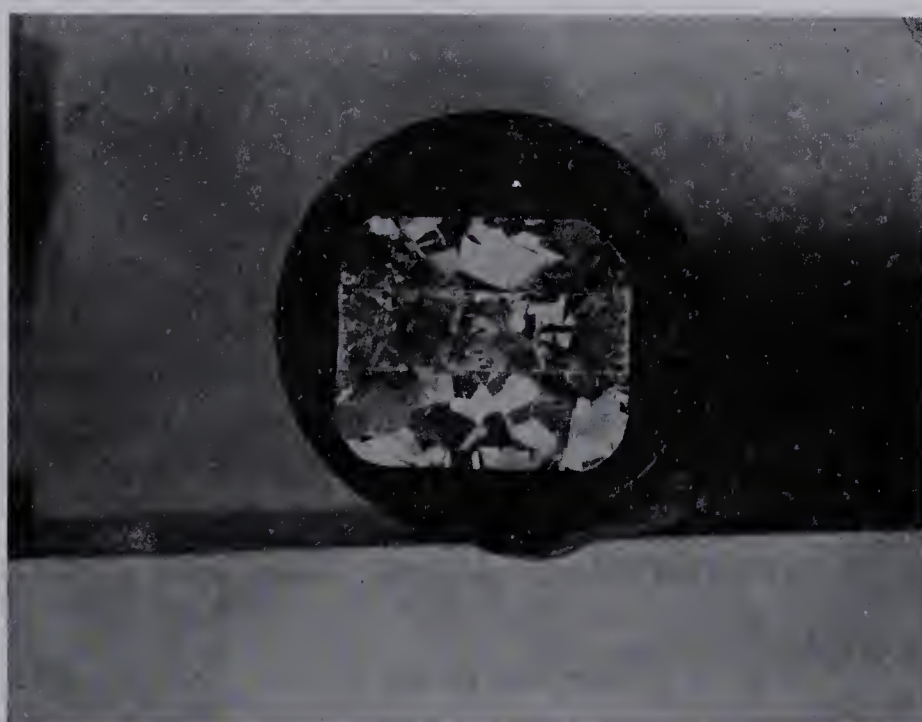
* The argument of the function $2(C(x)/C_0 - 0.5)$ is obtained from tables for the probability integral and plotted versus x to obtain the plot on ordinary graph paper.

+ The diffusion couples annealed at 630°C have larger errors due to the shorter diffusion zone. The standard deviation of the slope is $\pm 4\%$, and, adding 2.5% for a temperature variation, the resultant error in D for these two couples is $\pm 6.5\%$.

line which passes through the other six points. This anomaly is very likely due to the influence of grain boundary diffusion. Figure 20 compares the grain sizes of diffusion couples annealed at 630°C and 756°C , and from which it is apparent that the grain size of the couple annealed at 630°C is much smaller than that of the couple annealed at 756°C . Therefore, grain boundary diffusion is much more prevalent at 630°C than at higher temperatures, and for this reason the diffusivities obtained at 630°C were not included in the Arrhenius plot used to determine the activation energy and the frequency factor. The Arrhenius plot of the diffusivities (Fig. 19) for the remaining six diffusion couples gives an activation energy of 37.8 ± 1.5 kcal/g-atom and a frequency factor, D_0 , of $0.03^{+.03}_{-.016}$ cm.²/sec. where the limits given are standard deviations. The results of the present investigation are compared with those of the previous investigations in Figure 21, from which it is seen that the present results agree much better with those of Sawatzky¹³ who gave values of 46.1 ± 1.0 kcal/ g-atom and 1.23 ± 0.25 cm.²/sec. for the values of Q and D_0 respectively. Seith and Peretti¹² gave values of 24.8 kcal/g-atom and 5.9×10^{-5} cm.²/sec. for values of Q and D_0 , which were obtained from only three values of D . Two of these values agree reasonably well with the present investigation, but the third is sufficiently different to give very low values for both Q and D_0 . Actually, an activation energy of 24.8 kcal/g-atom is extremely low for diffusion in a substitutional type



Couple Ag-NF-3. Annealed at 630°C for 48 hrs.



Couple Ag-NF-6. Annealed at 756°C for 44 hrs.

Figure 20. Comparison of the grain sizes in couples annealed at 630°C and 756°C . X 1.

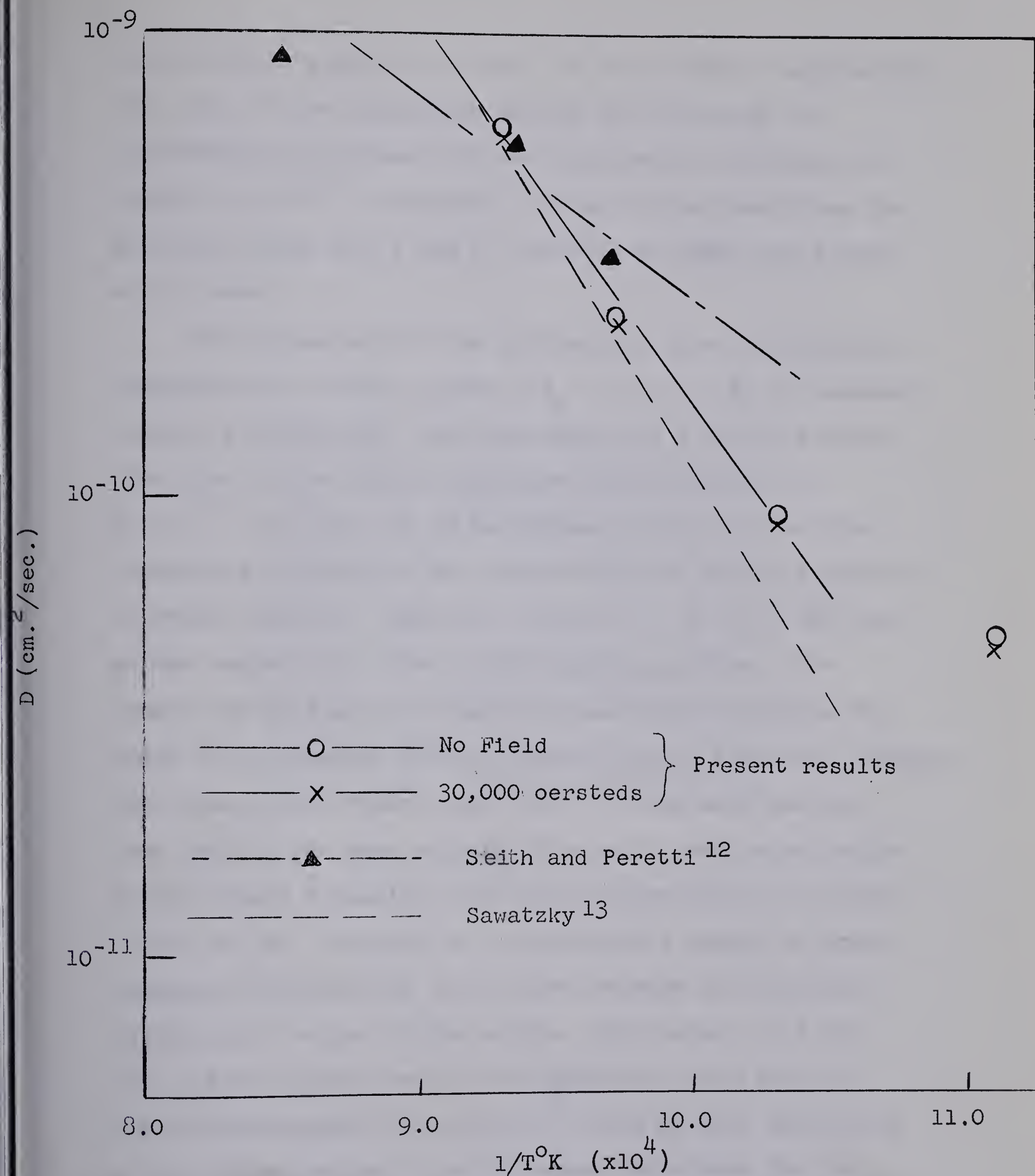


Figure 21. Comparison of previous data with present results.

alloy such as copper in silver, as this value is approaching the value of the activation energy for diffusion in interstitial solutions, 22.0 kcal/g-atom for diffusion of carbon in iron⁵⁰. Therefore, it can be concluded that the previous values for Q and D_0 obtained by Seith and Peretti are in error.

The dependence of the diffusivity upon concentration calculated for couple Ag-NF-7 ($C_0 = 11.9$ at. %) is somewhat unusual (see Fig.18). with the values of D on the Silver-rich side of the Matano interface being constant at 7×10^{-10} cm.²/sec. up to the Matano interface, and then increasing abruptly in the vicinity of the Matano interface to remain constant again at a value of 11×10^{-10} cm.²/sec. on the copper-rich side of the Matano interface. The reason for this abrupt change is made clear in Figure 22, where it is apparent that the grain size in the alloy (copper-rich side of the Matano interface) is very much smaller than that in the pure silver. The small grain size in the alloy, likely a result of the high concentration of copper (11.91 at. %), resulted in an appreciable amount of grain boundary diffusion and thus higher average diffusivities in the alloy region of the couple. The values of D for the 11.91% couples used for the Arrhenius plot (Fig.19) and the subsequent calculation of Q and D_0 were calculated at low concentrations (1 at.%) where the errors due to the grain boundary diffusion in the alloy would be minimal.

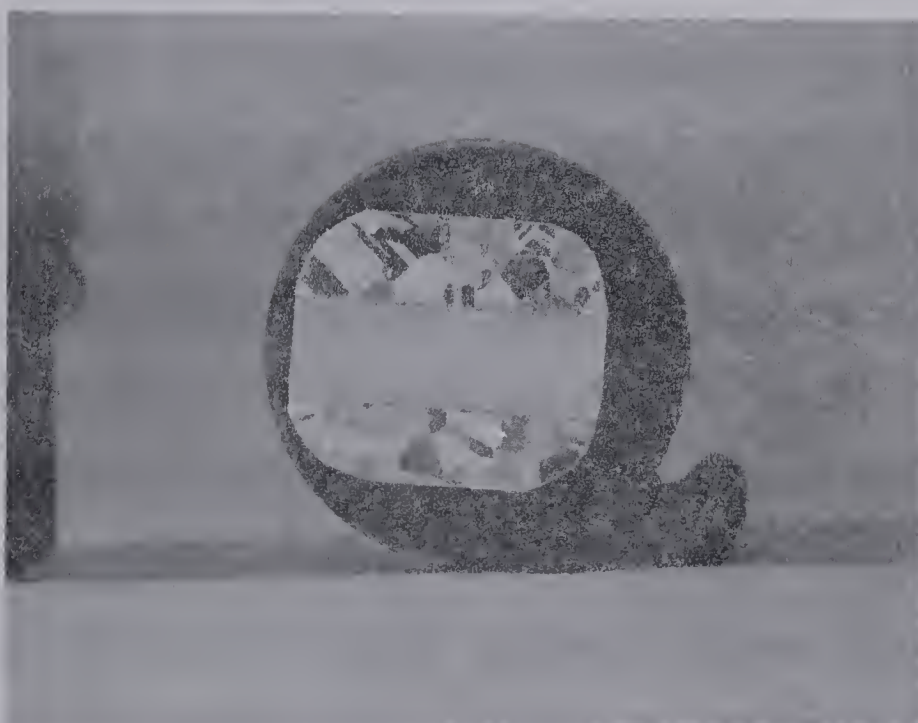


Figure 22. Different grain sizes in couple Ag-NF-7 annealed at 803°C for 24 hrs. X 1.

The results of direct measurements of the Kirkendall shift (see Table III) revealed a consistent movement of the weld (markers) into the pure silver portions of the diffusion couples. This shift was about 1.3% of the total length of the diffusion zone for all the diffusion couples except the two annealed at 800°C. For these two, the shift was about 2% of the diffusion zone but it is clear that this shift is not entirely due to a Kirkendall effect as it was shown previously that appreciable grain boundary diffusion occurred in the alloy sections of these diffusion couples. The grain boundary diffusion in these couples would tend to increase the interweld distance and apparently increase the Kirkendall shift. It appears that a small direct Kirkendall shift does exist, indicating that the diffusion of silver is slightly faster than the diffusion of copper in dilute silver(rich)-copper alloys. However, because the weld cannot be located with respect to the Matano interface, it would be presumptuous to draw any definite conclusions regarding the intrinsic diffusion coefficients of copper and silver.

C. DISCUSSION OF ERRORS

Because of the large number of operations involved in preparing diffusion couples, obtaining penetration curves, and calculating the diffusion coefficients, it is difficult to state an accurate probable error in the diffusion

coefficients. It is possible, however, to list the various sources of error and assess their approximate effect on the coefficients. The sources of error may be divided into two general classifications: experimental (measurement of temperature, analysis, inhomogeneity of base alloys, welding), and computational errors (fitting of curves to experimental points and measurement of areas and slopes). In the present investigation it was important to establish the highest possible precision between corresponding field and no-field results and the experimental methods were so designed.

1. Measurement of Temperature

In the Ag(rich)-Cu system, an error of 1°C in temperature measurement at 700°C will result in a 2.5% error in the diffusivity. Therefore, it is important to measure the temperature as accurately as possible. When thermocouples are used as the measuring device it is possible to minimize errors due to chemical inhomogeneities and compositional differences in the thermocouple wires by calibration against a standard thermocouple. In the present investigation, the thermocouples were calibrated against a platinum/platinum-10% rhodium thermocouple calibrated to $\pm 1^{\circ}\text{C}$ by the National Research Council of Canada. Therefore, the chromel-alumel thermocouples used were accurate to about $\pm 1^{\circ}\text{C}$, but since they were calibrated against the same standard they are likely accurate to better than 1°C relative

to each other. Therefore, the relative error in temperature between field and no-field thermocouples is not greater than $\pm 1^{\circ}\text{C}$, and possibly as good as $\pm 0.5^{\circ}\text{C}$.

It is known that a magnetic field can introduce errors in temperature measurement due to induced voltages in the thermocouple wires. The errors have been discussed in detail by Colton³³. The magnitude of this error can be most conveniently determined experimentally. During the course of the field experiments, the field was turned off and no resultant change in temperature was observed, which would have otherwise occurred if magnetovoltages of significant magnitude had been induced into the thermocouple wires. Therefore, errors in temperature measurement caused by the magnetic field are negligible.

2. Analysis

The errors due to the probe analysis are both random (due to background radiation) and systematic (due to errors in the standard samples used for calibration). In the present investigation the random errors were determined statistically, and quantitative values assigned by analyzing the probability plots using linear regression theory. For couple Ag-F-6, the standard deviation of the diffusivity was $\pm 1.5\%$. The systematic errors caused by errors in calibration are difficult to estimate, but will not affect the relative accuracy between field and no-field results.

3. Inhomogeneity of Base Alloys

Since corresponding field and no-field couples were obtained from the same welded composite, relative errors in the field and no-field couples would be minimal. In any case, they should be random errors and will be included in the standard deviation of the diffusion coefficient.

4. Welding

Again, since the corresponding field and no-field couples were cut from the same welded composite, relative errors in the field and no-field couples would be minimal. The errors due to different welds in the absolute values of the diffusivities should be random and will be included in the standard deviation of D_0 and Q obtained from the Arrhenius plot.

5. Computational Errors

The slopes of the probability plots are the best means for comparing the field and no-field results. For example, the slopes calculated for couples Ag-F-6 and Ag-NF-6 (Fig. 16) differ by 6% with the standard deviation of each slope being 1.5%. Therefore, a 6% difference in diffusivity is easily noticed on the probability plot. The errors in the diffusivities obtained from the Boltzmann - Matano treatment are likely random due to errors in slope and area

measurement and will be included in the standard deviations for D_0 and Q .

From the preceding discussion it is apparent that the field and no-field diffusivities can best be compared via their probability plots. For the present investigation, the relative values of the field and no-field diffusivities are likely accurate to $\pm 4\%$, 1.5% due to random scatter, and 2.5% due to an uncertainty of $\pm 1^\circ\text{C}$ in the temperature. The absolute accuracy of the diffusivities is given to a certain extent by the standard deviation in D_0 and Q , but a systematic error due to errors in the standard calibration samples does exist, which is difficult to estimate.

D. DIFFUSION IN THE MAGNETIC FIELD

In comparing the diffusion data for the field and no-field experiments, it is evident that a transverse magnetic field of 30,000 oersteds has no significant effect on diffusion in the homovalent Ag(rich)-Cu system. On the basis of the relatively high conductivity of the Ag(rich)-Cu alloys, a field effect of at least twice that observed for the Al(rich)-Cu alloys would be expected, if it is assumed that the electron density gradient per se, associated with the finite composition-density gradient in the diffusing system, behaves according to the laws of plasma dynamics so that equation (21) is valid. In the following, some

factors which determine the extent to which a metal alloy system in a non-steady state behaves as a plasma in a magnetic field are discussed in relation to the diffusion results obtained for the Ag(rich)-Cu and Al(rich)-Cu systems.

1. Electron Density Difference

In the development of the theory of diffusion in a magnetic field, it was emphasized that the expression given for the diffusivity in the field is valid provided: (i) that no (electrostatic) Hall fields develop as a result of charge accumulation against boundary surfaces, for this would cancel the Lorentz force on the electron and ultimately the diffusion inhibition effect, and (ii) that a finite electron density gradient exists in the diffusion system. As a consequence of the very short Debye distance in metals ($1-10\text{\AA}$) and the related requirement of electrical neutrality, ion motion (ambipolar diffusion) will be determined in a magnetic field by the retarded motion of the electrons even for very small electron density differences, provided macroscopic electron motion is involved. In the following, a rather simple relationship is developed between the magnitude of the electron density gradient, diffusivity of the system, and the time of the diffusion process in a magnetic field, to show what role these quantities play in the diffusion process.

Diffusion inhibition (in a magnetic field) will not

occur until the charge separation between the conduction electrons and ion cores approaches or exceeds the Debye distance given by equation (18). If charges of volume density n_e are moved a distance x from their equilibrium positions, a polarization P is set up given by

$$\vec{P} = n_e e \vec{x} , \quad (44)$$

which in turn gives rise to an electric field

$$\vec{E} = -4\pi \vec{P} . \quad (45)$$

The electrostatic energy density U is given by

$$U = k_o \frac{E^2}{2} , \quad (46)$$

which becomes, on substituting (45) for E ,

$$U = 8\pi^2 k_o e^2 n_e^2 x^2 . \quad (47)$$

The energy density per (affected) electron then becomes

$$U_e = 8\pi^2 k_o e^2 n_e x^2 , \quad (48)$$

given in c.g.s. units if k_o is taken as unity and e in e.s.u.

The mean distance of charge separation occurring during diffusion is, to a fair approximation, the difference in migration distances of the ion cores and electrons. The mean distance traversed by a diffusion ion in a given time t is the distance between the area centers under the diffusion composition curves, with the Matano interface taken as the zero reference line (see Appendix IV). Thus,

$$\bar{x}_i = \frac{C_0}{2} \int_0^{\infty} x \operatorname{erfc} \frac{x}{2\sqrt{D_i t}} dx \bigg/ \frac{C_0}{2} \int_0^{\infty} \operatorname{erfc} \frac{x}{2\sqrt{D_i t}} dx, \quad (49)$$

where erfc is the complimentary of the error function. On integration of (49) (Appendix IV) the mean distance of ion motion becomes

$$\bar{x}_i = \sqrt{\pi D_i t}. \quad (50)$$

The mean distance traversed by the electron in the same time and direction as the ion is clearly

$$\bar{x}_e = \bar{x}_i \sqrt{\frac{D_e}{D_i}}, \quad (51)$$

where the electron diffusivity in a transverse magnetic field is given by equation (25), i.e. $D_e = D_{\perp}$. Thus

$$\bar{x}_e = \sqrt{\pi D_{\perp} t}. \quad (52)$$

Since ion diffusion is relatively unaffected by the field $D_i = D$, the normal diffusion constant for the solute.

Dropping the subscript i , we can write for the mean separation distance

$$\bar{x} = \bar{x}_i - \bar{x}_e = \sqrt{\pi D t} \cdot \left(1 - \sqrt{\frac{D_{\perp}}{D}} \right), \quad (53)$$

or

$$\bar{x}^2 = \pi D t \cdot \left(1 - (D_{\perp}/D)^{1/2} \right)^2. \quad (54)$$

For interdiffusion in an alloy system it is reasonable to assume that only those electrons need move with the diffusing ion which are necessary to maintain electrical neutrality. That is, it is not the electron density gradient per se that is of importance in determining ion motion, but the electron density gradient per atom. Thus the effective electron volume density difference is

$$\delta n_e = \left| (n_e)_{\text{solute}} - (n_e)_{\text{solvent}} \right| .$$

Substituting δn_e for n_e into equation (48) and equating U to E_F gives

$$E_F = 8 \pi^3 k_o e^2 (\delta n_e) D t \left[1 - (D_{\perp}/D)^{1/2} \right]^2 , \quad (55)$$

or

$$t = \frac{E_F}{8 \pi^3 k_o e^2 (\delta n_e) D \left[1 - (D_{\perp}/D)^{1/2} \right]^2} . \quad (56)$$

Equation (56) for t may be assumed to give the order-of-magnitude time necessary for diffusion inhibition to commence in any non-steady state diffusing system, and shows its explicit dependence on the diffusivity of the system and the electron/atom concentration difference between solute and solvent. If δn_e is zero, that is, both the solvent and solute atoms contribute exactly the same number of electrons (per atom) to the common Fermi pool, then the inhibition effect due to the field is absent

($t \rightarrow \infty$). The field diffusion results obtained in this investigation suggest that this is most probably the situation for the homovalent Ag(rich)-Cu system. Diffusion in the Ag(rich)-Cu system essentially involves motion of the ion cores through a stationary electron gas. The electron density gradients associated with chemical composition differences, play no dynamic part in the diffusion process, and are dissipated without electron flow as the specific volume of the alloy changes during diffusion of the ion cores. In contrast, the heterovalent Al(rich)-Cu system shows significant diffusion inhibition in a magnetic field, and this may be attributed to the difference in electron concentration per atom between the solute Cu and the solvent Al, which gives rise to an electron density gradient (per atom) and a corresponding macroscopic electron flow during the chemical diffusion process. It is not obvious simply from a consideration of the valency of an alloy component whether a magnetic field will inhibit diffusion, for it requires some knowledge of the band structure of the alloy. For example, the field segregation results⁷ for the homovalent Bi - Sb system suggest a significant diffusion inhibition by the field, and have been explained on this basis. Assuming this is correct, it must be concluded that the free-atom valencies of Bi and Sb (+5) do not represent the actual number of 'free' electrons per atom in the liquid metal. Even for a monovalent metal, where the electron density is lower and the band structure considerably simpler,

the perturbation potential of a monovalent solute in the lattice might be sufficient to result in an overlap of the conduction and valence bands, so that electron/atom concentrations might differ significantly for the solute and solvent atoms. It is clear that the number of free electrons per atom and the plasma-like nature of the alloy becomes more difficult to assess as the electron densities increase and band structures become more complicated.

Finally, in regard to electron density gradients, it should be pointed out that a system in a stationary state will not experience a Lorentz force inhibiting diffusion. This is because a stationary state involves no time change in electron density at any given point, and consequently there are no macroscopic electron diffusion currents to interact with the magnetic field. For diffusion inhibition a non-stationary state is required, i.e. $\partial^2 c / \partial x^2 \neq 0$.

2. Electron Ground State Energy (E^0).

It is essential to consider what effect the electron ground state energy of the solute relative to the solvent has on motion of the solute atom in the solvent lattice. The energy of the lowest-energy electron in the conduction band of a metal is calculated with reference to the energy of an electron at rest in free space as zero. For monovalent metals it can easily be shown⁵¹ that

$$E^0 = -H + \bar{E}_F + I_1, \quad (57)$$

where H is the sublimation energy, \bar{E}_F the mean kinetic energy ($3/5 E_F$) of the electron, and I_1 the first ionization potential. For polyvalent metals the problem is complicated by the change in the interaction energies of the electrons when going from the sublimated to the condensed state. Varley⁵¹ shows that for a polyvalent metal which contributes Z electrons per atom to the conduction band

$$E^0 = -\frac{1}{Z} \left\{ H + 2 \sum_{i=1}^Z I_i + ZE_F - ZI_Z + (Z-2)I_T + Z\left(\frac{Z-1}{r}\right) \frac{e^2}{r} (0.284-b) \right\}, \quad (58)$$

where $b = b(r)$ and I_T is the $s - p$ transition energy. The value of E^0 in e.v. for some of the common metals calculated using equation (58) is given as follows⁵¹: Cu (-15.48), Ag (-13.85), Au (-16.47), Mg (-13.03), Cd (-14.33), Zn (-16.29), Hg (-15.38), Al (-18.30), Ga (-17.94), In (-16.08).

Now, when a solvent metal is perturbed by a potential $U(r)$ associated with an impurity atom, there is in general, a shift in the Fermi level from E_F to $E_F + \Delta E_F$. For low concentrations (approaching infinite dilution), $\Delta E_F = 0$. If it is also assumed that the linearization approximation may be applied, the self-consistent potential is given by equation (3). It is clear that the linearization approximation of the Thomas - Fermi equation is not valid when $V(r)$ (or Z) is large, i.e. $V(r) \sim E_F$, or when $r \rightarrow 0$ for

which $V(r) \rightarrow \infty$. For this case exact solutions of the Thomas - Fermi equation are required. Alfred and March^{2,3} obtain for the self-consistent potential, equation (7), with the parameter $\alpha < 1$ for positive, Z and > 1 for negative Z . For the case of homovalent solutes $Z = 0$; however, the ground state energies of the solute and solvent electrons differ, so that a perturbation potential $U = E_A^0 - E_B^0$, where A is the solvent metal and B the solute metal, will result in a potential well (if positive) and attract electrons into it. For negative U a potential hump arises to repel electrons in the vicinity of the impurity site. There is a polarization of the conduction electrons as a consequence, and the self-consistent potential is approximately given by equation(11) (see Le Claire⁹).

In Figure 23, the 'two-band model' representation of $N(E)$ vs. E for the Al-Cu and Ag-Cu alloys are shown, based on the calculated Fermi and ground state energies of the electrons in the pure metals. The eigenfunctions ψ_A^0 and ψ_B^0 , corresponding to the respective ground state energies E_A^0 and E_B^0 , will in general have different amplitudes at the cell boundaries and will not match. Each ψ^0 will thus be modified so that the ground state eigenfunction becomes single-valued and continuous throughout the alloy lattice. There will, therefore, be a corresponding modification in the ground state energies E_A^0 and E_B^0 , but the change will be small provided $E_A^0 - E_B^0$ is not too large (Varley⁵¹). It is evident from Figure 23, that when Cu is dissolved in an

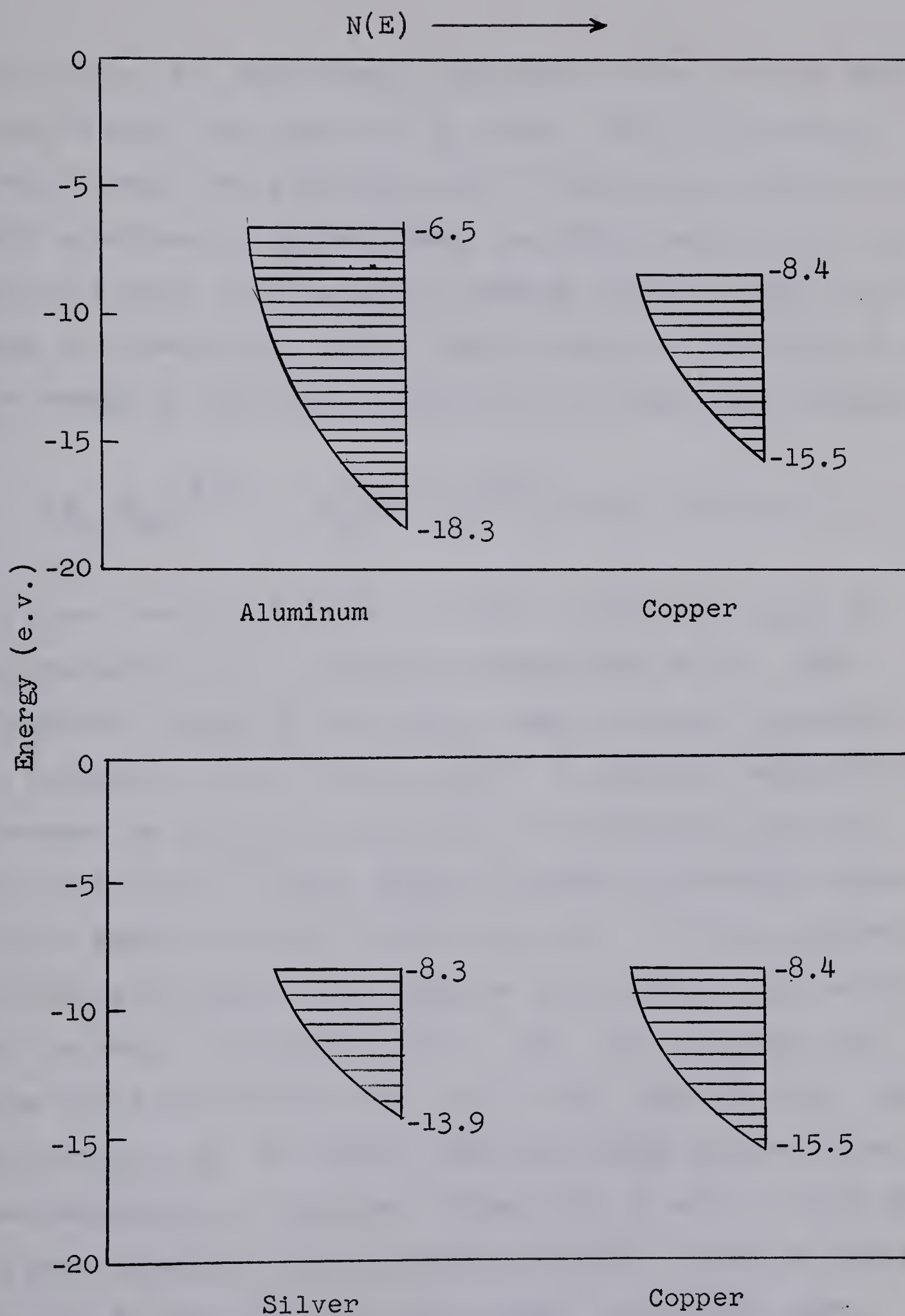


Figure 23. 'Two band' representation for $N(E)$ vs. E in the Al-Cu and Ag-Cu alloy systems.

Al lattice, the high energy electrons in the Al cells will tend to spill over into the Cu cells. The Cu cells will tend to repel the electrons, for if the copper cell was filled with electrons to approximately the Fermi level of Al, for dilute alloys, the increase in energy would be prohibitively high for stability. As the Fermi energy is a function of $(Z)^{2/3}$, the energy at the solute site would increase approximately

$$(Z_{\text{Al}}/Z_{\text{Cu}})^{2/3} \cdot E_F(\text{Cu}) = 3^{2/3} \cdot (7.10) = 14.8 \text{ e.v.},$$

to a new level of $(-15.48 + 14.8) = -0.68 \text{ e.v.}$, which is approximately 6 e.v. above the Fermi level of Al. The "negative" charge of the solute copper ion will therefore be screened, and the actual amount of electron redistribution between the Al and Cu cells will be determined primarily by the balance in Fermi energy decrease and electron interaction energy increase within the cells. If the calculations of Alfred and March³ for negative Z in a monovalent solvent may be used, the parameter $\alpha = 1.85$. On the other hand, when Cu is the solvent metal and Al the impurity atom, the situation is not as drastic from the energy point-of-view. Redistribution of electrons between the Al and Cu cells will be more extensive, with a greater transfer to the Cu cells because of the relatively low energy, large Fermi sink. However, most of the electrons associated with the Al will remain in the Al cell to screen out the excess positive charge more effectively, and this agrees with the value of

0.67 for the parameter α calculated by Alfred and March for an atom of valency 3 dissolved in Cu.

It is interesting to speculate what effect the charge redistribution or polarization of the conduction electrons has on ion motion in a magnetic field. The screening model for a negative ion submerged in an electron gas is quite different physically from that of a positive ion. For a positive ion, screening is effected by the attraction of electrons into the cell region, while for an effective "negative ion", such as Cu in Al, the Cu ion is screened by the repulsion of electrons out of its cell to give an effective 'positive' charge in the electron cloud surrounding the ion. In the former case (Al in Cu) the Al ion is more effectively neutralized by the electrons drawn into its cell, and this is indicated in the value of the parameter $\alpha < 1$. In the latter case (Cu in Al) there is a greater physical separation of the Cu ions from the conduction electrons, and this is also indicated by the values of the parameter α , which are greater than unity for negative Z. In this sense, 'negatively' charged solute ions in a solvent lattice may be considered as closer to a true plasma model than solute ions which have an excess positive charge relative to the solvent metal. It might be reasonable to conclude that if the charge separation was significant, motion of the electron cloud would be retarded in a magnetic field, which would in turn retard ion motion across a magnetic field even where no macroscopic composition and corresponding

electron density gradients existed. This, of course, implies an anisotropic negative charge distribution about the ion. On this basis it would be expected that self-diffusion of Cu in Al (in very dilute alloys) would be retarded in a magnetic field to approximately the same degree as chemical diffusion of Cu in Al is found to be⁶. For the opposite situation, i.e. Al dissolved in Cu, charge separation is considerably less, so that the magnetic effect on the polarized conduction electrons is absent (or minimal), and diffusion inhibition for self-diffusion of Al may be absent. However, in chemical diffusion, where finite concentration and electron density gradients exist, diffusion inhibition due to the field would still exist as the Fermi level would vary with composition and tend to equilibrate by electron redistribution during diffusion. Self-diffusion experiments in both extremities of the Al-Cu system would be of obvious interest in testing the above theory.

From Figure 23 it is evident that the maximum energy of the electrons for both Ag and Cu are approximately at the same position on an absolute energy scale. Consequently, no electron redistribution between Ag and Cu cells occurs as a direct result of the difference in the Fermi levels of the two atoms. However, the difference in ground state energies of the electrons does result in transfer of high energy electrons from the Ag to the Cu cells. The approximate number of (excess) electrons attracted into the Cu cells (when Cu is the solute) is given by $(\propto Z)_{\text{eff}}$ calculated

using equation (11), which Le Claire gives as 0.6 electrons. The attraction of electrons into the Cu cells is also indicated by a decrease in the Knight shift of the Ag atoms in an Ag-Cu alloy. This polarization of the conduction electrons apparently has no effect on diffusion in the field as surmised from the results of the present investigation. The absence of a field effect on diffusion in the Ag(rich)-Cu system is therefore attributed to the absence of an electron density gradient (per atom) corresponding to the composition gradient in a diffusion couple. For diffusion of the solute Ag in the solvent Cu lattice, an electron density gradient (per atom) would also be absent, but because $E_{\text{Cu}}^{\text{O}} > E_{\text{Ag}}^{\text{O}}$, U is negative and electrons are repulsed from Ag sites. The charge separation is greater, and this may result in diffusion retardation in a magnetic field. Here a study of diffusion in the Cu(rich)-Ag system in a magnetic field may shed some light on the screening effect.

3. Screening

The absence of a field effect on diffusion of Cu in Ag supports the original assumption that the screening constant q is unaffected in metals by a magnetic field. It was shown in the theory that a change in the screening parameter would result in a significant change in the activation energy for diffusion, since the interaction energy between the impurity ion and a vacancy would be affected in the field.

The plasma oscillation frequency, which is related to the screening parameter, was shown (by a theoretical argument) to be unaffected by a magnetic field of strength $< 10^7$ oersteds, and therefore it was concluded that the diffusion inhibition effect observed in Al(rich)-Cu alloys occurs through plasma-magnetohydrodynamic forces. Since the screening effect is independent of concentration gradients, it would have resulted, if present, in a decreased field diffusion in the Ag(rich)-Cu system. The screened potential of an impurity atom is not affected by the field. The implication of a possible diffusion inhibition related to screening and charge polarization, as discussed in the previous section, is associated with a possible magneto-hydrodynamic drag of the polarized conduction electrons.

SUMMARY AND CONCLUSIONS

1. The interdiffusion coefficient in Cu-Zn (γ -phase) alloys, calculated from boundary migration data, was found to be $7.1 \pm 0.6 \times 10^{-9} \text{ cm.}^2/\text{sec.}$ at 509°C.

2. The interdiffusion coefficient in Ag(rich)-Cu alloys, calculated using the Boltzmann - Matano method on diffusion data obtained by electron probe microanalysis of standard diffusion couples, is given by

$$D = 0.03_{-.016}^{+.03} e^{-(37,800 \pm 1500)/RT}.$$

3. A magnetic field of 30,000 oersteds applied perpendicular to the diffusion direction has no significant effect on the interdiffusion coefficient in the heterovalent Cu-Zn, γ -phase. A theoretical investigation shows that the inhibition factor is independent of the effective mass of the electron if the classical, phenomenological definition of the electron collision frequency is used (collision frequency equal to the ratio of the Fermi velocity to the mean free path). The absence of a diffusion inhibition effect in the Cu-Zn γ -phase is associated with the low conductivity of the alloy.

4. A magnetic field of 30,000 oersteds applied perpendicular to the diffusion direction has no significant effect on the interdiffusion coefficient in the homovalent Ag(rich)-Cu system. The absence of a diffusion inhibition effect, similar to that observed in the heterovalent

Al(rich)-Cu system, is attributed to the absence of an effective electron density gradient (per atom) associated with composition differences. Diffusion in the Ag(rich)-Cu system essentially involves ion motion through a stationary electron gas, with no macroscopic electron diffusion current involved.

5. The different ground state energies of the electrons of Ag and Cu had no apparent effect on diffusion in the homovalent Ag(rich)-Cu system. A consideration of the screening models for positively and 'negatively' charged solutes (relative to the lattice), suggests that the greater charge separation or polarization of conduction electrons for the 'negative' solute may have an inhibition effect on diffusion in a magnetic field. The effect would be magneto-hydrodynamic in nature, resulting from the magnetic drag of the polarized conduction electron cloud. It is suggested that self diffusion studies in a magnetic field in the solid solution extremities of the Ag-Cu and Al-Cu alloy systems would be useful in testing the 'screening' hypothesis.

6. The absence of a field effect of diffusion in the Cu-Zn phase and the Ag(rich)-Cu alloys supports the assumption developed in the theory that the field effect is via plasma-magnetohydrodynamic forces, and that the screening factor or screened potential per se remains unaffected by the field.

BIBLIOGRAPHY

1. Lazarus, D., Phys. Rev., 93, 937 (1954).
2. Alfred, L.C.R., and March, N.H., Phil. Mag., 46, 759 (1955).
3. Alfred, L.C.R., and March, N.H., Phys. Rev., 103, 877 (1956).
4. Alfred, L.C.R., and March, N.H., Phil. Mag., 2, 985 (1957).
5. Le Claire, A.D., Phil. Mag., 7, 141, (1962).
6. Youdelis, W.V., Colton, D.R., and Cahoon, J., Can. J. Phys., 42, 2217 (1964).
7. Youdelis, W.V., Colton, D.R., and Cahoon, J., Can. J. Phys., 42, 2238 (1964).
8. Youdelis, W.V., and Dorward, R.C., Can. J. Phys., to be published.
9. Le Claire, A.D., Phil. Mag., 10, 641 (1964).
10. Mehl, R.F., and Lutz, C.F., Trans. AIME, 221, 561, (1961).
11. Jost, W., Z. Physik, 127, 163, (1950).
12. Seith, H.W., and Peretti, E.A., Z. Electrochem., 42, #7, 570, (1936).
13. Sawatzky, A., University Microfilms Publication #24851, Doctoral Dissertation Series.
14. Camp, F.W., and Johnson, E.F., Effect of Strong Magnetic Fields on Chemical Engineering Systems, (U.S. Atomic Energy), (1961).
15. Cowling, T.G., Magnetohydrodynamics, (Interscience Publication, New York), p.3, (1957).
16. Spitzer, L., Physics of Fully Ionized Gases, Second Edition, (Interscience Publication, New York), p. 30, (1962).

17. Mangelndorf, P.C., Physical Chemistry of Process Metallurgy, (Interscience, New York), pt. 1, p. 429, (1961).
18. Ziman, J.H., Electrons and Phonons, (Clarendon Press, Oxford), p. 494, (1964).
19. Kapitza, P., Proc. Roy. Soc., (London), Sec. A, 123, 292, (1929).
20. Kittel, C., Introduction to Solid State Physics, Second Edition, (John Wiley & Sons, New York), p. 239, (1956).
21. Bohm, D., and Pines, D., Phys. Rev., 82, 625, (1951).
22. Bonch - Bruevich, V.L., and Mironov, A.G., Soviet Phys. Solid State, 2, 454, (1960).
23. Stephen, M.J., Phys. Rev., 129, 997, (1963).
24. Salpeter, E.E., Phys Rev., 122, 1663, (1961).
25. Birchenall, C.E., Metals Rev., 3, 235, (1958).
26. Borg, R.J., and Birchenall, C.E., Trans. AIME, 218, 980, (1960).
27. Stanley, J., and Wert, C., J. Appl. Phys., 32, 267, (1961).
28. Buffington, F. S., Hirano, K., and Cohen, M., Acta Met., 9, 434, (1961).
29. Hirano, K., Cohen, M., and Averbach, B.L., Acta Met., 9, 440, (1961).
30. Hume - Rothery, W., Acta Met., 11, 630, (1963).
31. Hirano, K., Agarwala, R.P., Averbach, B.L., and Cohen, M., J. Appl. Phys., 33, #10, 3049, (1962).
32. Borg, R.J., J. Appl. Phys., 34, #5, 1562, (1963).
33. Colton, D.R., Ph. D. Thesis, University of Alberta, p. 21, (1964).
34. Metcalfe, A.G., Acta Met., 1, 609, (1953).

35. Hendricks, S.B., Jefferson, M.E., and Schultz, J.E., Z. Krist., 73, 376, (1930).
36. Borg, R.J., and Lai, D.Y.E., Acta Met., 11, 861, (1963).
37. Borg, R.J., Lai, D.Y.E., and Krikorian, O.H., Acta Met., 11, 867, (1963).
38. Cahoon, J.R., and Youdelis, W.V., Trans. AIME, 230, 1734, (1964).
39. Bitter, F., and Read, F.E., Rev. Sci. Instr., 22, (3), 171, (1951).
40. da Silva, L.C.C., and Mehl, R.F., Trans. AIME, 191, 155, (1951).
41. Jacquet, P.A., Metallurgical Reviews, (Institute of Metals), 1(2), 235, (1956).
42. Shewmon, P.G., Diffusion in Solids, (McGraw Hill, New York), p. 32, (1963).
43. Jost, W., Diffusion in Solids, Liquids, and Gases, (Academic Press Inc., New York), p. 77, (1960).
44. Kirkaldy, J.S., Decomposition of Austenite by Diffusional Processes (Interscience, New York), p. 65, (1962).
45. Wilson, A.H., The Theory of Metals, (Cambridge University Press), 168, (1954).
46. Mott, N.F., and Jones, H., The Theory of the Properties of Metals and Alloys, (Dover Publications Inc., New York), 211, (1958).
47. Putley, E.H., The Hall Effect and Related Phenomena, (Butterworths, London), p. 73, (1960).
48. Dekker, A.J., Solid State Physics, (Prentice Hall Inc.), p. 215, (1957).
49. Sato, T., and Noguchi, S., J. Phys. Soc. Japan, 12, 335, (1957).
50. Smith, R.P., Trans. AIME, 224, 105, (1962).
51. Varley, J.H.O., Phil. Mag., 45, 887, (1954).

52. Van Horn, D.D., Trans. ASM, 51, 185, (1959).
53. Peirce, B.O., and Foster, R.M., A Short Table of Integrals, 4th. Edition, (Ginn and Company, Boston), p. 68, (1956).

APPENDIX I

ANALYSIS OF MATERIALS

1. High Purity Zinc

The following analyses were furnished by the supplier, the Consolidated Mining and Smelting Co. of Canada, Ltd.

<u>Element</u>	<u>Amount Present (p.p.m.)</u>
Cd	3.0
Cu	0.5
Fe	1.0
Pb	1.0
Ag	0.2

2. High Purity Silver

<u>Element</u>	<u>Amount Present (p.p.m.)</u>
Bi	0.5
Cu	0.5
Fe	2.0
Pb	0.5

3. High Purity Copper - Johnson, Matthey and Co., Ltd.

Analysis furnished by the supplier.

<u>Element</u>	<u>Amount Present (p.p.m.)</u>
Fe	2
Si	1
Ag	1
Mg	1

4. High Purity Copper - L. Light and Co., Ltd.

<u>Element</u>	<u>Amount Present (p.p.m.)</u>
Fe	2
Mg	1
Si	5
Ag	1

APPENDIX II

DETERMINATION OF THE DIFFUSIVITY BY THE
BOUNDARY SHIFT BETWEEN A SINGLE
PHASE AND TWO PHASE REGION

In this derivation the following assumptions are considered valid.

1. The diffusivity is independent of concentration.
2. No diffusion occurs in the two-phase region.
3. No Kirkendall shift occurs.

If a diffusion couple having the initial concentrations C_1 and C_2 is annealed at temperature T (Figure 24a), after time t the concentration profile will be similar to that shown in Figure 24b. If k is the constant composition at the initial interface, then the concentration, C , in the single phase region is given by⁵²

$$C = k - (k - C_1) \operatorname{erf} (x / \sqrt{4Dt}) \quad . \quad (59)$$

Considering the flux of solute at the phase boundary,

$$D \frac{dC}{dx} = (C_2 - C_{1,0}) \frac{d\epsilon}{dt} \quad , \quad (60)$$

where ϵ is the boundary movement and $C_{1,0}$ is defined in Figure 24. Taking the derivative of C with respect to x in equation (59), equation (60) becomes

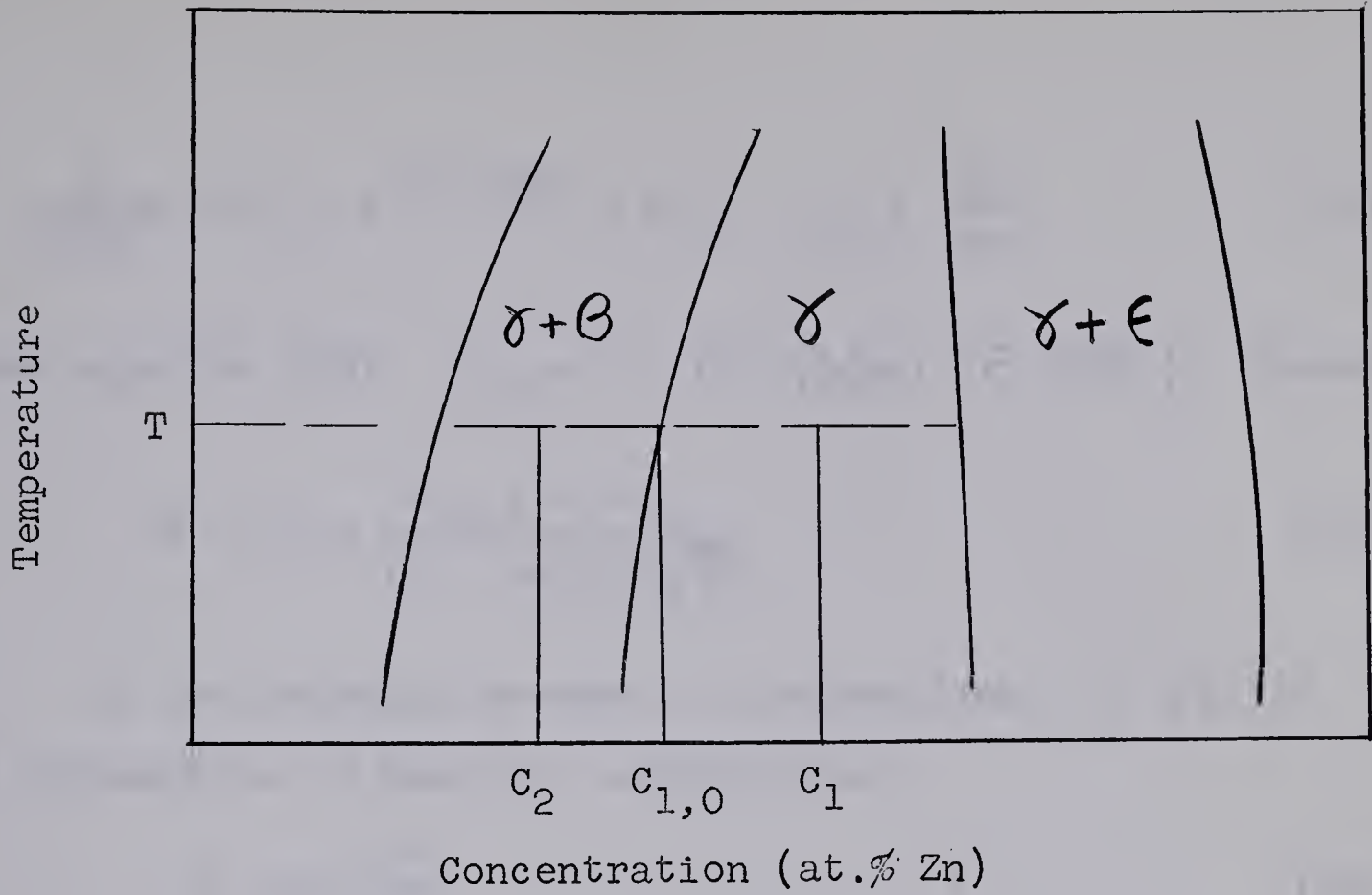


Figure 24a. Phase diagram showing limiting concentrations for diffusion from a two-phase region into a single phase region.

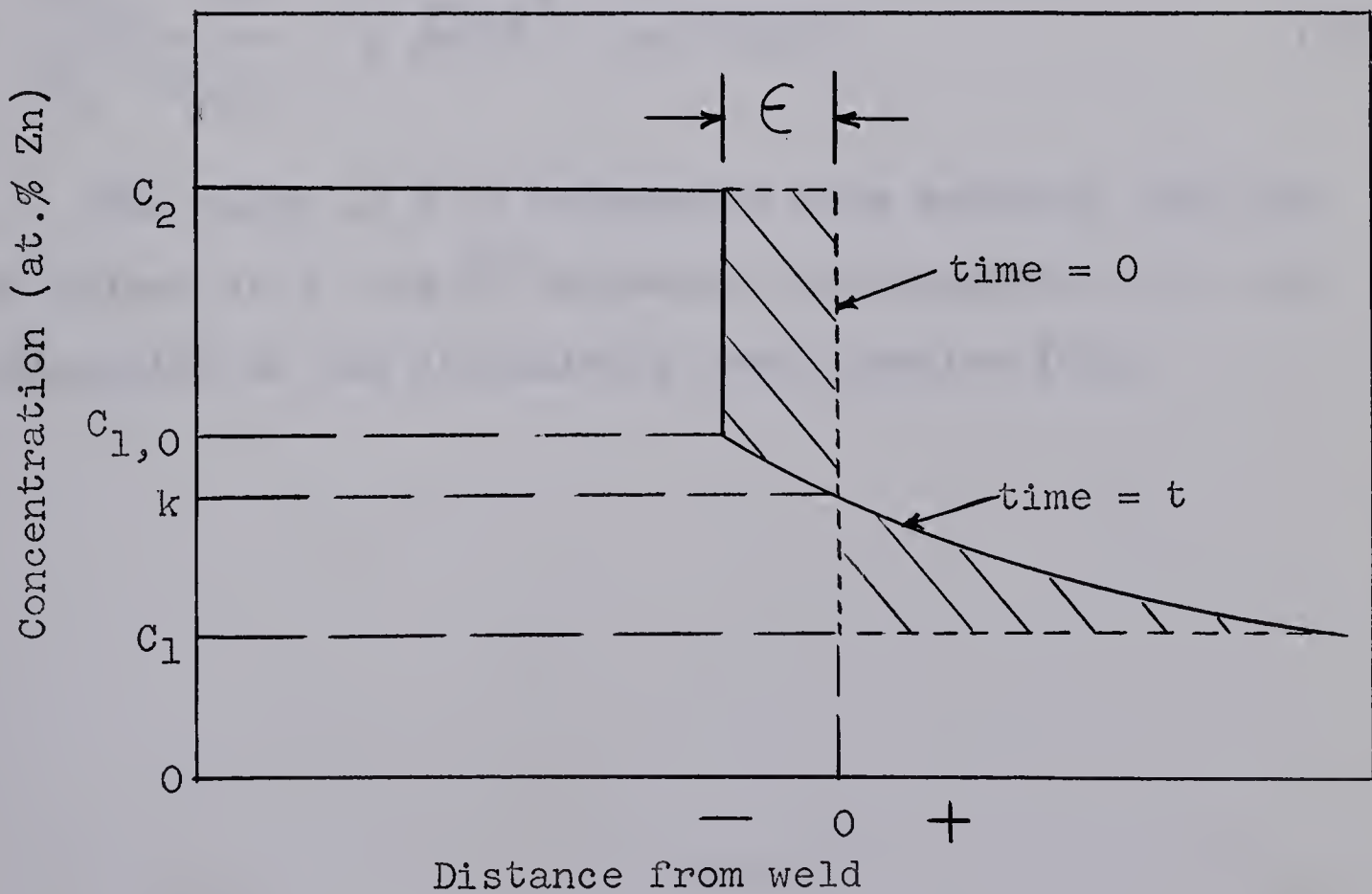


Figure 24b. Concentration profile after diffusion at temperature ' T ' for time ' t '.

$$-\frac{D}{\sqrt{\pi Dt}} (k - c_1) e^{-\epsilon^2/4Dt} = (c_2 - c_{1,0}) \frac{d\epsilon}{dt} . \quad (61)$$

From equation (59), $c_{1,0} = k - (k - c_1) \cdot \left(\operatorname{erf} \epsilon / 2\sqrt{Dt} \right)$. Therefore,

$$k - c_1 = \frac{c_{1,0} - c_1}{(1 - \operatorname{erf} \epsilon / 2\sqrt{Dt})} . \quad (62)$$

If the boundary movement is proportional to \sqrt{t} , it is permissible to make the substitution

$$\epsilon = 2K \sqrt{Dt} , \quad (63)$$

where K is a constant. Using this substitution and equation (62), equation (61) becomes

$$\frac{c_{1,0} - c_1}{c_2 - c_{1,0}} = K \sqrt{\pi} e^{K^2} (\operatorname{erf} K - 1) . \quad (64)$$

The value of K is determined from equation (64) and the values of ϵ and \sqrt{t} determined experimentally for the calculation of the diffusivity from equation (63).

APPENDIX III
CONCENTRATION PROFILES FOR THE Ag-Cu
DIFFUSION COUPLES

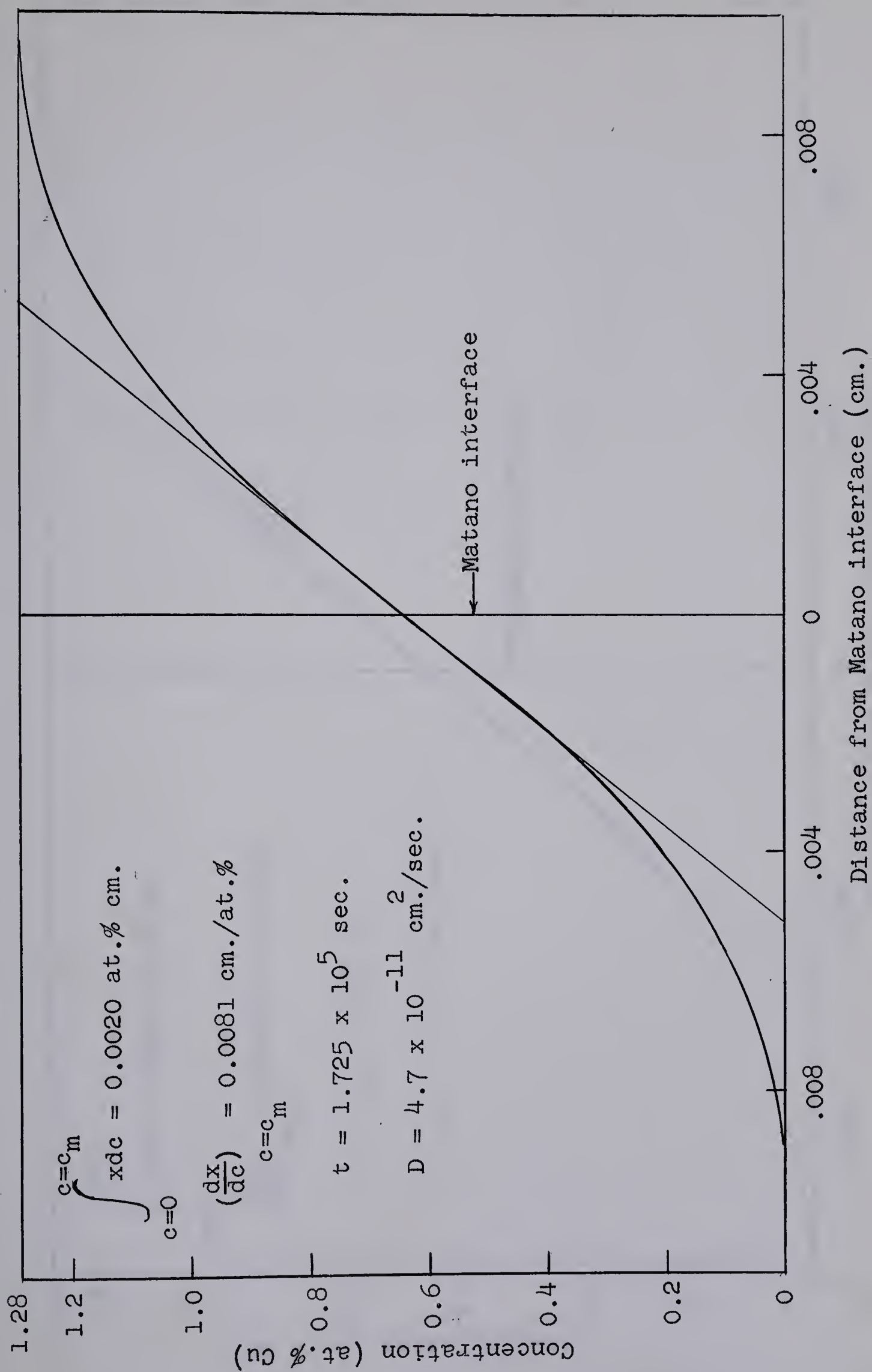


Figure 25. Penetration curve for couple Ag-F-3 annealed at 629°C for 48 hrs.

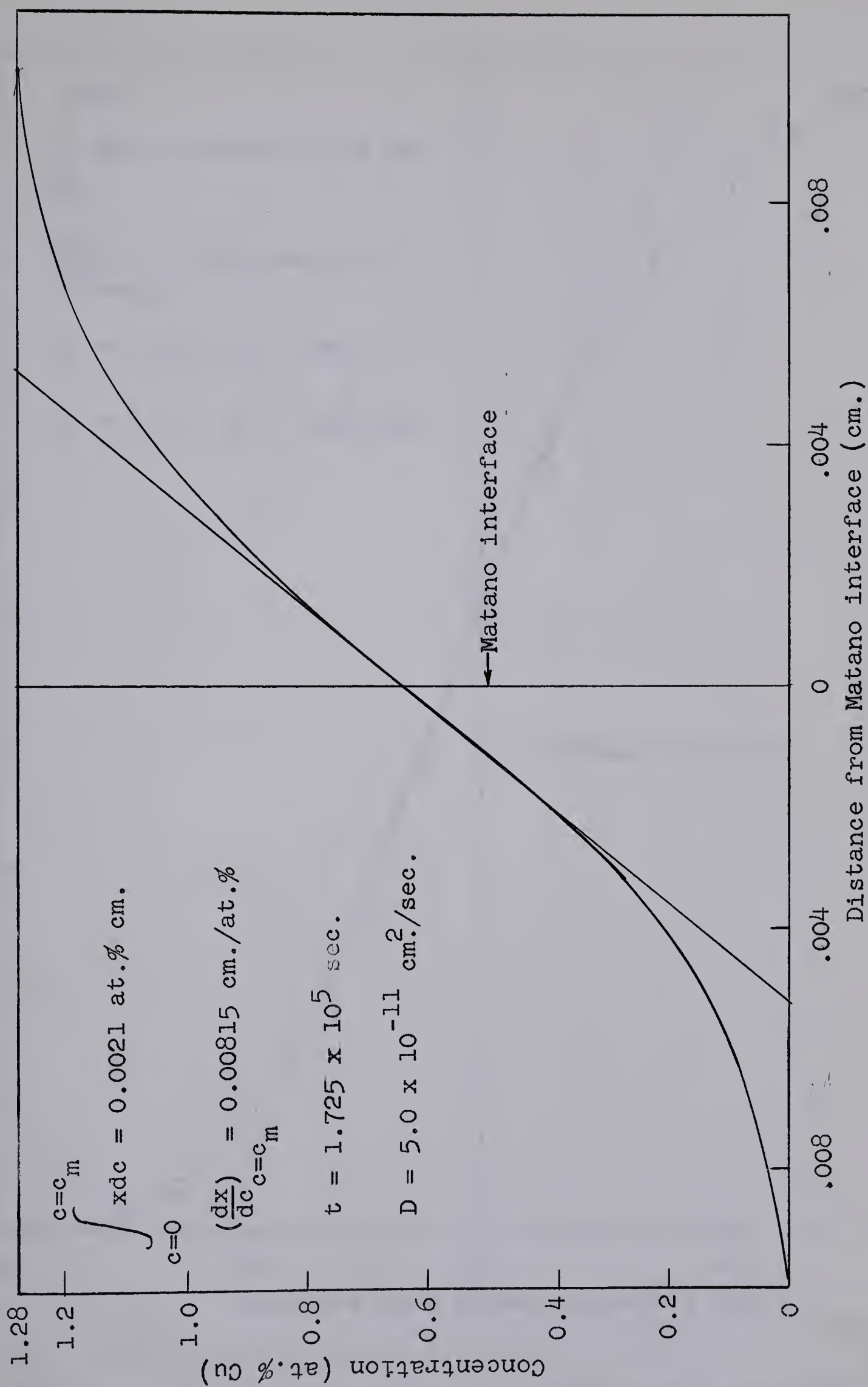


Figure 26. Penetration curve for couple Ag-NF-3 annealed at 630°C for 48 hrs.

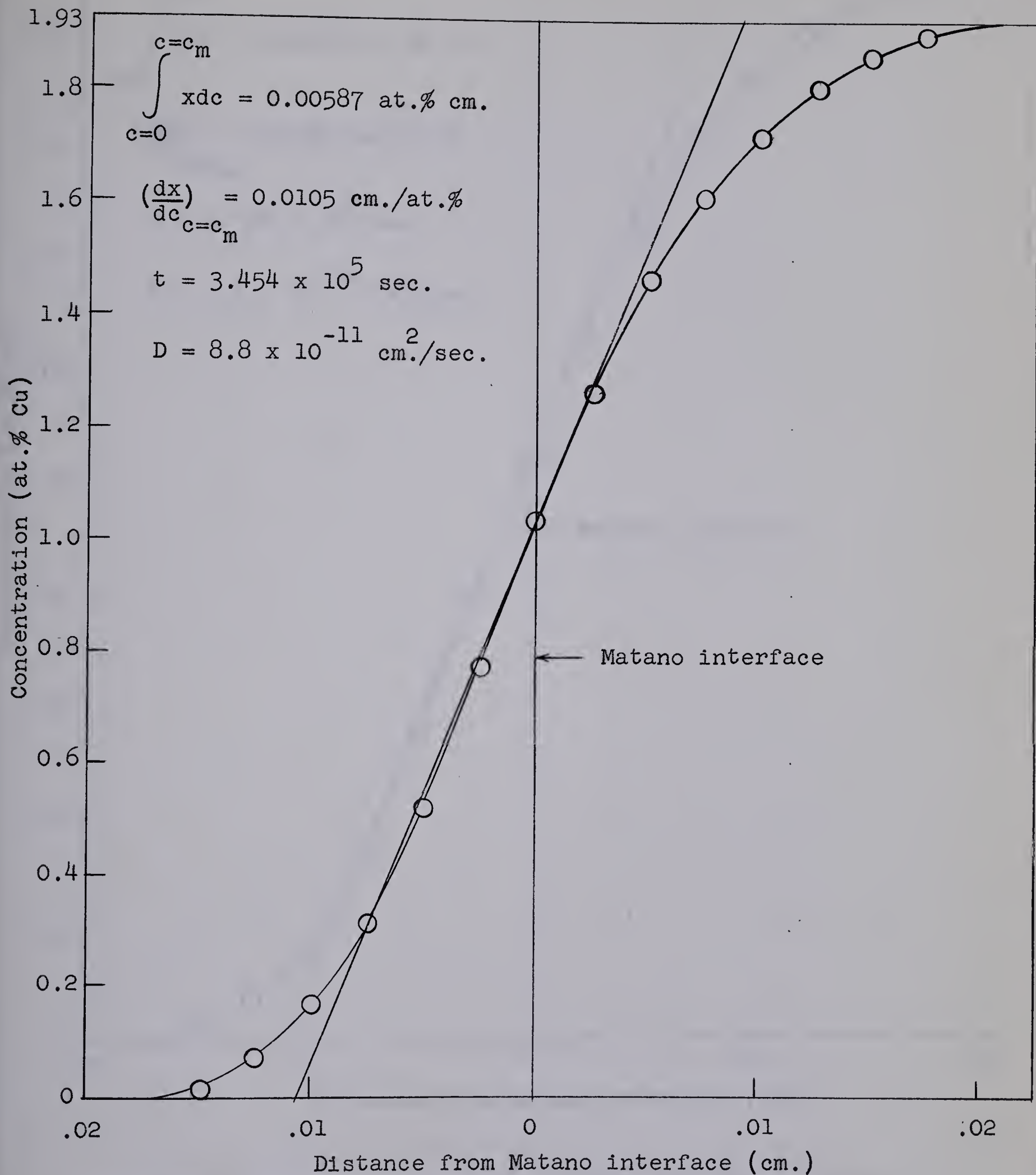


Figure 27. Penetration curve for couple Ag-F-5 annealed at 699°C for 96 hrs.

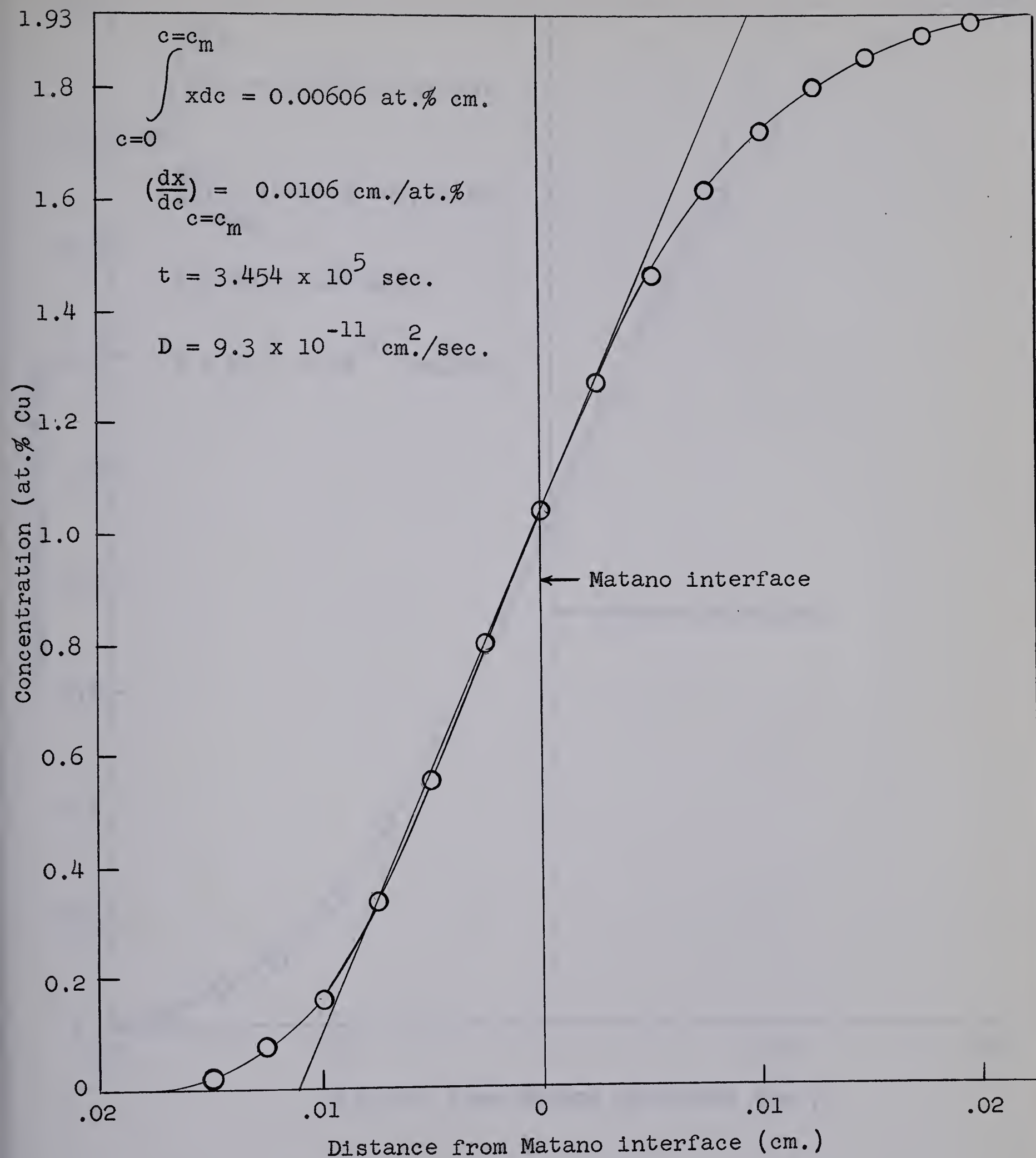


Figure 28. Penetration curve for couple Ag-NF-5 annealed at 698°C for 96 hrs.

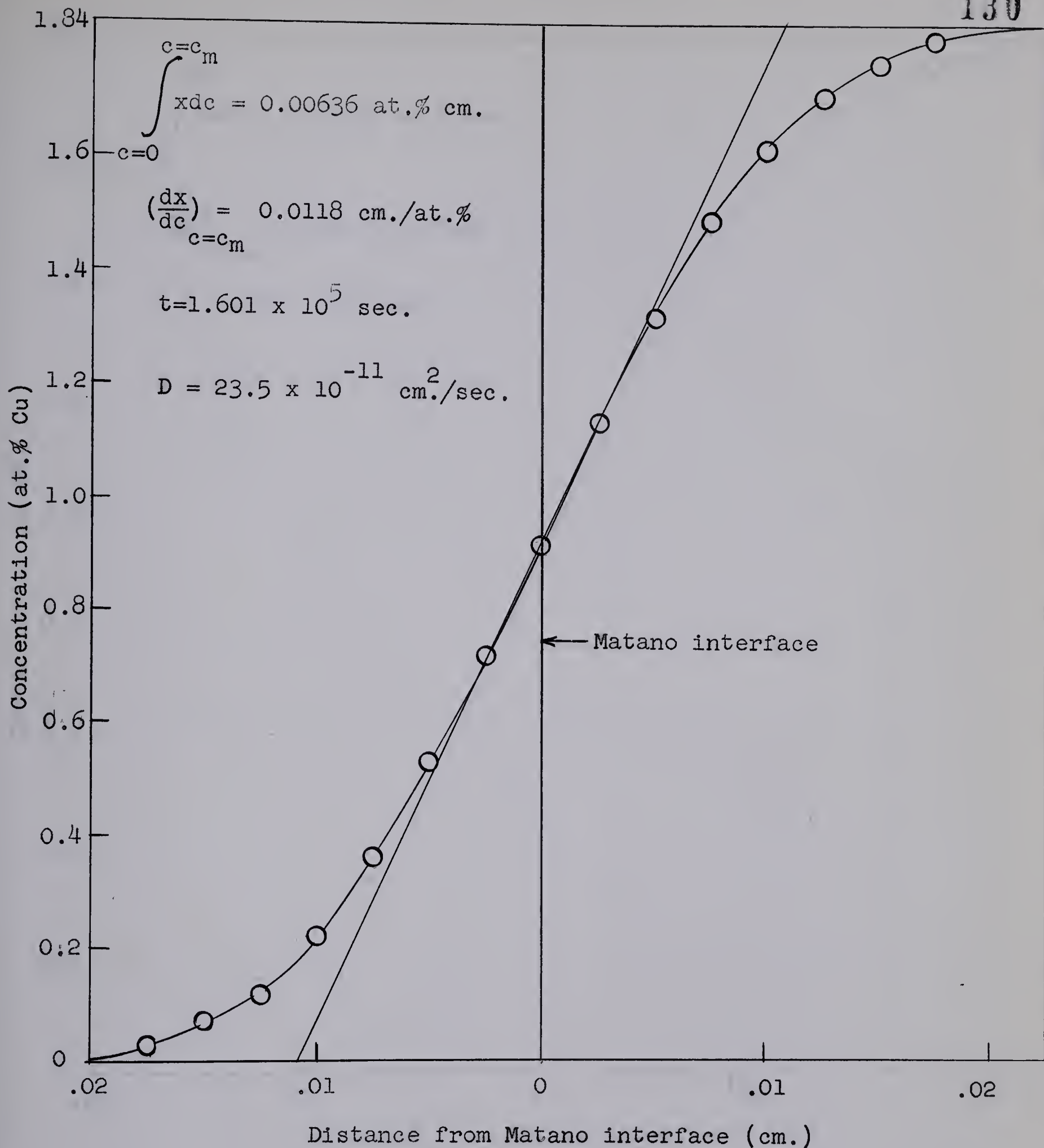


Figure 29. Penetration curve for couple Ag-F-6 annealed at 754°C for 45 hrs.

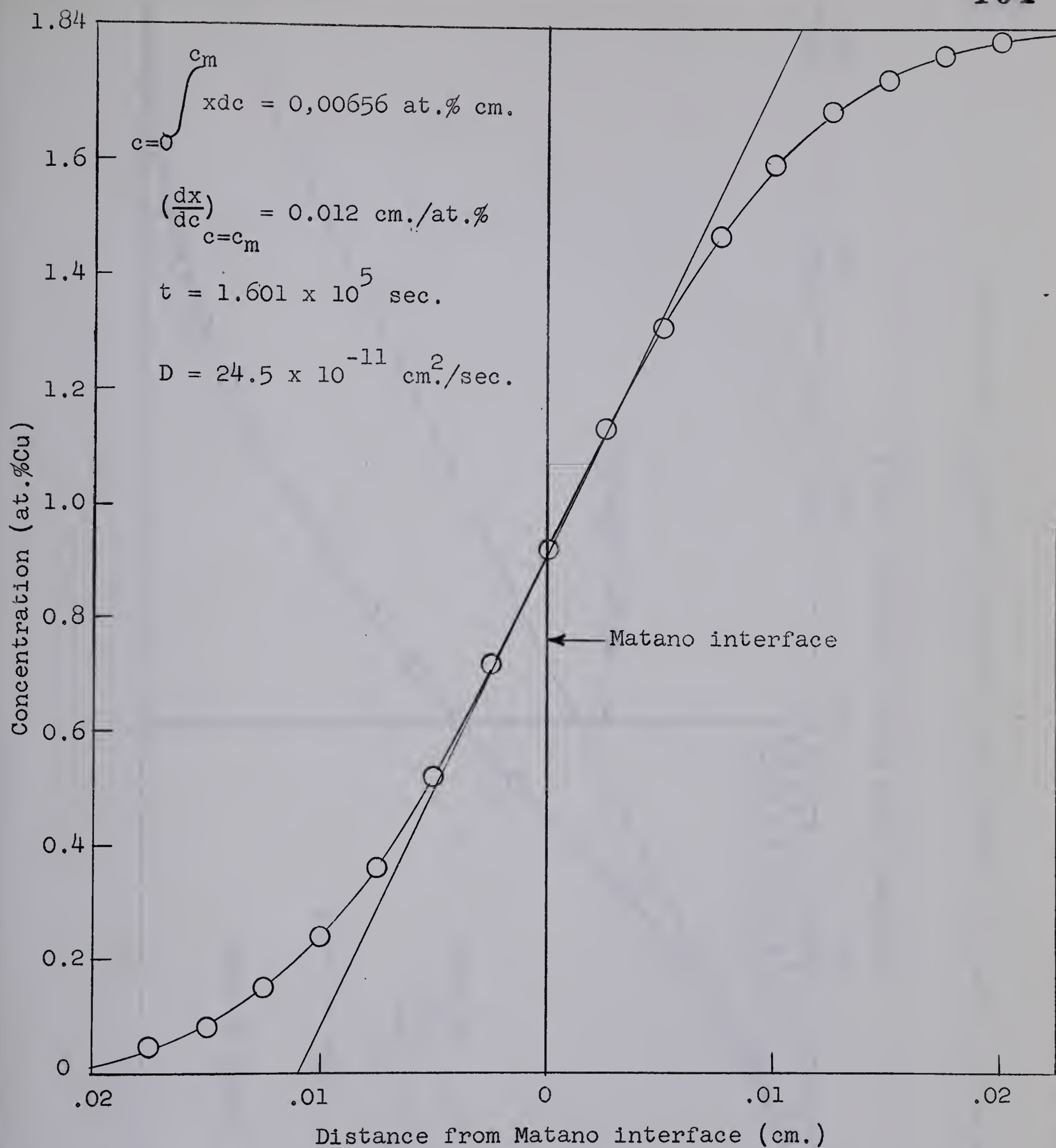


Figure 30. Penetration curve for couple Ag-NF-6 annealed at 756°C for 45 hrs.

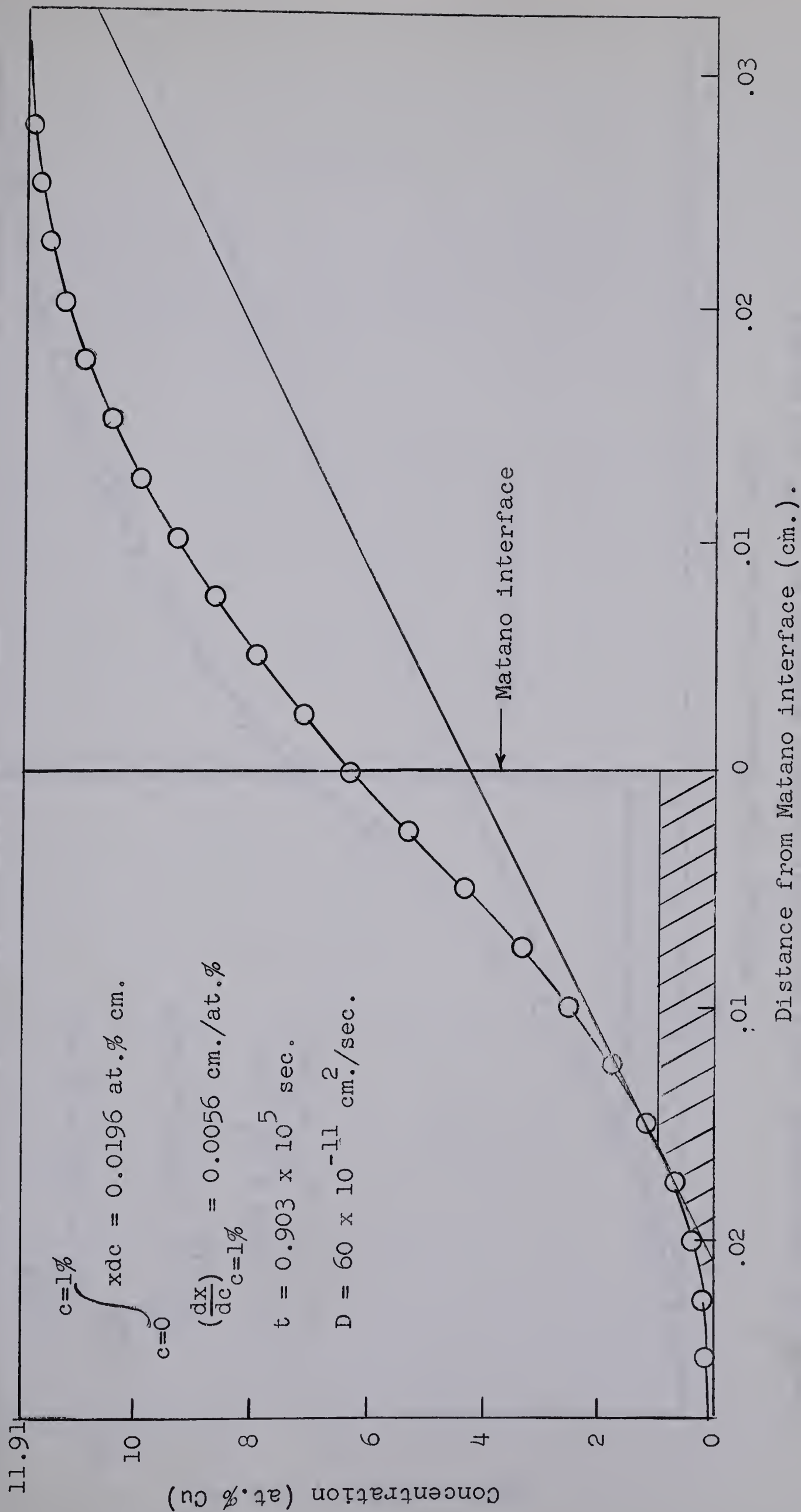


Figure 31. Penetration curve for couple Ag-F-7 annealed at 802°C for 25 hrs.

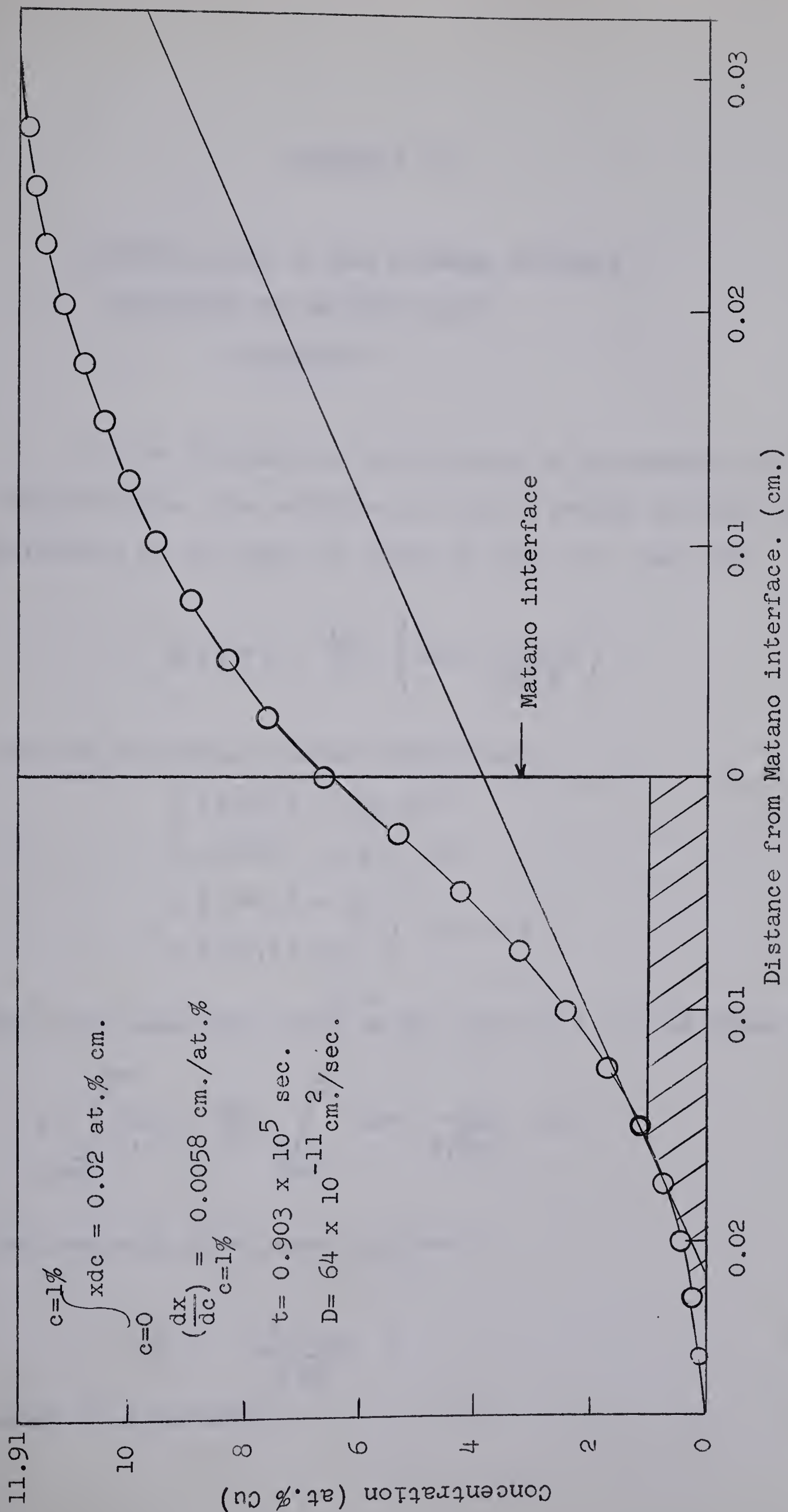


Figure 32. Penetration curve for couple Ag-NF-7 annealed at 803°C for 25 hrs.

APPENDIX IV

DETERMINATION OF THE AVERAGE DISTANCE
TRAVERSED BY AN ION DURING
DIFFUSION

If the diffusivity of the ions is independent of concentration, the solution of Fick's second law for the diffusion of the ions is given by (ref. 43, page 20)

$$C(x,t) = \frac{C_0}{2} \cdot \left(\operatorname{erfc} \frac{x}{2\sqrt{D_i t}} \right), \quad (65)$$

for the following boundary conditions:

$$\left. \begin{aligned} C(x,0) &= 0 \text{ for } x > 0 \\ C(x,0) &= C_0 \text{ for } x < 0 \\ C(-\infty, t) &= C_0 \\ C(+\infty, t) &= 0 \end{aligned} \right\} \text{ for all } t.$$

The area under the curve on one side of $x = 0$ is given by

$$A = \int_{x=0}^{\infty} C dx = \frac{C_0}{2} \int_{x=0}^{\infty} \operatorname{erfc} \frac{x}{2\sqrt{D_i t}} dx. \quad (66)$$

The centroid of an area is given by

$$\bar{x} = \frac{\int x dA}{\int dA}, \quad (67)$$

where A is the area.

Thus, the centroid of the area under the concentration curve is

$$\bar{x}' = \frac{\frac{C_0}{2} \int_0^{\infty} x \operatorname{erfc} \frac{x}{2\sqrt{D_i t}} dx}{\frac{C_0}{2} \int_0^{\infty} \operatorname{erfc} \frac{x}{2\sqrt{D_i t}} dx} \quad (68)$$

Introducing the change of variable $y = x/2\sqrt{D_i t}$, equation (68) becomes

$$\bar{x}' = \frac{\int_0^{\infty} 4D_i t y \operatorname{erfc} y dy}{\int_0^{\infty} 2\sqrt{D_i t} \operatorname{erfc} y dy} \quad (69)$$

The first derivative of the complementary error function and the first integral (from 0 to ∞) are, respectively

$\left[(-2/\sqrt{\pi}) e^{-y^2} \right]$, and $(1/\sqrt{\pi})$. Upon integration, equation (69) becomes

$$\bar{x}' = \frac{\frac{4D_i t}{\sqrt{\pi}} \int_0^{\infty} y^2 e^{-y^2} dy}{2\sqrt{D_i t/\pi}} \quad (70)$$

Now, $\int_0^{\infty} y^2 e^{-y^2} dy = \sqrt{\pi}/4$.⁵³ Therefore,

$$\bar{x}' = \sqrt{\pi D_i t}/2 \quad (71)$$

Now, \bar{x}' is the centroid for one side of the diffusion curve. Considering the other half of the diffusion curve, the average distance an atom moves is $\bar{x} = 2\bar{x}'$ or

$$\bar{x} = \sqrt{\pi D_i t} \quad .$$

B29849